NUE UNIQUE

NANOTECHNOLOGY
UNDERGRADUATE
EDUCATION:

USING NANOSCIENCE
INSTRUMENTATION
FOR QUALITY
UNDERGRADUATE
EDUCATION

Nanoscience on the tip

a workshop in scanning probe microscopy

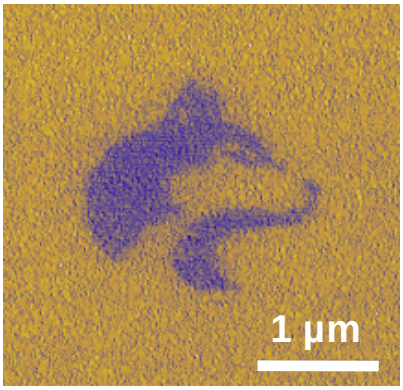

Seattle, Washington

June 25–29, 2007

NSF

nanoSurf

nanoScience Instruments

UNIVERSITY OF WASHINGTON

Nanoscience on the tip

a workshop in scanning probe microscopy

TABLE OF CONTENTS

Laboratory Unit Descriptions and Assignments

Scope

Motivation

Since the invention of the scanning tunneling microscope (STM) in 1981 by Gerd Binnig and Heinrich Rohrer (Nobel Prize in Physics 1986) scanning probe microscopy (SPM) techniques have dazzled scientist and engineers in nearly every field from natural sciences to liberal arts, and nucleated the new discipline of Nanoscience and Nanotechnology. The birth of such a highly interdisciplinary field is an attest to the changing times in a world that moves from educating specialists to generalists. The true power of SPM techniques, which assisted in removing boundaries between disciplines, lays in its simplicity to provide access to the nanoworld in terms of visualization and manipulation. Hence, it is only perceivable that SPM offers an outstanding educational tool for schools.

Objective

The overarching objective of the NUE UNIQUE Program is to develop a nationally *replicable* model of a *sustainable* and *up-to-date* undergraduate teaching laboratory of scanning probe methods applied to nanosciences and nanotechnology. To this end, a partnership between researchers and educators at the University of Washington (UW) and the North Seattle Community College (NSCC), and two companies - Nanosurf, AG (Liestal, Switzerland) and nanoScience Instruments (Phoenix, AZ) has been forged within this partnership a new paradigm of initiating, operating and maintaining a SPM laboratory will be developed and tested that provides a truly hands-on experience in a classroom laboratory setting for a small number of students per instrument involving a variety of SPM techniques and nanoscience/engineering topics.

Preface

This first workshop organized within the boundaries of this paradigm of initiating, operating and maintaining a SPM laboratory serves a class of 16 undergraduate students of diverse academic background with a one-week hands-on experience in small groups of 4 students per instrument. The students gain experience in a variety of different areas from nanolithography, photovoltaics, contact mechanics, polymer relaxation, Van der Waals and capillary forces to quantum mechanical properties.

René M. Overney, Director
NUE UNIQUE
University of Washington, Seattle, WA 98195

roverney@u.washington.edu

June 25, 2007

Organization of the 2007 SPM Workshop

Format – Daily Schedule

<table>
<tr><th>Monday</th><th>Tuesday</th><th>Wednesday</th><th>Thursday</th><th>Friday</th></tr>
<tr><td>June 25</td><td>June 26</td><td>June 27</td><td>June 28</td><td>June 29</td></tr>
<tr><td></td><td>8:00 a.m.
SFM Lecture on Surface Electronic Properties
Prof. Ginger
Mueller 154</td><td>8:00 a.m.
SFM Lecture on Contact Mechanics
Prof. Overney
Mueller 154</td><td></td><td rowspan="2">8:00 a.m.
Work on the assigned Lab Unit for the day
(a) Prelab Assignment
(b) Lab Assignment
(c) Lab Report
(start with the lab report around 1 p.m.)</td></tr>
<tr><td>9:00 a.m.
Welcome
Profs Overney and Ginger
Mueller 154</td><td colspan="3" rowspan="3">9:00 a.m.
Work on the assigned Lab Units for the day
(a) Prelab Assignment
(b) Lab Assignment
(c) Lab Report
(start with the lab report around 2 p.m.)

Wilcox 233 and 335
Shared Experimental Facilities of GEMSEC</td></tr>
<tr><td>9:15 a.m.
Lab Overview
Prof Overney
Mueller 154</td><td rowspan="2">2:30 p.m.
Final Discussion
Certificates and Awards
Evaluation
Mueller 154
3:30 p.m.
Adjourned</td></tr>
<tr><td>10:00 a.m.
Laboratory
UNIT 1:
Introduction to SFM and Nanolithography

Wilcox 233 and 335</td></tr>
<tr><td colspan="4">4:30 p.m. Daily discussion about the lab Milnor-Roberts Room</td></tr>
<tr><td colspan="4">Individual preparation for the assigned Lab Unit the next day: Involves reading of the background information and answering the theoretical questions. Due at the beginning of the lab the next morning.</td></tr>
</table>

See maps on next pages for directions.

Local Map

Map of University of Washington Campus with NUE-UNIQUE Facilities Highlighted

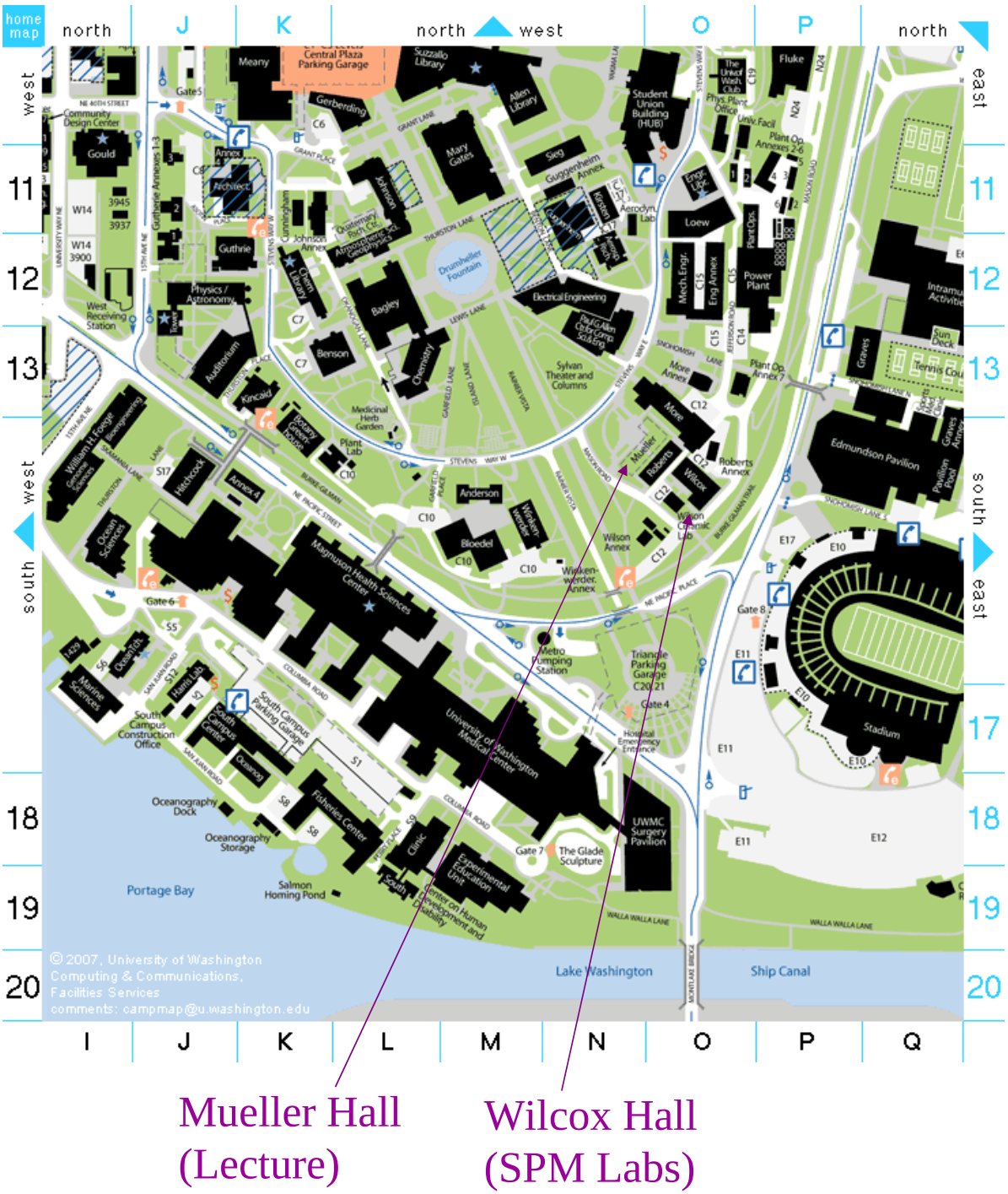

Parking Information at the UW: http://www.washington.edu/commuterservices/get_to_uw/maps_directions/

Local Map

Map of Mueller Hall

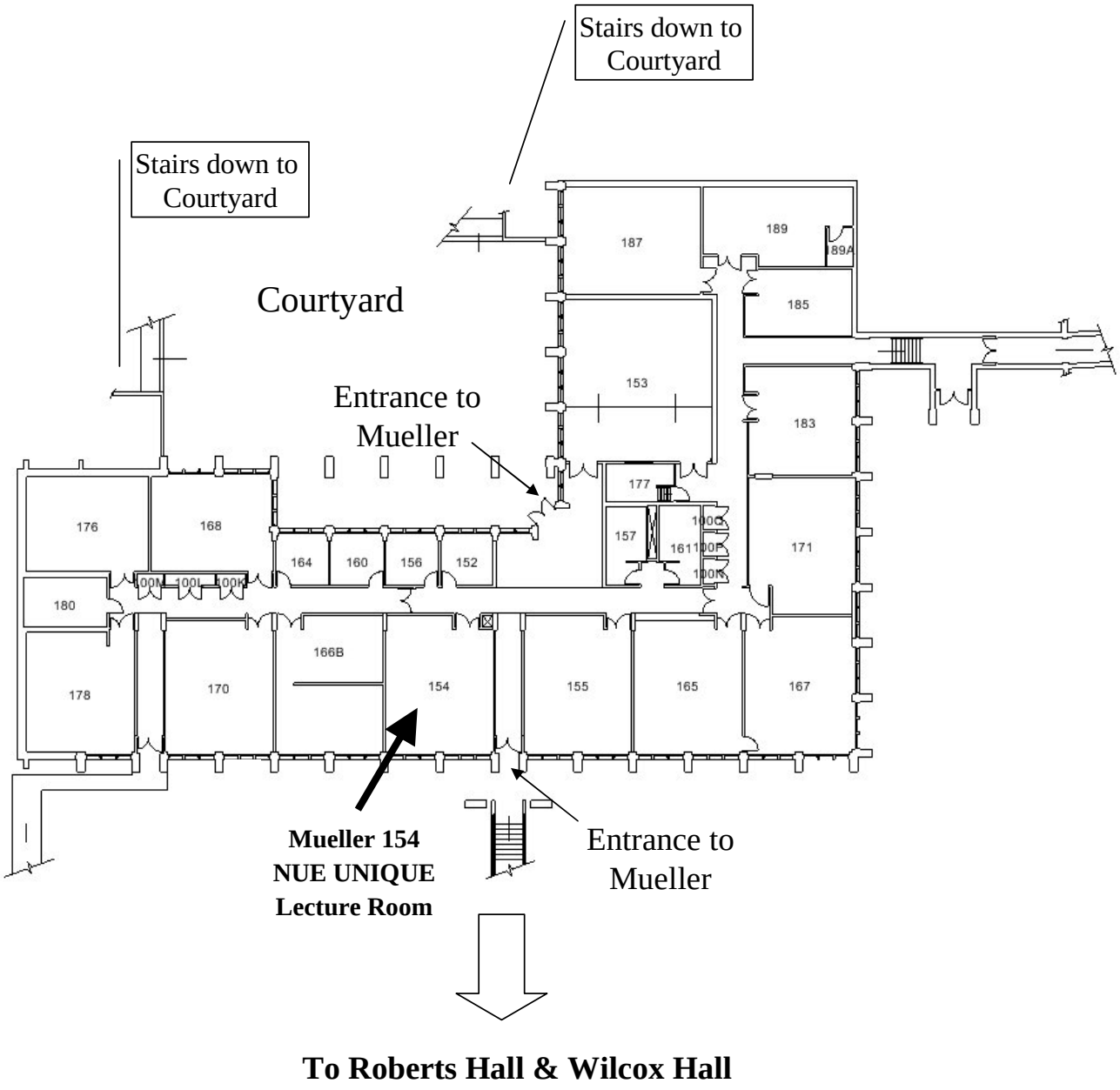

Local Map

Map of Wilcox 2nd Floor

Shared Experimental Facilities of GEMSEC

To Roberts Hall & Mueller Hall

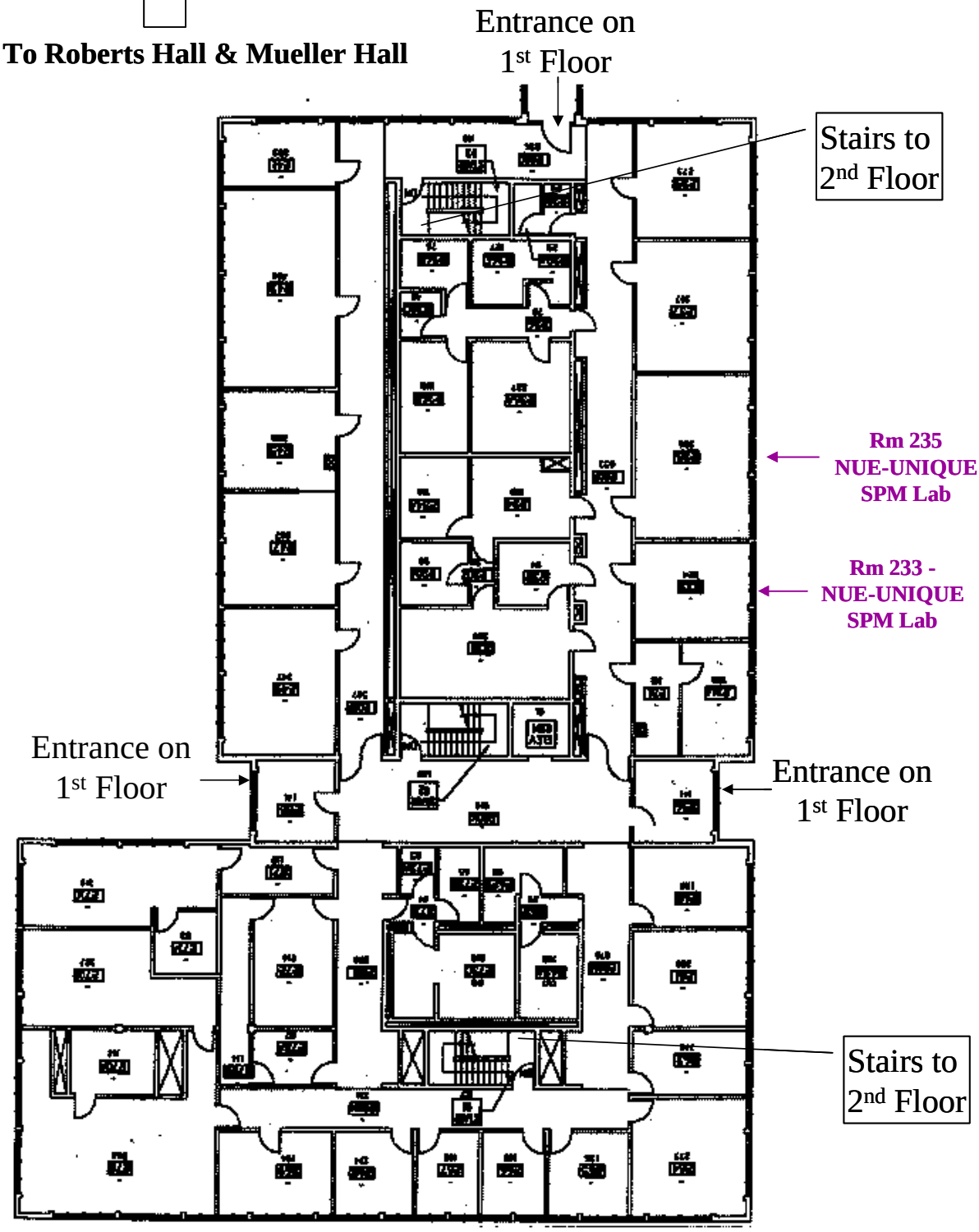

NUE UNIQUE PARTNERS & SPONSORS

- UW - Genetically Engineered Materials Science & Engineering Center GEMSEC (NSF-MRSEC)
- UW - Center for Nanotechnology (CNT)
- North Seattle Community College (NSCC), Seattle, WA
- Nanosurf, AG (Liestal, Switzerland)
- nanoScience Instruments (Phoenix, AZ)

NUE UNIQUE (Nanotechnology Undergraduate Education - Using Nanoscience Instrumentation for Quality Undergraduate Education), Grant 06-538, is a National Science Foundation sponsored program.

Biographical Sketches

Instructors

David Ginger (*ginger@chem.washington.edu*, Prof. in Chemistry) research focuses on the creation and study of nanostructured materials with unique optoelectronic and photonic properties. His group has pioneered novel scanning probe microscopy and lithography methods to further our understanding of nanostructured organic solar cells. His group is also developing bio-inspired assembly strategies for controlling near-field electromagnetic coupling between fluorophores and plasmon resonant nanoparticles. Ginger is also known for his work in the development of semiconductor nanocrystals for photovoltaics and LEDs, and as a pioneer of Dip-Pen Nanolithography methods for biomolecules. In recognition of his research and education efforts, he has been named a Research Corporation Cottrell Scholar.

René Overney (*roverney@u.washington.edu*, Prof. in Chemical Engineering) is known for his pioneering work in nanorheology and transport properties. His group has developed various SPM nano-characterization methods particularly applicable to polymer science and related technologies. The research of his group ranges from mesoscale material aspects in photonics, optoelectronics, electronic storage media, separation membranes, tribology to human implant technology. Overney coauthored one of the early textbooks in Nanoscience (*Nanoscience*, World Scientific 1998), and is teaching on the undergraduate and graduate level nanoscience related courses since 1996.

Mehmet Sarikaya (*sarikaya@u.washington.edu*, Prof. in Materials Science and Engineering) is known for his pioneering efforts and ideas in *Molecular Biomimetics.* By merging recent advances in molecular biology and genetics with state-of-the-art engineering and nanocharacterization from the physical sciences, his and his collaborators' goal is to shift the biomimetic materials science paradigm from imitating Nature to designing materials to perform artificial nanofunctions. It is the intent to combine Nature's proven molecular tools, such as proteins, with synthetic nanoscale constructs to make molecular biomimetics a full-fledged methodology. To this end, at the Genetically Engineered Materials Science and Engineering Center, an NSF-MRSEC, Sarikaya is directing a multidisciplinary team with diverse expertise to genetically select inorganic-binding short polypeptides, tailoring them via molecular manipulation and bioinformatics to make heterofunctional molecular constructs and using them as synthesizers, assemblers, and molecular erectors in materials science and medicine.

Teaching Assistants

Yeechi Chen (yeechi@u.washington.edu) is a graduate student working with Prof. David Ginger. She received her A.B. in physics from Dartmouth College in 2000, and her M.S. from the University of Washington in 2003. Her research focuses on the characterization of metal nanoparticle-modified fluorescence.

Biographical Sketches

Teaching Assistants cont.

Hanson Fong (*hfong@u.washington.edu*) received his Ph.D. in Materials Science & Engineering from University of Washington in 2003. His is currently a post-doc fellow at the University of Washington working under the supervision of Drs. Mehmet Sarikaya and Martha Somerman on dental tissue regeneration. He is also the facilities coordinator for GEMSEC at the University of Washington.

Dan Knorr (*knorrdb@u.washington.edu*), currently a graduate student, is studying with Dr. René Overney and Dr. Alex Jen in the fields of atomic force microscopy and photonic materials. Dan earned B.S. and M.S. degrees in chemical engineering at Texas A&M University and then spent five years in the chemical industry as a process engineer with Chevron Phillips before returning to school to pursue a Ph.D.

Jason Killgore (*killgoj@u.washington.edu*) is a 5th year graduate student studying with Dr. René Overney. Jason received a BS degree from Western Washington University in 2002 and an MS degree from the University of Washington in 2005. His research focuses on using scanning probe microscopy to study local fluxes in nanocomposite polymer membranes. He expects to complete his Ph.D. in spring 2008.

Chris So (*crso@u.washington.edu*) graduated in 2006 with a BS from the Biochemistry program at the University of Washington. He is currently a graduate student in the Materials Science and Engineering Department working with Prof. Mehmet Sarikaya at the Genetically Engineered Materials Science and Engineering Center (GEMSEC). He is interested in bio-inspired materials and molecular biomimetics, particularly in using the AFM as a tool for their study.

Joseph Wei (*wei@u.washington.edu*) is a Chemical Engineering graduate student working in the lab of Prof. David Ginger. His current interests are applying Dip-Pen Nanolithography to template-directed organization in polymer thin films, assembling engineered polypeptides on inorganic surfaces, and direct patterning of positive etch resists. He received his BS (2002) and MS (2004) degrees in Chemical Engineering from the University of Washington under the direction of Prof. René Overney on direct surface permeability analysis and nanoscopic material characterization of membrane systems using scanning probe microscopy.

Acknowledgment

Our foremost thanks go to Dr. Tomoko Gray (UW, ChemE) for developing a great part of the laboratory units. Furthermore, we gratefully acknowledge the lab unit development efforts by Michael Brasile, Yeechi Chen, Dan Knorr, Jason Killgore, and Joseph Wei, and the logistic support efforts by Dr. Hanson Fong (UW, GEMSEC). We also like to express our gratitude to Dr. Ethan Allen (UW, CNT) and Dr. Tom Griffith (NSCC) for their support of this program from the very beginning. NUE UNIQUE is funded by the Nanotechnology Undergraduate Education (NUE) program of the National Science Foundation (Grant 06-538) and supported by GEMSEC (a UW based Mat. Res. and Eng. Center), Nanosurf AG (Switzerland) and nanoScience Instruments (AZ), and the Department of Chemical Engineering at the University of Washington.

Workshop 2007 Participants

Name:		Email:	Current College/University:
Bleecker	Joan	bleecj@gmail.com	University of Washington
Chen	Yu-Chun	yuchun@u.washington.edu	University of Washington
Christin	Brian	BRChristin@hotmail.com	University of Washington
Deleo	Francesco	deleof@aa.washington.edu	University of Washington
Gill	Kristina	korynn@kyriani.org	North Seattle Community College
Jaramillo	C'havala	chavallaneous@hotmail.com	University of Washington
Koniges	Ursula	koniges@washington.edu	University of Washington
Marciniak	Monika	monik956@u.washington.edu	University of Washington
Nair	Tara	nairt@seattleu.edu	Seattle University
Quarfoth	Ryan	rquarfoth@hmc.edu	Harvey Mudd College
Schneider	Anna	ars7@u.washington.edu	University of Washington
Smith	Rebecca	smit1105@seattleu.edu	Seattle University
Stapleton	Sarah	stapls@u.washington.edu	University of Washington
Stephen	Zachary	zrs420@u.washington.edu	University of Washington
Tey	Johnson	johnson.tey@gmail.com	University of Washington
Yaghoobi	Parham	pyaghoobi@gmail.com	University of British Columbia


NUE UNIQUE
Class of 2007
including TAs and Instructor

LAB UNIT 1: Introduction to Scanning Force Microscopy and Dip-Pen Nanolithography

Specific Assignment: Introduction to Scanning Force Microscopy (SFM) and Dip-Pen Nanolithography (DPN) Gold Etching with DPN-generated Templates and Contact Mode Imaging

---

Objective

The student will become familiar with contact mode Scanning Force Microscopy (SFM) as an imaging technique, and be introduced with Dip-Pen Nanolithography (DPN).

Outcome

At the end of this lab, you will be familiar with the basic principles and techniques of contact mode SFM and DPN, and you will obtain some familiarity with script-based control of the NanoSurf SFM.

Synopsis

In this lab, you will use DPN to generate nanoscale resists for gold etching, and you will subsequently use SFM to image the patterned structures in contact mode.

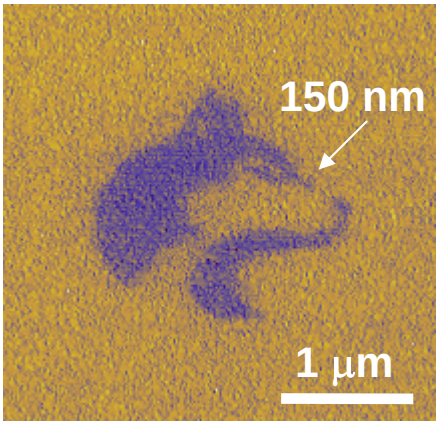

DPN-Patterned Alkanethiols on a Gold Surface

Materials

16-mercaptohexadecanoic acid, gold films on silicon oxide wafers, and gold etchant solution (thiourea and ferric nitrate)

Techniques

Contact mode SFM and DPN

Table of Contents

1. Assignment

In this lab, you will use the Scanning Force Microscope (SFM), also known as Atomic Force Microscope (AFM), as both an imaging tool, and as a writing tool. As an imaging tool, you will use the most basic SFM imaging method: contact mode imaging. You will use the SFM tip as a nanoscale writing tool to deliver chemical "inks" to a surface very much like a nanoscale fountain pen. These inks will serve as etch resists that you will develop into patterns that can be imaged using contact mode SFM.

The unpatterned region of gold surface will be etched in a solution of thiourea and ferric nitrate. We will then use SFM in contact mode to image the resulting nanostructures.

The steps are outlined here:

1. (***pre-lab)*** Read the Material Safety Data Sheets (MSDS) of all chemicals used in this lab
2. (***pre-lab)*** Read background information of Scanning Probe Microscopy and Dip-Pen Nanolithography in section 4
3. Take the quiz on your theoretical understanding in section 2
4. Generate mercaptohexadecanoic acid patterns on gold surface as negative resists for gold etching using dip-pen nanolithography
5. Etch the unpatterned gold region to generate nanostructures using wet chemistry
6. Image the resulting gold patterns with atomic force microscopy in contact mode
7. Perform cross-section analysis on the topography of the structures to determine their diameter and height
8. Compare the feature size as a function of DPN dwell time
9. Compile a report to summarize your findings from this lab. Your report should include the following with a brief discussion:

    - Topography image showing your DPN-generated structures with scale bar
    - Cross-section profile of your structures
    - Dimensions of your structures (report average diameter and height with standard deviation)
    - Compare diameters with those predicted from eq. (4) and plot of dot sizes *vs.* dwell time of DPN

Chemical Hazards: See Experimental Assignment (section 3)

2. Quiz

2.1 Short Answers

(1) How many hydrogen atoms would you have to line up to make one nanometer?

(2) A student takes a SFM image like the one shown below to measure the size of some gold nanoparticles attached to a surface. What are the dimensions of the nanoparticles?

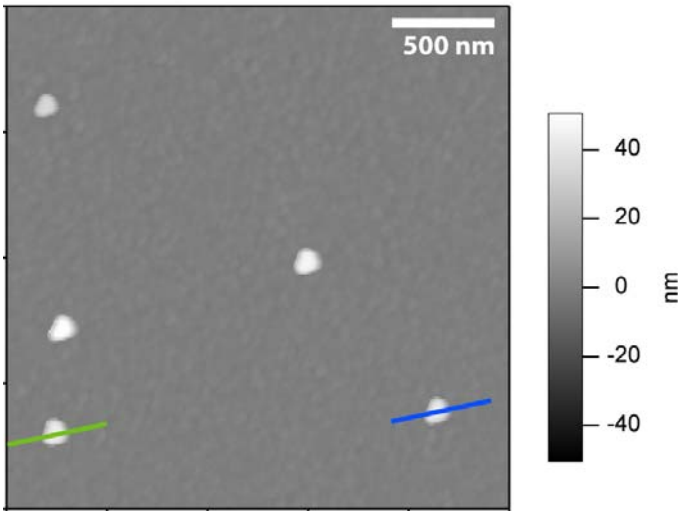

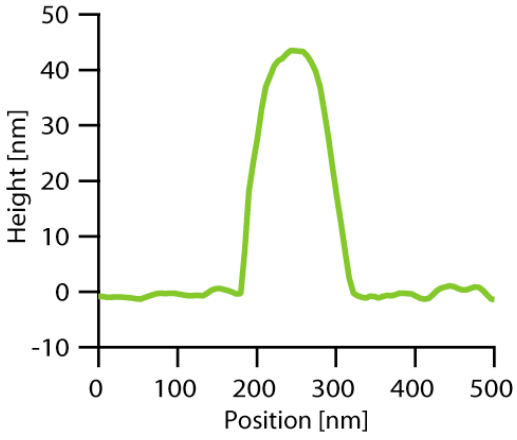

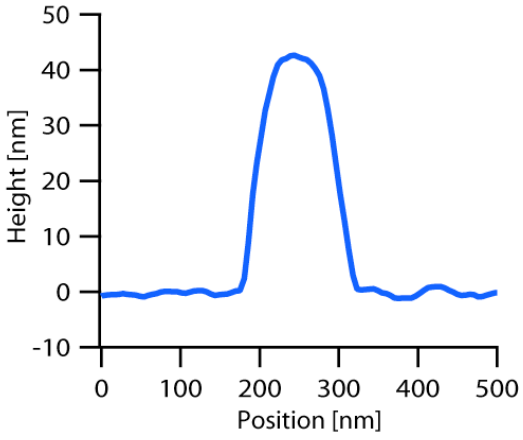

(3) A student takes an SFM like the one shown below. Explain what has gone wrong.

(4) A) What is the force constant of the cantilevers you will be using in this lab?
B) How much force does it take to deflect such a cantilever by 1nm?
C) Provide an order of magnitude estimate of how much force is needed to break a covalent bond (remember typical ~1 Angstrom long, ~80 kcal/mol).
D) Calculate the force that a 1 mW beam of 830 nm photons exerts on a mirror.

(5) Using the same SFM cantilever as in problem (4) the deflection set point is set to 10 nN.
A) How far is the cantilever deflected from equilibrium?
B) What is the pressure beneath the SFM tip if the contact area is 30 nm in diameter?

(6) How does the SFM scan the tip across the surface?

(7) If you are scanning an area of 80 μm by 80 μm with 512 lines and 512 points per line, what is the resolution of your image (specify in both μm and nm)?

3. Experimental Assignment

3.1 Goal

At the end of this lab, you should understand the concept and operation of SFM contact mode and able to use DPN to create nanostructures.

Specifically perform the following:

(1) Use DPN to generate patterns of thiols on gold surfaces to act as resists in gold etching
(2) Create a few nanometers tall gold structures from the DPN-generated patterns
(3) Use SFM in contact mode to obtain topography of the generated gold structures

3.2 Safety

- Wear safety glasses and gloves
- Use extreme cautious when handling chemicals and be sure you have read the MSDS
- Refer to the General rules in the SFM lab

Chemical Hazards: You will be using a solution of thiourea and ferric nitrate to etch gold films in this lab. This solution is a strong oxidizer. It is **toxic** and a **carcinogen**. Not only can it burn your skin, but it can cause a fire if it is brought into contact with combustible material. The solution should be stored away from heat, strong acids, strong bases, and organic materials. Wear goggles, gloves and lab coats when handling the thiourea solutions. Never generate or handle more than 10 mL of etching solution. If you spill the solution on your skin, you should flush the area with copious amounts of water for at least 15 minutes and remove the contaminated clothing and shoes. After that you should contact a physician. If you spill the solution on the bench you should ask the TA for assistance. The area should be evacuated immediately. You should wear a self-contained breathing apparatus, a pair of rubber boots, and heavy rubber gloves to clean. The spills should be absorbed on sand or vermiculite and be placed in a closed container for proper disposal. After the spills have been picked up, you should wash the spilled area and ventilate the area. Always handle the solutions in a well-ventilated area. The solution is highly toxic to aquatic species and must not be poured down the drain. It must be properly disposed at the designated chemical waste jar.

Warning: The AFM contains a Class 1 laser (830 nm wavelength). Although class 1 lasers are deemed safe for brief exposure, you should NOT look directly into the laser beam behind the cantilever alignment chip. The laser is infrared, meaning your blink reflex will not protect you.

3.3 Instrumental Setup

- Easy Scan 2 AFM system with contact mode AFM tip (Vista probes; CL-25) with 0.2 N/m spring constant, resonant frequency of 12 kHz, and the tip radius of ~10 nm
- 20 mL vials
- A stir bar
- A stir plate
- Plastic Petri dishes
- Tweezers

3.4 Materials

- 15 nm gold films thermally-evaporated onto silicon oxide wafers
- 16-mercaptohexadecanoic acid (MHA); $HS(CH_2)_{15}CO_2H$

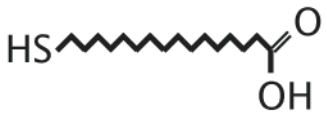

- Thiourea; NH_2CSNH_2

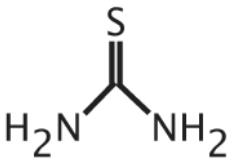

- Ferric nitrate nonahydate; $Fe(NO_3)_3*9H_2O$

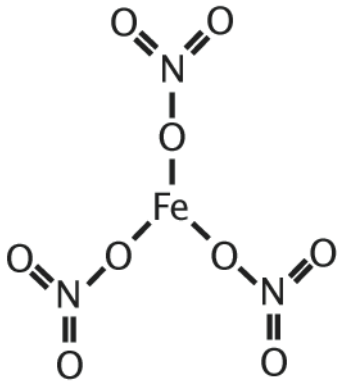

- Acetonitrile
- Ultra pure Milli Q water

3.5 Experimental Procedure

Read the instructions below carefully and follow them closely. If you are uncertain about anything, please consult your TA first.

(i) Inking tips for DPN (this step may be performed by the TA)

(1) Use a pair of tweezers to place a contact-mode AFM tip (CL-25; Vista probes; spring constant of 0.2 N/ m) in a saturated MHA solution of acetonitrile for 5 seconds

Figure 3.1. Dipping an AFM tip into the chemical ink

(2) Gently blow on the inked tip with compressed air for a few seconds to remove excess solvent.

Figure 3.2. Water Condensation Formed in a Vial at 70^{o}C

(3) Heat a vial of deionized water at 70^{o}C until condensation forms on the sides.

Figure 3.3. Tip attached inside the Vial Lid

(4) Adhere the inked-tip to the inside of the lid of the vial using double-stick tape. Seal the vial with the tip inside for 5 minutes. Seal the vial with the tip inside for 5 minutes.

(5) Reink the tip in MHA solution for 5 seconds, and redry the tip.

(6) Store the tip in a Petri dish if not using immediately.

(ii) Preparation of the experiment

(1) Scratch an alignment mark by gently scratching a "4" on a gold substrate using a razor blade or the tip of your tweezers. BE GENTLE, you only want to lightly scratch the gold, if you press to hard you will scratch into the silicon oxide layer and create lots of dust which will make the subsequent steps more difficult.

(2) System set-up: follow the start up procedure in Easy Scan 2 AFM System SOP (Standard Operational Procedure).
   a. Use a MHA-inked contact-mode cantilever (CL-25)
   b. Operating mode: static force (contact mode)
   c. Lower the stage by clicking *Advance* in the Approach panel until you see the shadow of your cantilever.
   d. Change the positioning view to *Top View* and use the translation stage to locate the cross area of the alignment mark
   e. Make sure the *auto start imaging* is unchecked. It's under the *Positioning windows* → *Approach Panel* → *Approach options*

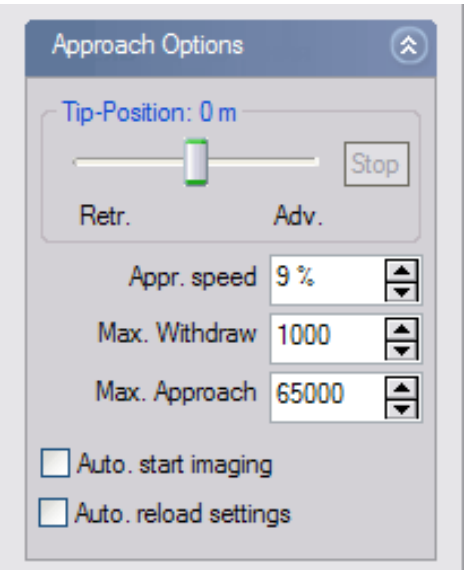

Figure 3.4. Approach Options Panel

(3) If your tip is in contact, withdraw the tip from the surface by clicking the "withdraw" bottom once

(4) Mark the position of the alignment and the cantilever on the transparency by placing the transparency over the computer monitor

(iii) Dip-Pen Nanolithography

The goal of this section is to utilize a lithography program to write with AFM a series of dots of different sizes by varying the dwell time, and to compare your data against a theoretical prediction (see background information). The lithography program is written in the script function of the easyScan 2 software.

(1) Open the lithography program by clicking
   a. *Script* on the tool bar
   b. *Script Editor*
   c. *Load* the file from the desktop, DPN.vbs
   d. The Script will write four 5 × 5 grids of dots, each with a different dwell time, as shown in Fig. 3.5. The dwell times are stored in an array called, appropriately, diptimes. Change these four diptimes to four different times of your choosing, between 1 and 20 seconds.

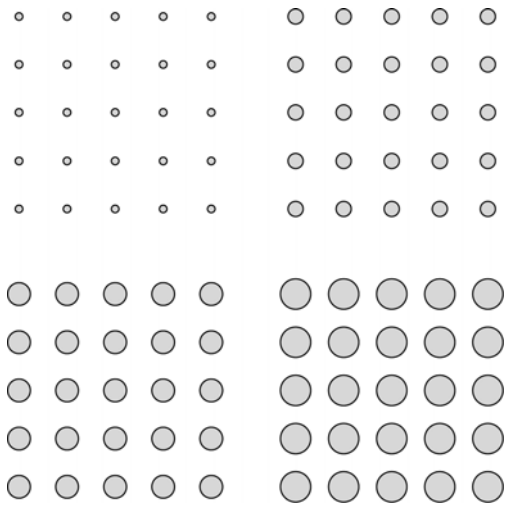

Figure 3.5. DPN Patterns

(2) Running DPN
   a. Make sure the tip is within approaching distance to the surface
   b. Click *run* on the Script Editor
   c. Wait until the script finishes running. A dialog box will pop up that says "Done writing!"

(3) Removing patterned substrates
   a. Retract the cantilever by first clicking on the *withdraw* (in the *Approach panel*). When the tip stops moving, click and hold the *Retract* bottom until there is enough clearance between the tip and the substrate.
   b. Remove the AFM scan head
   c. Remove the gold substrate

(iv) Gold etching

In this section, we will use the DPN-generated patterns from the previous section as resists in the gold etching to create gold structures. The unpatterned gold regions will be etched first and faster than the MHA-patterned gold areas.

(1) Make a 20 mM ferric nitrate and 30 mM thiourea in DI water and mix the solution well

(2) Pour the solution into a Petri dish with a stir bar on a stir plate

(3) Adjust the stir plate to about 200 rpm for gentle mixing

(4) Place the patterned-gold substrate in the solution for 1 minute

(5) Rinse the substrate with DI water for 5 seconds

(6) Blow the substrate with nitrogen

(7) Repeat steps (4) to (6)

(v) AFM imaging of the generated nanostructures

Finally, we use AFM contact mode to image the generated gold structures, determine the diameters of the structures, and perform the cross-section analysis of the structures from the topography images.

(1) Place the substrate on the AFM translation stage

(2) Place the AFM scan head on the stage

(3) Follow the *Easy Scan 2 AFM System SOP Startup Procedure* to approach the tip

(4) Withdraw the tip from the surface by clicking the “withdraw” bottom once

(5) Use the marked transparency from before to locate your patterned region by adjusting the translation stage

(6) Approach the tip and scan a 110 micron by 110 micron area following the instruction step 9 to 11 on the *Easy Scan 2 AFM System SOP Startup Procedure*

(7) Save the image by clicking *photo* and wait until the scan has reached the end

(8) Zoom-in to your DPN-patterned structures by clicking *zoom* in the imaging bar and use mouse cursor to define the interested area. Then, click *zoom* on the left side *Tool results panel*.
(9) Scan the selected area

(10)Save the image

(11) Process image and perform cross-section analysis using the options under the *Tools*. Keep in mind that you want to obtain the following information,

- Cross-section profile of your structures
- Dimensions of your structures (report average diameter and height with standard deviation)
- Compare diameters with those predicted from eq. (4) and plot of dot sizes *vs.* dwell time of DPN

(vi) AFM shut down

(1) Follow the *Easy Scan 2 AFM System SOP Shutdown Procedure*

(2) Dispose all of the chemical waste properly

3.6 Easy Scan 2 AFM system components and tools

1. Easy Scan 2 Controller
2. USB Cable
3. Main Power Cable
4. Easy Scan 2 Scan Head with Video Camera
5. Scan Head Case
6. Scan Head Cable
7. Video Camera Cable
8. AFM Sample Stage
9. Ground Cable
10. Sample Holder
11. Screwdriver
12. Pointed Tweezers for Cantilever Installation and Sample handling
13. Cantilever Insertion Tool and Drop Stop

The Scan head

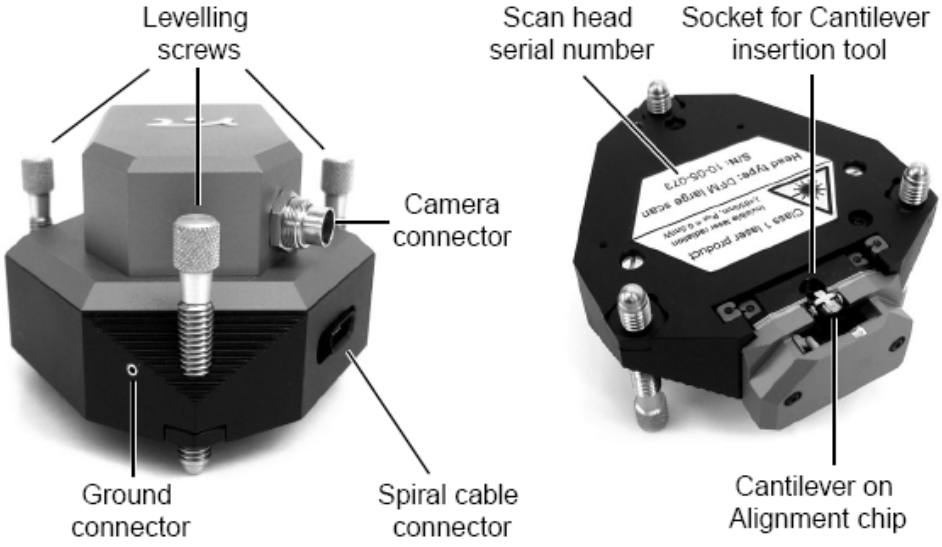

The Controller

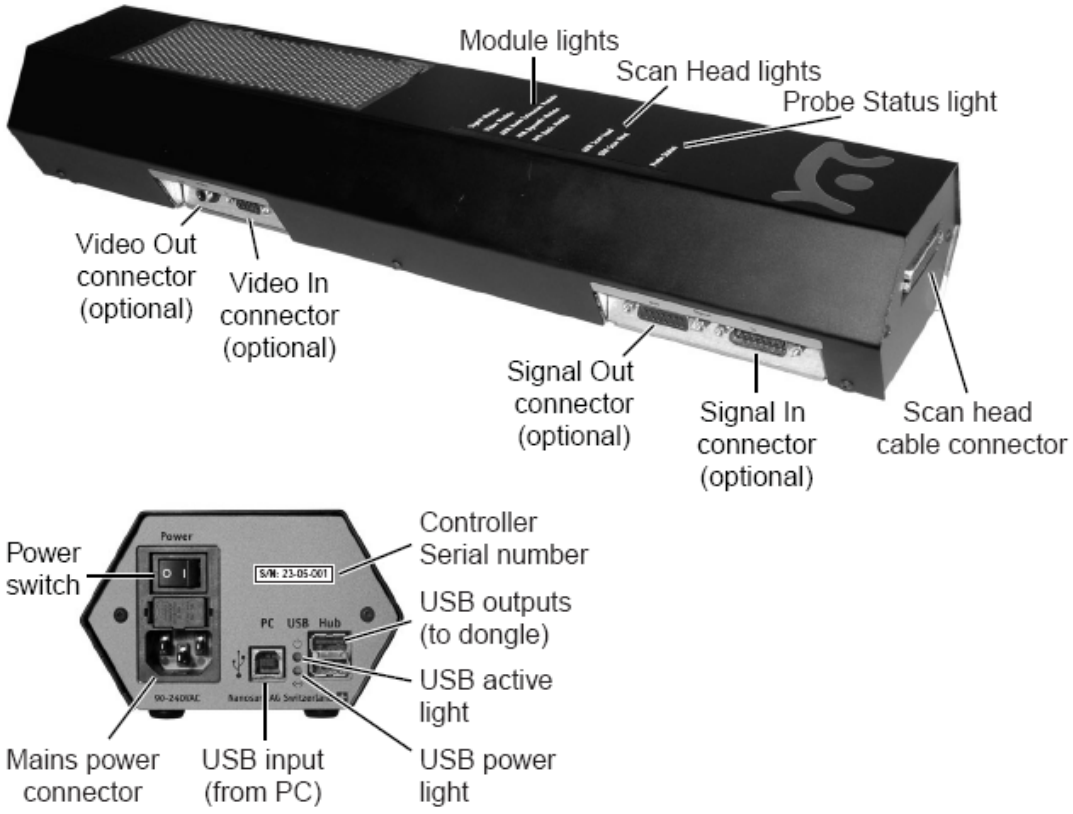

3.7 Easy Scan 2 AFM System Standard Operational Procedure

3.7.1 Startup Procedure

1 Take the *Scan Head* out from the *Scan Head Case* and place it on the *AFM Sample Stage*

Note: Whenever the Scan Head is handled, take the extreme care!

2 **Connect Cables.**

a. Connect *Scan Head Cable* using the screwdriver at the spiral cable connector of the *Scan Head* and at the scan head cable connector on the *Controller*.
b. Connect *Video Camera Cable* at the camera connector of the *Scan Head* and at the video in connector on the *Controller*
c. Check if *Main Power Cable* and *USB Cable* are connected appropriately.

Easy Scan 2AFM System with break-out box

3 **Mount the Cantilever.**

a. Place the *Scan Head* up-side-down on a flat space on the AFM work station.
b. Slide in the *Drop Stop* over the detection system as shown below. The *Drop Stop* prevents from dropping the cantilever accidentally into the scan head.

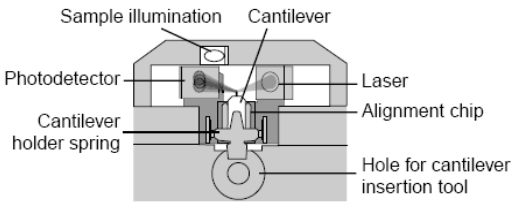

Schematic of signal detection system

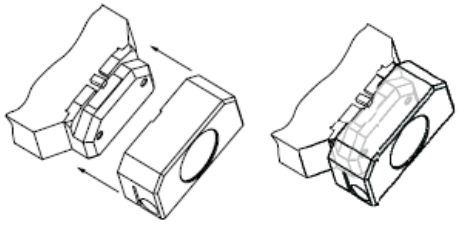

Sliding the *Drop Stop*

c. Confirm a blank cantilever (for storage) is placed at the cantilever holder.
d. Place the *Cantilever Insertion Tool* into the hole behind the alignment chip. This opens the cantilever holder spring. (See below)

Note: The Cantilever Holder Spring is very delicate. Do not bend.

e. Use the tweezers to remove the blank cantilever from the holder.
   i. Hold lightly the cantilever on the sides with the tweezers.
   ii. Slide it out onto the Drop Stop and rest it.
   iii. Again hold the cantilever with the tweezers to transfer into a cantilever case.

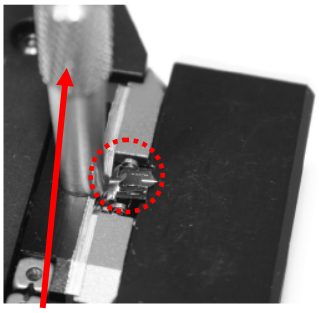

The *Cantilever Insertion Tool* opens the cantilever holder spring.

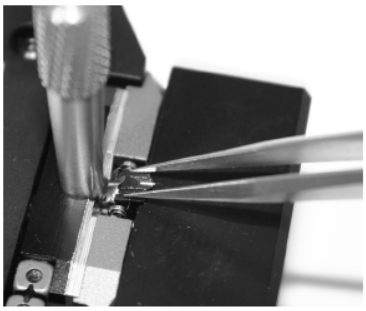

Hold the sides of the cantilever lightly and slide it out onto the *Drop Stop*

f. Place a new cantilever into the Scan Head.
   i. Take an appropriate cantilever out of its box and place it on the *Drop Stop*. *Note: The cantilever is extremely fragile. Never touch the cantilever, especially at the tip end.*
   ii. Using the tweezers (holding the sides of the cantilever lightly), slide the cantilever into the alignment chip.
   iii. By tapping the cantilever lightly with the tweezers, move the cantilever so that it sits correctly on the alignment chip. (See below)
   iv. Gently pull the cantilever insertion tool out of the hole. Closes the spring.
   v. Slide the *Drop Stop* out. Be cautious no to touch the cantilever.

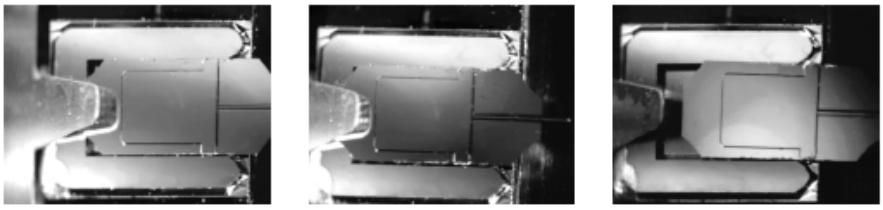

Cantilever Alignment: left: Correct, the mirrored environment light shows a pattern that is continuous on the cantilever and the alignment chip; centre, right: Incorrect, the mirrored environment light shows a different pattern on the cantilever than on the alignment chip.

g. Place the *Scan Head* back on the AFM stage. *Note: Take extra care not to touch the cantilever.*

4 Turn the power switch (on the controller) on. The LED lights on top of the *Controller* light up and blink.

5 Start the *Easy Scan 2 Software* on the control computer. The interface window opens. (See below)

6 If all components and modules are detected correctly, the LEF lights will stop blinking and light up. Make sure the AFM Scan Head status light and the Probe status light are on.

*Note: If the Probe Status light **blinks red**, it does not detect the cantilever in place. In that case, turn off the power switch, and readjust the cantilever following the step in 3.*

7 Set Operating Mode

a. Click the Operating Mode icon on the Navigator Bar. The Operating Mode Panel opens.
b. Select appropriate cantilever type (NCLR for non-contact, CONR for contact mode, etc).
c. Select operating mode (static force, dynamic force, etc.)

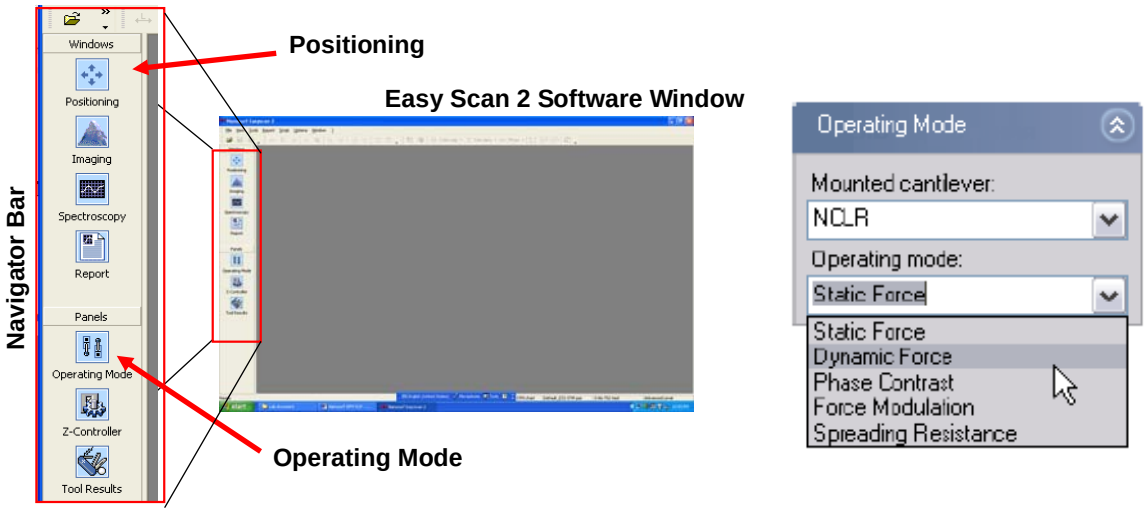

8 Position Cantilever

a. Open the Positioning Window by clicking the Positioning icon on the Navigator Bar. The video monitor shows the cantilever tip.
b. Place a sample on the *Sample holder* under the AFM *Scanner Head*. Make sure the Head is high enough (~ 0.5 cm gap) so that the cantilever tip won't crash into the sample surface.
c. Level the *Scan Head* relative to the sample surface.
   i. Measure the tilt with the *Leveler* on the *Sample Stage*.
   ii. Place the *Leveler* on top of the *Scan Head.* By adjusting the height of three leveling screws, achieve the same tilt as that of the *Sample Stage*. *Note: When lowing the Scan Head, be cautious about the relative positioning of the cantilever.*
   iii. Without changing the tilt, lower the *Scan Head* so that the cantilever is within 1 mm from the sample surface. The distance can be estimated by the shadow of the cantilever tip. (see below)
   iv. Check again if the *Scan Head* is still level with the *Sample Stage*.

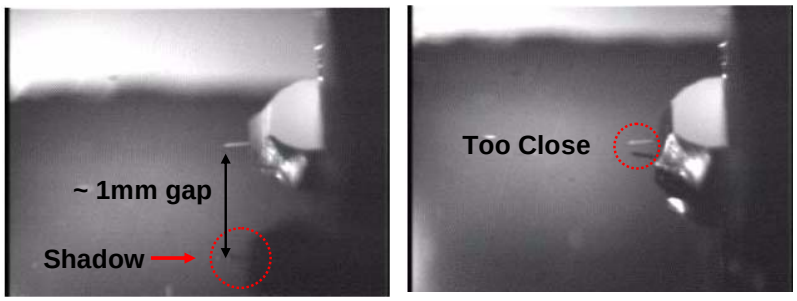

9 Automatic Approach of Cantilever

a. Once the cantilever is approximately 1mm from shadow, automatic approach is used to bring the cantilever into contact.
   i. Open the Z-Controller Panel by clicking the icon in the Navigator bar.
   ii. Set the set point to be 5 nA(contact)/50%(non-contact). Use the default values for the P-Gain, I-Gain, and D-Gain.
   iii. Click the Approach icon in Approach panel on the left side of the Positioning window.
   iv. The software lowers the SFM tip till it comes in contact with the sample surface.

b. Once the approach is complete a message 'Approach done' appears and the imaging panel automatically appears in the active window.

c. Look at the Probe Status Light on the Controller. If it is NOT green, it is not operating correctly. Immediately come out of contact by clicking Withdraw in the Approach Panel. Consult to a lab assistant.

d. The set point can be adjusted while the tip is in contact. In contact mode, increase of the value increases the normal force. In non-contact mode, increase of the value (%) decreases degree of tip-sample interaction.

Click off the Auto start imaging

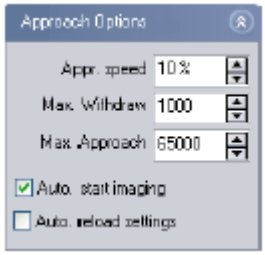

Automatic Approach

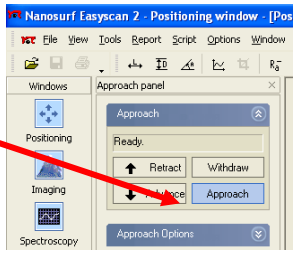

10 Adjust the measurement plane

For higher quality imaging and data collection, the sample surface is adjusted to be in parallel to the XY-plane of the SFM Scanner Head.

a. Look at the slope of the sample surface on the Topography line graph, located below the Topography image.

b. If the slope of the topography in the imaging window is negative, the X-slope will need to be increased. Start by increasing the slope by 0.1°.

c. Increase the slope till the line is relatively parallel (no general slope) and the mean fit scale (y-scale) is small.

d. If the slope is positive decrease the slope by -0.1.
e. Once the slope is adjusted, the Y-direction slope is also adjusted. To do so, change the scan direction by typing in 90 ° in Rotation in Imaging Area window in the Imaging panel. Adjust the Y-slope in the same manner as X-slope.

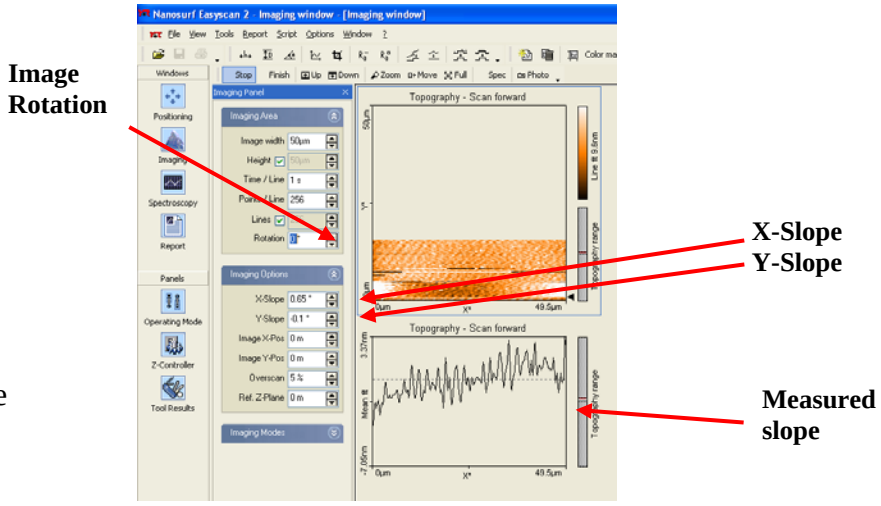

11 Adjust the Controller Settings

Click on the Z-controller icon found on the Navigating bar (see below) and adjust the controller settings to keep tip-sample interactions constant. This is done by adjusting the feedback parameters, P, I, and D gain of the Z-controller.

i. Leave the P-gain at default value. Increase I-gain by 10% of the default value. Check in the topographic image if the contrast improves. If it shows a periodic stripe (shown in figure below), the I-gain is generating noise. Reduce it till the noise disappears.

ii. Increase the P-gain by 10 % of that default value. Stop when increasing the P-gain does not improve.

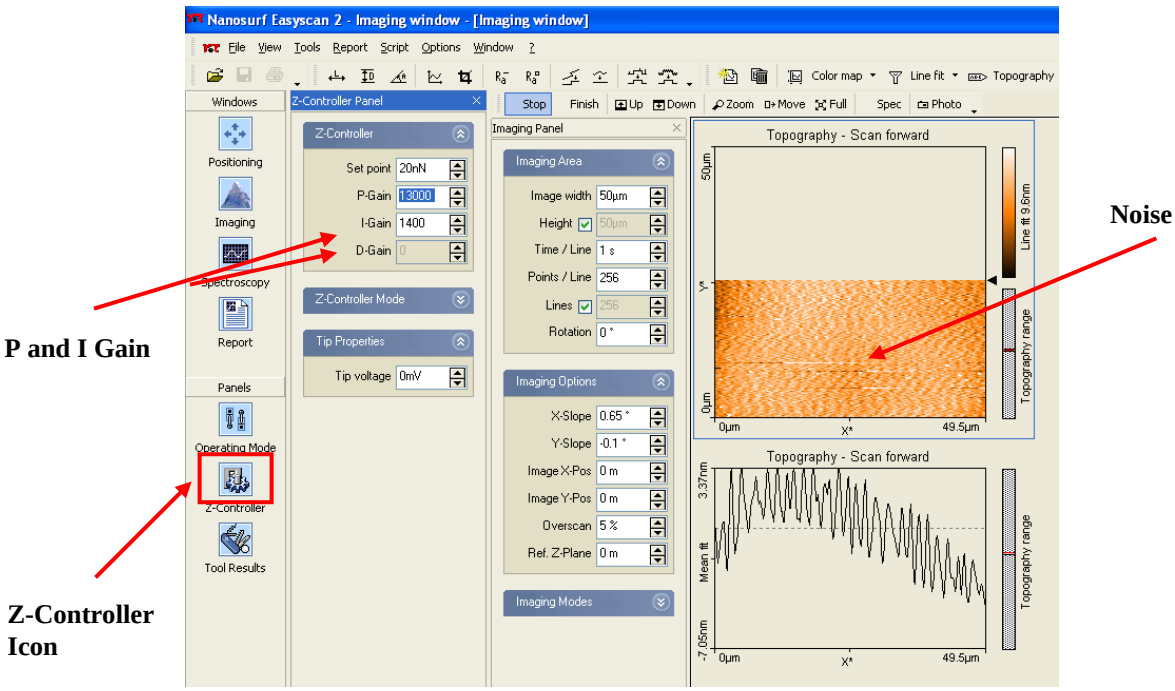

12 Ready for measurements. Proceed with instrument operational instructions specific to the lab unit.

3.7.2 Shutdown Procedure

(1) Retract the cantilever as far as possible by auto-positioning.

(2) Close the Easy Scan 2 soft ware window.

(3) Remove the cantilever (follow the instruction given in the Startup procedure step (3)), and place the blank cantilever for the storage.

(4) Turn of the power switch on the *Controller*.

(5) Disconnect the *Scan Head Cable* and the *Video Camera Cable.*

(6) Place the *Scan Head* in the *Scan Head Case*.

4. Scanning Probe Microscopy and Dip-Pen Nanolithography

Table of Contents:

4.1 Historic Perspectives

In 1982, Gerd Binnig and Heinrich Rohrer of IBM in Rüschlikon (Switzerland) invented scanning tunneling microscopy (STM). Although STM is not the focus of this lab, it is the ancestor of all the variations of scanning probe microscopy (SPM) that followed: although the mechanism of image contrast may vary, the idea of building up an image by scanning a very sharp probe across a surface has endured. As the name suggests, STM scans a sharp tip across a surface while recording the quantum mechanical tunneling current to generate the image. STM is capable of making extremely high resolution (atomic resolution) images of surfaces and has been extremely useful in many branches of science and engineering. For their invention, Binnig and Rohrer were awarded the Nobel Prize in Physics in 1986[1].

Although STM is able to obtain images with better than atomic resolution (some scientists even use it to image the electron orbitals around atoms in molecules), one limitation is that STM can only be used to image conductive surfaces. In an effort to overcome this restriction, Gerd Binnig, Christoph Gerber, and Calvin Quate at IBM and Stanford Univeristy developed scanning force microscopy (SFM), also known as atomic force microscopy (AFM), in 1986. SFM is a surface imaging technique that images both conductive and nonconductive surfaces by literally "feeling the surface", i.e. measuring the force between a surface and an ultra sharp tip (typically 10 nm in radius). Fig. 4.1 shows a SFM image of a lipid bilayer.

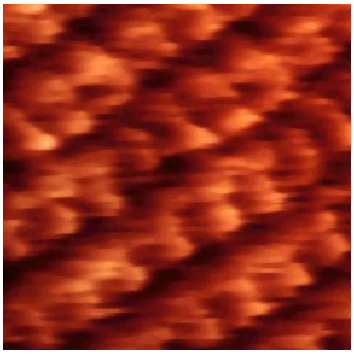

Figure 4.1. SFM Image of Lipid Bilayer (scan size: 10 nm)

4.2 Scanning Force Microscopy (SFM)

4.2.1. Contact Mode

As noted above, an SFM acquires an image by scanning a sharp probe across a surface. This can be done by contacting the surface (contact mode) or by a variety of other scanning modes (intermittent contact and others are covered in more detail in separate lab modules). Contact mode imaging is perhaps the most straightforward SFM mode, and is the technique you will use in this lab. In contact mode, a sharp tip attached to the end of a long flexible cantilever is brought into contact with a surface (Fig. 4.2). The harder the tip presses into the surface, the more the cantilever bends. The tip moves in regardless of the sample in the x-, y- and z-directions using a piezoelectric actuator. The actuator contains a piezoelectric crystal that expands and contracts as an external voltage is applied across its crystal faces (voltages of a few hundred volts may be applied to move the sample tens of microns).

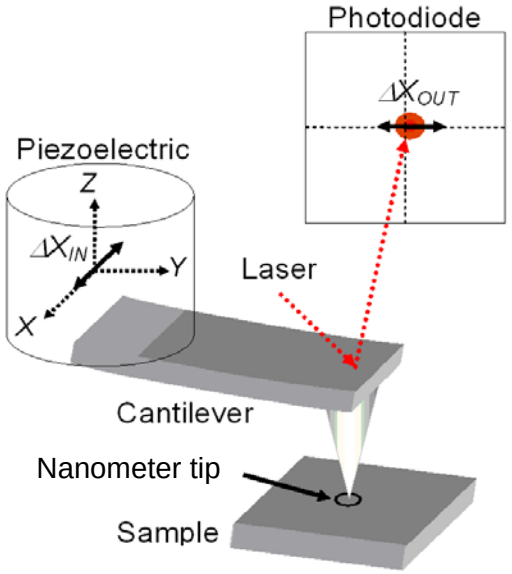

Figure 4.2. Schematics of scanning force microscopy (also known as atomic force microscopy, AFM) operated in contact mode

The deflection of the cantilever is most commonly monitored by a laser-beam deflection scheme. A laser is reflected off the back of the cantilever tip onto a segmented photodiode (top and bottom segments for vertical deflection) or a four-quadrant photodiode (for both vertical and lateral detection of the cantilever deflection). One way to acquire an image is to use the piezo to scan the tip in the x-y plane and record the deflection of the tip as a function of position. As the tip moves over a bump, the deflection of the cantilever increases, which increases the tip-sample force. If the bump is too large the tip may scratch the surface, or the lever may break. This scanning mode is called "force mode." For a topographical imaging mode, a feedback loop (Fig. 4.3) is implemented to keep the cantilever deflection constant by changing the tip height (z) while scanning in x and y. In this way, a nearly constant force is maintained between the tip and sample, and the topographical image is created by recording the voltage applied to the z-piezo as a function of the x and y position. As the tip is scanned, lateral force are

achieved on the lever on the lever due to friction causing the lever to torque. The motion can be with 4-quadrant segmented photodiodes.

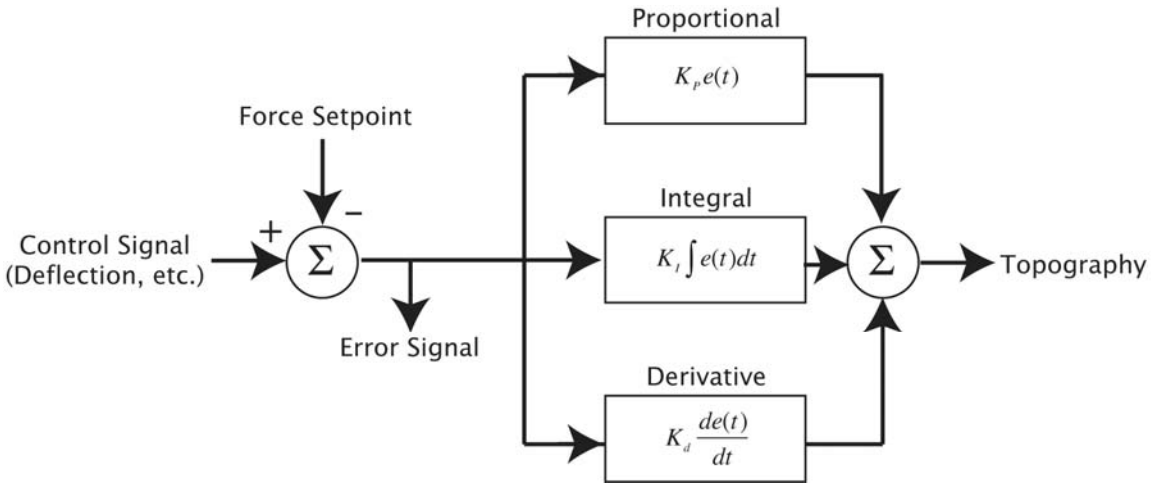

Figure 4.3. Block Diagram of an SFM Feedback Loop. K_c is proportional gain; K_i is the integral gain; K_d is the derivative gain; *e* is the error.

4.2.2. AC Mode Imaging

The SFM can also image a surface without continuously touching the surface. Such imaging modes—which can be classified as non-contact or intermittent-contact (Tapping Mode™ imaging by certain manufacturers)—are widely used, and are particularly suited to imaging soft surfaces such as polymers or biological samples. AC mode imaging gets its name from the fact that the tip is raised slightly above the surface and the cantilever is driven to vibrate near its resonant frequency (by yet another piezoelectric crystal). The amplitude, phase, and/or frequency of the cantilever are then monitored as the tip is scanned across the surface. The forces between the tip and the sample change the properties of the cantilever resonance, which can be used to generate a feedback signal and thus create an image. AC Mode imaging will be covered further in other lab modules so we will not discuss it further here.

4.2.3. Applied Force: Cantilever Deflection and Hooke's Law

The dimension, shape, and material of the cantilever tip can affect its resolution and sensitivity to different forces. In addition, tips with different coatings can be used in different applications of SPM. A conductive coating is required for electrostatic force microscopy (EFM), conductive atomic force microscopy (c-AFM), and etc. The most common commercial SFM tip is microfabricated from silicon or silicon nitride using conventional photolithography and semiconductor processing techniques, processes similar in many ways to those used to generate silicon computer chips. Hundreds to thousands of cantilever tips can be fabricated on a single wafer at once. The tip (with a tip radius of ~10 nm) is located at the free end of the cantilever that is typically 100 to 200 micron long (refer to Fig. 4.2). Shorter or thicker cantilevers have higher spring

constants and are more stiff. The cantilever acts like a spring and can be described by Hooke's law:

$$F = -k_N z \qquad \text{Eq. (1)}$$

where F is the force, k_N is the normal spring constant, and z is the cantilever normal deflection. Typical spring constants available on commercially manufactured SFM cantilevers range from 0.01 N/m to 75 N/m. This enables forces as small as 10^{-9} N to be measured in liquids or an ultra-dry environment with the SFM. Analogous, lateral forces acting on the lever can be expressed as the product between a lateral spring constant k_x and a lateral deflection x.

For a bar-shaped cantilever with length L, width W and thickness t, and an integrated tip of length r, the normal and lateral spring constants, k_L and k_x, are related to the material stiffnesses, as

$$k_N = \frac{EWt^3}{4L^3} \quad \text{and} \quad k_x = \frac{GWt^3}{3Lr^2}. \qquad \text{Eq. (2)}$$

where E and G respresent the normal Young's modulus and the shear modulus, respectively.

The thickness of the cantilever, typically poorly defined by the manufacturers, can be determined from the first resonance frequency of the "free" cantilever using the following empirical equation:[2]

$$t = \frac{2\pi f_1}{(1.875104)^2} L^2 \sqrt{\frac{12\rho}{E}}. \qquad \text{Eq. (3)}$$

The Young's modulus and density of silicon cantilevers are around $E = 1.69\times10^{11}$ N/m^2 and $\rho=2.33\times10^3$ kg/m^3.[2]

4.2.4. SFM Tips

The lateral imaging resolution of SFM is intrinsically limited by the sharpness of the cantilever. Most commercial cantilevers have a tip with a 10 nm radius of curvature, although more exotic probes (such as those tipped with carbon nanotubes) are also available. Keep in mind that the resolution is also limited by the scanning parameters. For instance, if you take a 10×10 micron scan with a resolution of only 256×256 points, the size of each image pixel represents a lateral distance of 1×10^{-6} m / 256 = 39 nm.

As SFM images are generated by scanning a physical tip across the surface, this can lead to several image artifacts. One type of imaging artifact results from tip convolution. When the tip size is larger than the imaging feature size, the resulting image will be dominated by the shape of the tip. In this case, the observed features from the topography images will have very similar shapes despite the fact that the real features might be different (think of it as taking a picture of the tip with each of the surface features). Fig 4.4 shows two different sized tips scanned over a substrate with both small and large features. Also, damaged tips can often lead to distorted images. A tip with a piece of dirt stuck to it, or one that has been broken near the end can yield, for instance,

doubled features as illustrated in Fig 4.5. One way to check for tip-induced artifacts is to rotate the scan angle by 90 degrees. If the shapes you are seeing do not rotate, the tip might be damaged!

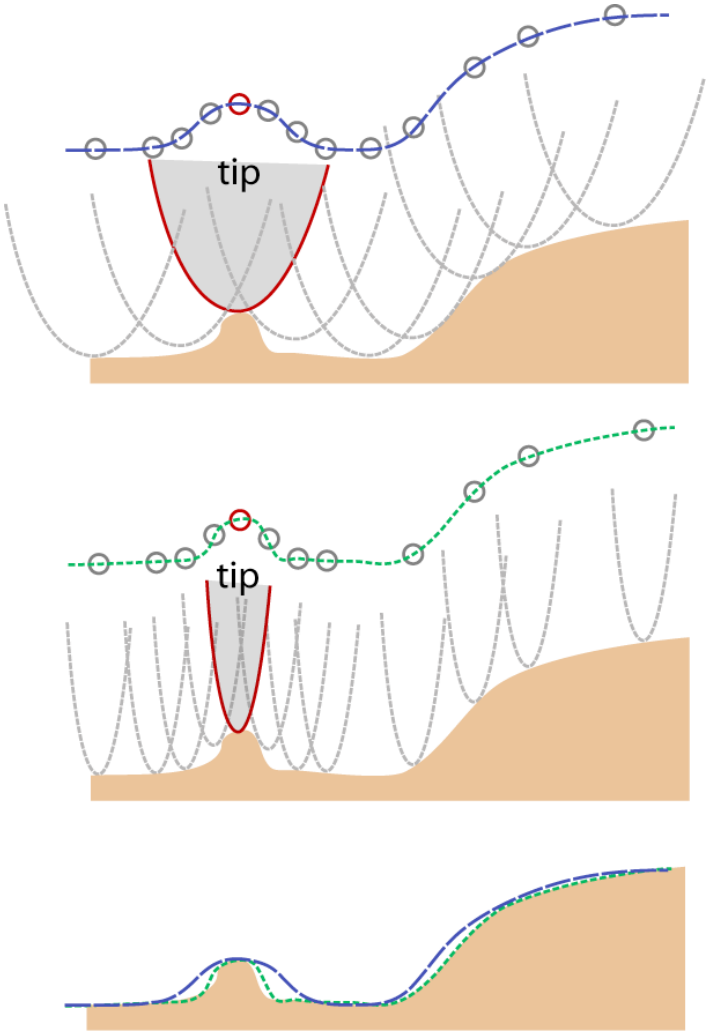

Figure 4.4. Limitations of Tip Size. (Top) The large tip is much bigger than the small substrate feature. Each circle on the figure represents the position of the z-piezo recorded by the SFM as it moves across the sample. (Center) A small tip tracks both surface features better. (Bottom) The two line traces (large tip is dashed blue; small tip dotted green) from each tip are shown with the actual surface topography.

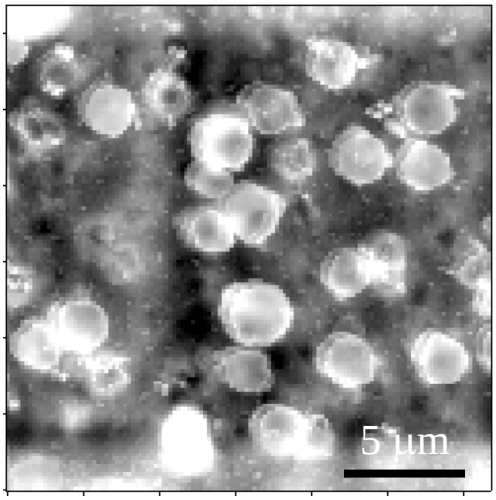

Figure 4.5 A minor case of doubled features caused by a damage tip. The image shows salt crystals embedded in polymer matrix.

In addition, image artifacts can also result when the feedback system is not optimized. The feedback loop consists of a set point value and feedback gains (proportional, integral, and derivative of the error signal). When the feedback gains are too high, the controller will overcompensate and amplify random noise in the system. Sometimes the tip oscillates and creates periodic noise in the images (showing periodic stripes in the image). On the other hand, if the gains are too low, the tip cannot accurately track the features due to the slow response of the feedback loop. Fig. 4.6A-C show some SFM images taken with the gains set just right, too low, and too high.

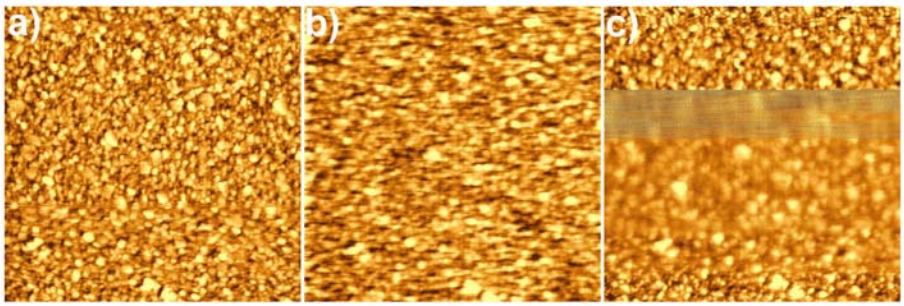

Figure 4.6 Topography of Gold Surface (Scan Size: 1µm*1µm). a) with optimal feedback loop gains, b) with gains set too low, and c) with gains set too high

In contact mode, the set point determines the amount of force applied on the cantilever tip, which also affects the cantilever deflection. You can specify the set point value in nN in the NanoSurf easyScan 2 software. (Note: this value depends on the accuracy of the spring constant assigned to the tip, via Eq 1). In non-contact mode, the set point is specified in a percentage of the amplitude at resonance. Tuning of the NanoSurf cantilevers should be performed far from the surface, i.e. when there are no short- or long-range forces acting on the tip. The SFM controller will bring the tip close to the surface until the vibration amplitude becomes the specified value.

4.3 Dip-Pen Nanolithography (DPN)

In addition to imaging with the SFM, there have been numerous methods developed to use STM and SFM techniques as lithographic tools. STM is capable of actually moving individual atoms, and many interesting examples of STM images can be found online[3].

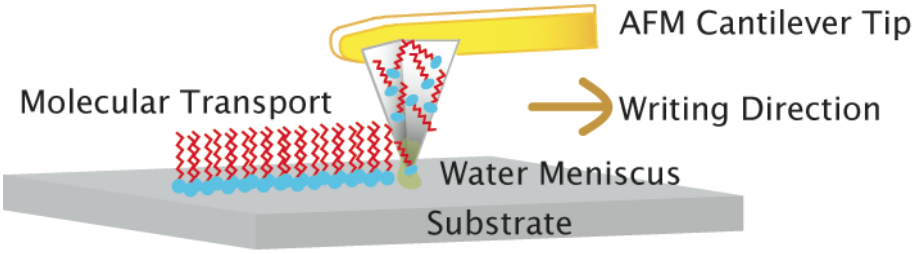

Figure 4.7. Schematics of Dip-Pen Nanolithography

Dip-pen nanolithography (DPN) is a scanning probe-based lithography tool that uses an SFM tip to "write" chemicals onto surfaces. It is a direct-write additive process. It is analogous to a conventional fountain pen, with the SFM tip as the pen and the substrate being the paper (Fig. 4.7). Although there are now more sophisticated systems for delivering chemical "inks" to the tip using microfluidics, etc. (such as built-in ink reservoir or ink wells), the basic DPN approach is still the easiest to implement. To coat the tip with the chemical ink it is simply dipped (using tweezers and a steady hand) into an ink solution. Alkanethiols, DNA, proteins, polymers, etc., have all been used as inks in DPN[4,5]. After the tip is inked, excess solvent is blown off the tip and it is loaded into the SFM. When the tip contacts the substrate the chemical ink flows to the surface and is deposited onto the surface of the substrate. For many inks, such as depositing alkanethiols on gold, the tip can be approximated as a small source delivering a constant flux of molecules to the surface per unit time. Thus, the area of the features increases linearly with the dwell time (the time of contact between the tip and the surface). The diameter of a DPN patterned feature scales approximately to the square root of the contact time:

$$d \approx t^{1/2} \qquad \text{Eq. (4)}$$

where d is the diameter of the patterned dots and t is the dwell time.

DPN is a direct-write technique that does not require a design mask, and it can generate various complex structures on demand using any atomic force microscope. However, like other scanning-probe based lithography tools, DPN is a *serial* process (one feature is created at a time). Nevertheless, it is inexpensive and suitable for rapid prototyping applications. Attempts to improve the serial natural of the DPN technique have resulted in commercially available multiple arrays of DPN probes for mass DPN-patterning[6].

Writing patterns of a thiol (16-mercaptohexadecanoic acid, "MHA") on a gold surface is the most common ink-surface chemistry in DPN. Thiols chemically bond to gold

surfaces through their sulfur atom to form a gold-sulfur bond. The chemical reaction is generally accepted to be[7]:

$$R-SH+Au \rightarrow R-S-Au+\frac{1}{2}H_2$$

Long-chain alkanethiols tend to form well-ordered monolayers on gold surfaces, known as self-assembled monolayers, or SAMs. Typically, DPN-generated patterns are characterized with LFM, allowing images of patterned SAMs to be made based on friction contrast (i.e. the lateral defleciton of the lever if moved over the surface), e.g. Fig. 4.8 (though with care it is possible to image the SAM pattern based on topography alone; it will be very challenging to image height differences of less than a few nanometers).

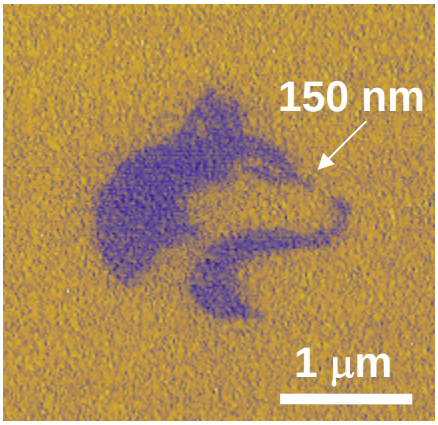

Figure 4.8. Lateral Force Image of DPN-Patterned 16-Mercaptohexadecanoic Acid on Gold

Alternatively, the features can be more easily scanned in the topography mode by using the DPN patterns as etch resists to generate topography on the gold layer after gold etching. A common gold etching solution is a solution of thiourea and ferric nitrate[8]. The amount of etched gold is proportional to the etching time. The bare, unmodified gold (unwritten) regions will etch faster than the regions protected by the alkanethiol SAM, as the SAM prevents the etchant molecules from reaching the gold surface.

References

1 http://nobelprize.org/nobel_prizes/physics/laureates/1986/index.html
2 *Nanoscience - Friction and Rheology on the Nanometer Scale*, E. Meyer, R. M. Overney et al., World Scientific, NJ (1998).
3 http://www.almaden.ibm.com/vis/stm/gallery.html
4 D. S. Ginger, H. Zhang, and C. A. Mirkin, Angew. Chem.-Int. Edit. **43**, 30 (2004).
5 K. Salaita, Y. Wang, and C. A. Mirkin, Nature Nanotechnology, **2**, 145 (2007).
6 K. Salaita, Y. Wang, J. Fragala, R. A. Vega, C. Liu and C. A. Mirkin, Angew. Chem.-Int. Edit. **118**, 7378 (2006).
7 J. B. Schlenoff, M. Li, and H. Ly, J. Am. Chem. Soc. **117**, 12528 (1995).
8 M. Geissler, H. Wolf, R. Stutz, E Delamarche, U.-W. Grummt, B. Michel, and A. Bietsch, Langmuir **19**, 6301 (2003).

LAB UNIT 2: Electrostatic Force Microscopy (EFM)

Specific Assignment: Electrical Properties of Conjugated Polymer Films

Objective

This lab unit introduces Electrostatic Force Microscopy to characterize the electrical properties of a blended conjugated polymer film by studying the changes in tip oscillation due to electrostatic force gradients between the tip and the sample.

Outcome

Learn the basics of electrostatic force microscopy, applying concepts including Coulomb force, capacitance, force gradients and damped driven simple harmonic motion.

Synopsis

We learn the basics of electrostatic force microscopy by characterizing a thin film composed of a blend of electron-donating and electron-accepting organic semiconductors.

Materials

Thin film of 4:1 PCBM:MDMO-PPV on gold
Gold film
Indium tin oxide-coated glass

Tweezers
Alligator clip mounted on a glass slide
Alligator clip-terminated wire (both ends)
Voltmeter
Pair of small magnets

Easy Scan 2 AFM system
Pt-coated non-contact mode EFM tip with 1–5 N/m spring constant (probe model: ANSCM-PT from AppNano)

Technique

Intermittent-contact mode AFM imaging, electrostatic force microscopy (EFM)

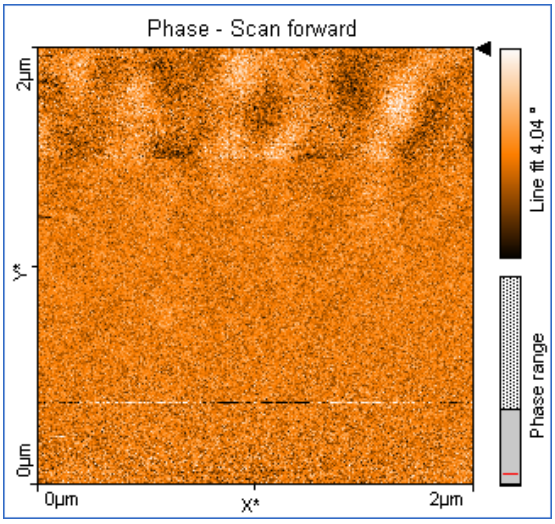

Table of Contents

1. Assignment

The assignment is to learn about the basic concepts of electrostatic force microscopy, apply them to measure surface potentials and to characterize a phase-separated blend of conjugated polymers as might be done in studying organic solar cells.

1. Familiarize yourself with the background information provided in Section 4.
2. Test your background knowledge with the provided Quiz in Section 2.
3. Prepare a grounded sample of a conductive polymer blend, evaporated Au and ITO for EFM as instructed in Section 3.
4. Perform topographical, electrostatic measurements and study the phase shift as a function of applied bias as instructed in Section 3.
5. Fit a function to collected data to determine the work function difference between indium tin oxide (ITO) and Au.
6. Finally, provide a written report discussing the following results:
   (i) What is the Q factor of the tip you used? Include a graph of the frequency sweep and corresponding phase shift.
   (ii) Using the phase shift versus voltage plots for ITO and Au, fit the data to the following function (just like PreLab Question 2):

$$f(x) = -\arcsin(A(x - V_0)^2)$$

   What value of V_0 do you get for each metal? Calculate the difference in work function between ITO and Au.
   (iii) Include the topography image and the EFM images of the surface: arrange them by increasing distance from the surface.
   (iv) What is the maximum variation in height (look at your topography scan)? How does this value compare to the changes in the phase contrast at different heights?
   (v) What causes the contrast in the EFM scans (ie, what physical property are you measuring?) How does the contrast change as you increase the tip-surface distance?
   (vi) How does the EFM image compare to the topographical image? What might this say about the polymers?
   (vii) What are the limitations of this method of EFM? How might you improve the experiment?

2. Quiz – Preparation for the Experiment

Theoretical Questions

(1) Derive the expression for the amplitude and resonance frequency of a damped, driven simple harmonic oscillator with damping constant b and natural frequency ω_0. (See Section 4.) The following steps will guide you:

a. Give the differential equation describing the motion of a damped, driven simple harmonic oscillator. What do each of the variables represent?

b. In the text, we give the form of the solution for $z(t)$. Plug this into (a). Group the terms into a $\cos \omega t$ and a $\sin \omega t$ term. For this equation to be true at all t, both terms must be 0, i.e. the prefactors of these two terms must go to zero independently.

c. Using the prefactor for the $\sin \omega t$, solve for the phase shift, δ.

d. Using the prefactor for $\cos \omega t$, solve for A, the amplitude of oscillation as a function of frequency. (Hint: To get the expression into the form given in the text, remember that if $\tan x = a/b$, then $\sin x = a/\sqrt{(a^2+b^2)}$.)

e. For what driving frequency ω is the amplitude of oscillation the greatest? (Hint: Find ω for which A has a local maximum.) This is the resonance frequency ω_R.

f. Assume that the damping factor is very small, so $\omega_R \approx \omega_0$. What is the phase shift between the driving force and the oscillator response at this frequency? (Your answer should be an actual number.)

(2) Write down the functional forms for the distance dependence of van der Waals (vdW) and Coulomb forces. Do these forms explain why electrostatic forces can still affect the tip motion at ranges where vdW forces cannot? Explain.

(3) Consider a simple parallel plate capacitor consisting of two circular plates 200 nm in diameter, spaced 50 nm apart.

a. What is the capacitance of this structure?

b. If this capacitor is charged to 5 V, what is the charge on each plate?

c. How much energy is stored in the capacitor?

d. What is the force acting between the capacitor plates when they are charged to 5 V?

(4) Write a description in words explaining what is meant by the quality factor, or ”Q” of an oscillator. Write down at least three different formulas for determining the Q of an oscillator.

(5) In an ideal instrument the minimum detectable force is limited by the thermal noise in the cantilever motion. In this case the minimum detectable force gradient is $F' = \sqrt{\frac{4k_B TBk}{Q\omega_0 A^2}}$ (where k_B is Boltzmann’s constant, T is the absolute temperature

(Kelvin), B is the measurement band, k is the spring constant of the cantilever, ω_0 is the natural frequency of the spring, Q is the quality factor of the resonance and A is the amplitude of oscillation). What is the minimum theoretically detectable F' for a typical cantilever operating at room temperature at B=1000 Hz? (Use k= 1 N/m, ω_0=30 kHz, A=1 nm, Q=100). At what distance is the force gradient between two point charges comparable to this value?

Prelab Quiz

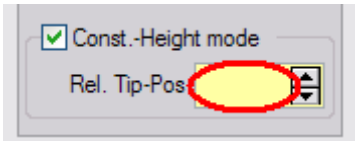

(1) Suppose you want to position the cantilever 75 nm above the surface in constant height mode. What value should you type in the highlighted box?

(2) Use the following data points into Excel (in the provided worksheet). Fit the points with the following function:

$$f(x) = -\arcsin(A(x - V_0)^2) + B$$

Hint: Solve the equation for $A(x-V_0)^2$, then use Excel to fit the parabola. The best fit to B is reasonably approximated by the maximum value of the phase shift.

What value do you get for A? V_0?

What physical quantity does V_0 represent?

(3) Given the following plot (see exact points in spreadsheet), find Q.

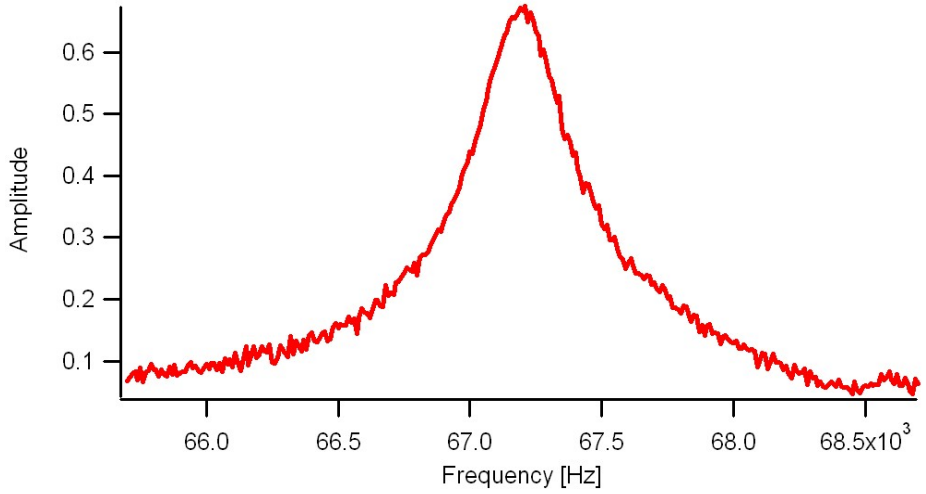

3. Experimental Assignment

Goal

Perform intermittent contact mode imaging and electrostatic force microscopy on a polymer blend sample. Examine domains of PCBM and MDMO-PPV with both intermittent-contact SFM and EFM. Find the difference in work function between ITO and gold.

Materials

Instrumental Setup

- Easy Scan 2 AFM system with Pt-coated non-contact mode EFM tip with 1–5 N/m spring constant (probe model: ANSCM-PT from AppNano)
- Alligator clip-slide holder
- Alligator clip-terminated wire (both ends)
- Pair of small magnets
- tweezers (one for the EFM tip, one for the sample)
- Samples: Au film, polymer film on Au film, ITO (see sample prep below)

Sample Preparation

- spin coater
- sonicator (with acetone and isopropanol)
- voltmeter with probes
- thermal evaporator with gold (for the silicon/silicon oxide gold-coated substrate)
- silicon/silicon oxide substrate with a thermally evaporated 15 nm gold layer
- indium tin oxide (ITO) coated glass
- poly[2-methoxy-5-(3',7'-dimethyloctyloxyl)])-1,4-phenylenevinylene (MDMO-PPV)
- methanofullerene [6,6]-phenyl C61-butyric acid methyl ester (PCBM)
- toluene
- acetone
- isopropanol

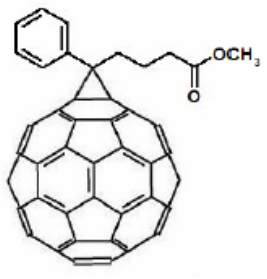

PCBM

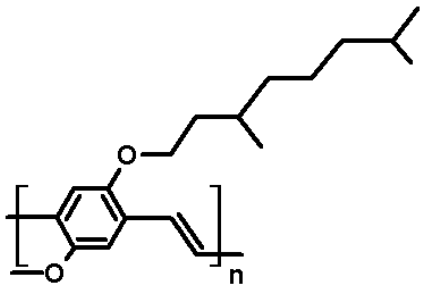

MDMO-PPV

Safety

- Wear protective gloves and safety glasses when working with solvents and the spin-coater
- Review the Chemical Hazards below

- Refer to the General rules of the AFM lab

Chemical Hazards: This is only a summary of the Material Safety Data Sheets for the chemical reagents we will be using.

Toluene: Flammable liquid and vapor. Causes eye, skin, and respiratory tract irritation. Breathing vapors may cause drowsiness and dizziness. May be absorbed through intact skin. Aspiration hazard if swallowed. Can enter lungs and cause damage. Possible risk of harm to the unborn child. May cause central nervous system depression. Target Organs: Central nervous system, respiratory system, eyes, skin.

Isopropanol: Flammable liquid and vapor. Irritant to eyes and skin. Vapors can cause drowsiness or dizziness. Target Organs: nerves and kidneys

Acetone: Irritant, especially to eyes. Repeated exposure may cause skin dryness or cracking. Vapors may cause drowsiness and dizziness. Target organ(s): liver and kidneys

MDMO-PPV poly(2,5-bis(3',7'-dimethyloctyloxy)-1,4-phenylenevinylene
PCBM ([6,6]-Phenyl C61 butyric acid methyl ester)
These polymers have not been fully characterized for toxicity.

Experimental Procedure

Reagent preparation

(1) Prepare a ~10 mg/mL stock solution of MDMO in toluene. This may take a few days and/or mild heating/stirring to completely dissolve.

(2) Prepare a ~20 mg/mL stock solution of PCBM in toluene.

(3) Mix a volume of 1 part MDMO and 2 parts PCBM. The final weight ratio should be 4:1 PCBM:MDMO.

Substrate preparation

Substrates should be cut to a size that is small (to conserve materials), yet large enough to be handled easily. A 1 cm x 1 cm square is a good size.

(4) After cutting the substrate to size, sonicate both ITO slides and silicon/silicon oxide in an acetone bath, then an isopropanol bath for 20 minutes each

(5) Blow the substrates dry with a nitrogen stream.

(6) (Optionally, plasma clean the ITO for about 5 minutes.) Store the cleaned ITO in a covered container (petri dish) to keep it clean.

(7) Evaporate about 15 nm of gold onto the silicon/silicon oxide substrates.

(8) Set the spin-coater to spin at 2000 rpm for 30 seconds. Gently deposit about 50 µL of 4:1 PCBM/MDMO-PPV (in toluene) onto the gold-coated substrate and start the spin-coater. Reserve a gold-coated substrate for later use.

Initial Set-Up of the Instrument

See start up procedure in Easy Scan 2 AFM System SOP (Standard Operational Procedure) for more details.

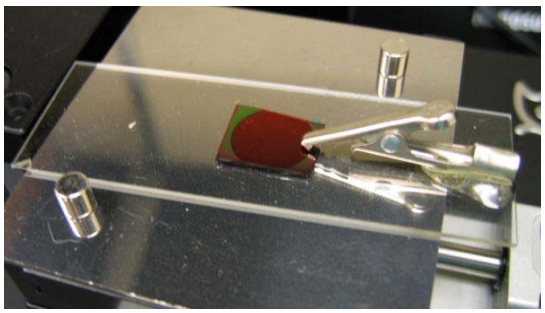

(1) Clip the polymer-film substrate into the substrate holder. Set the voltmeter to measure resistance. Touch one probe to the conductive part of the substrate and the other probe to the alligator clip holding down the substrate. A resistance of ~10-15 Ω indicates a satisfactory contact has been made. If not, gently push the clip down on the substrate, and wiggle the clip to "clean the contact" if necessary.

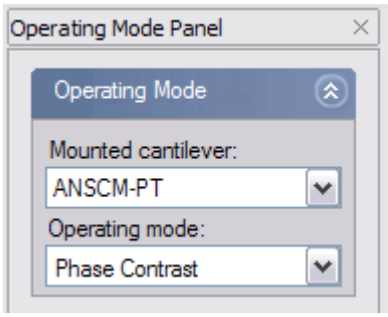

(2) Load an EFM cantilever (k=1–5 N/m) into the AFM head. (ANSCM-PT tips)

(3) Select the Operating Mode Panel: Select *ANSCM-PT* for the cantilever, and the *Phase Contrast* operating mode. (If the cantilever option is not there, go to *Options* > *Cantilever*

Options, create a new cantilever profile with the tip name, and enter in the properties for the ANSCM-PT cantilever. Save, then select the tip in *Operating Mode*.)

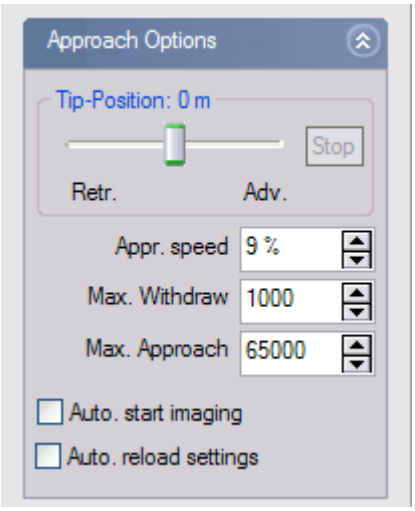

(4) *Uncheck* the auto start imaging under *Approach Options* in the Positioning Window

(5) Make sure the AFM tip has enough clearance (>1 mm) for the substrate and glass slide before carefully sliding under the tip.

(6) Anchor the glass slide to the translation stage with the small magnets.

(7) Ground the sample by connecting the clip to the Nanosurf controller by the alligator-clip terminated wire.

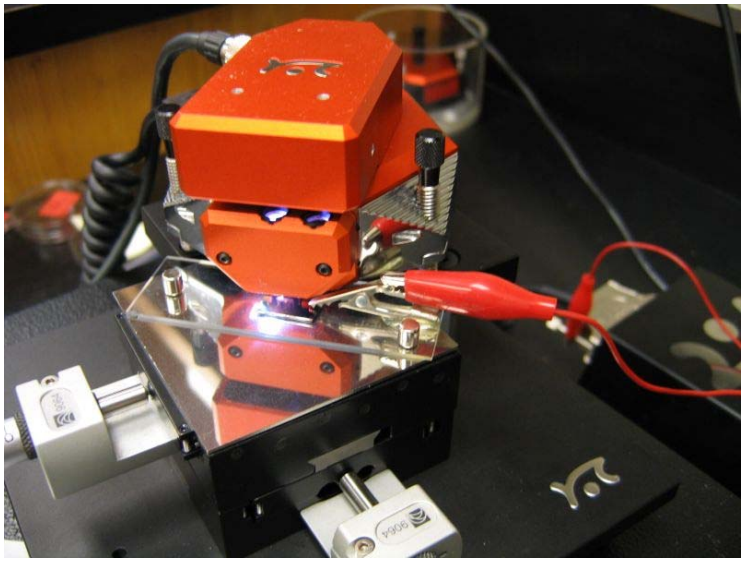

Non-Contact/Intermittent-Contact Imaging

(8) In the Operating Mode Panel: Mode Properties, make sure the checkboxes for *Auto set* and *Display sweep chart* are checked. Tune the cantilever tip manually by clicking *Set*. Note the shape of the response curve (cantilever amplitude versus driving frequency).

Click on the graph, then save the data from the resonance curve (File > Export > Current Chart… and save as a Comma Separated z-Values (*.CSV) file). You will need this later to determine the Q-factor for your cantilever.

Examine the oscillation amplitude as a function of drive frequency and record the resonant frequency of your cantilever (shown grayed out in *Mode Properties: Vibration frequency)*.

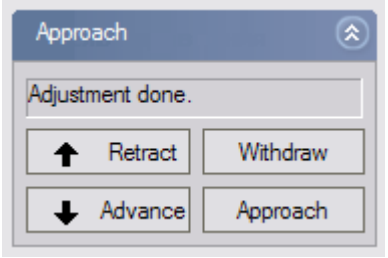

(9) Quickly advance the tip closer to the surface by clicking and holding down on the *Advance* button in the Approach panel. Approach the tip to the surface by clicking on 'Approach' in the Approach panel.

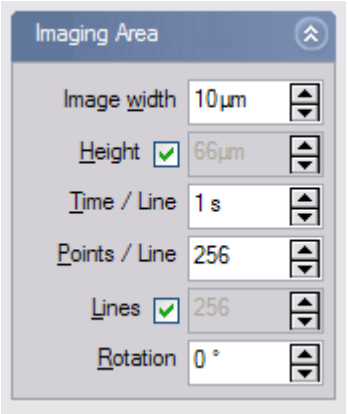

(10) In the Imaging Panel, adjust the image width to image a 10 µm wide square on the sample, and check that the other parameters are set to the same as the image on the right. Click *Start* to start the scan. As you scan, make sure you have a relatively "flat" region of the sample. If the line trace appears crooked, use the menu option: *Script* > *Imaging – Adjust Slope* to straighten it out. Repeat for *Rotation: 90º*. Large pieces of dirt will adversely affect the EFM imaging in the next step.

(11) Once you have scanned a region that is mostly free of dirt, click *photo* to save the image when the scan is done. Allow the scan to finish. When the window pops up with the completed image, click on the image, then *File* > *Export*, and save it as a Windows Bitmap Image (*.BMP).

(12) We will choose a smooth subsection of this region to perform EFM. Click on *Zoom* in the toolbar above, and draw a box (try for about 2 µm) around the cleanest region. The *Tool Results Panel* will pop up on the left as you do. Click *Zoom* to confirm your selection.

(13) Obtain a topography image of this narrowed region. Check that you have a good saved image and area. If the height variation is bigger than 50 nm, image a new area. Once you have a good image you can stop imaging, by clicking *Stop*.

Electrostatic force microscopy

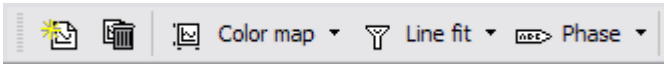

(1) We need to rearrange the chart window to show EFM data. From the toolbar (shown above), click  to create a new display graph. Choose 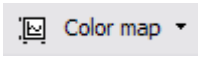 to show a 2D graph, and select 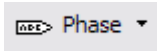 as the data to be shown. Add yet another display, except choose:  to make a line graph of the phase data.

(2) In the Imaging Panel: Imaging Modes, set *Rel. Tip_Pos* to –150 nm. This is the distance that the EFM will withdraw from the surface during the measurement, i.e. the tip will retract 150 nm above the surface from the initial "contact" point. You should know if the current spot is "clean" from the topography scan you just did. If there are features taller than 50 nm (most likely dirt), NanoSurf will not remember they are there, and try to run the tip through them when we scan at lower heights.

(3) Set the tip bias to 5 V, in *Z-Controller Panel: Tip Properties*.

(4) Check the *Const.-Height mode* to start EFM measurements.

(5) Click *Start* in the Imaging Panel and watch the phase map. Let the AFM scan for a few lines up (at least 1/5 of the total image area). Do you see any contrast? Move the tip closer to the surface by 25 nm. Keep decreasing the tip-to-substrate distance (be careful not to go below –50 nm). How does the contrast change? Save this scan when it completes.

(6) Once you find a good distance for contrast, scan the entire area at the same height. Make sure to select *photo* to save the image when it is done scanning.

(7) Recall the height variation you observed in the AC mode topography scan. Increase the tip-sample distance by half this value, and reimage the area. Save the image. Increase the distance again by the same amount, and obtain another scan of the area.

(8) When you are done, reset the tip voltage to 0 V.

"Calibrating" the EFM scan

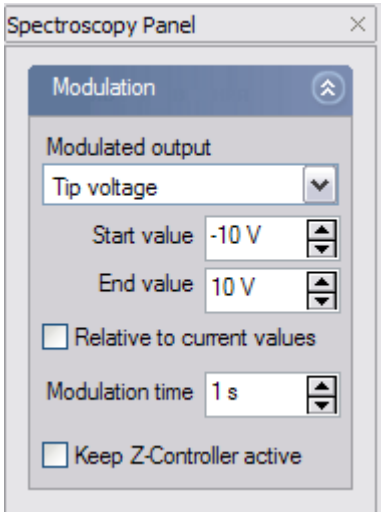

(9) Withdraw, retract the tip, and then carefully raise the AFM head from the sample. Switch samples to the gold substrate.

(10) Approach the surface. As before, make sure *Autostart Imaging* is **not** checked.

(11) Click on *Spectroscopy* in the left panel. Change the *Modulated Output* to *Tip voltage*.

(12) Configure the display panel to show *Phase*, as before. Use only the line graph, and display *Raw Data*.

(13) Select *Const-Height* mode, in the Imaging Panel, and set the distance to –70 nm.

(14) In the *Spectroscopy: Measurement* panel, change the number of averages to 20.

(15) Click on Start. If the shape that emerges is not a downward-facing parabola, first check that the substrate is firmly grounded. Alternately, withdraw the tip, move to a new location and repeat. You may also want to approach the tip to the surface to dissipate any charges collected on the tip. You will have to reselect *Constant Height Mode* after doing so.

(16) Save the trace, and repeat 4 times.

(17) Repeat with the ITO substrate, or try other conductive surfaces.

4. Background: Intermittent-Contact Mode Force Microscopy & Electrostatic Force Microscopy (EFM)

Table of Contents:

Motivation

Contact mode, non-contact mode, and intermittent-contact mode scanning probe microscopy (SPM) all use short range van der Waals forces to probe the topographic features of a sample. However, if we move the scanning probe further away from the surface (~20-60 nm), we can examine longer range forces, such as electrostatic and magnetic forces. In doing so, we can learn about the electrical properties of a material with high spatial resolution. Electrostatic force microscopy (EFM) and its variants are used to study topics as diverse as dopant profiles in silicon transistors, charge injection in organic diodes, and changes in photosensitive reaction complexes in biological membranes. Both intermittent-contact mode and EFM make use of the changes of the motion of an oscillating tip to produce images. In order to understand these imaging modes we first need to review the motion of an oscillating tip. If you have studied simple harmonic motion in your physics or math classes, the next section may be familiar to you.

Simple Harmonic Motion

The SPM tip sits at the end of a long, flexible cantilever. This cantilever is flexible and behaves like a spring: if the tip is pushed in one direction the cantilever exerts a force in the opposite direction in an attempt to restore the tip to its original position. Since we are going to be examining the motion of the tip in more detail, we first define some parameters:

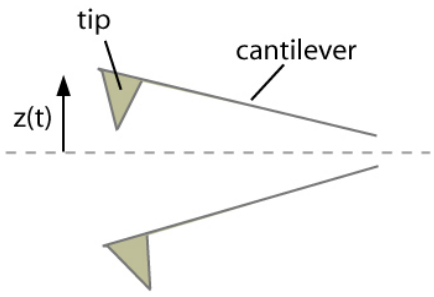

z(t)	position of the tip as a function of time
F	force exerted on the tip
m	mass of the tip
k	effective spring constant of the cantilever

Remember that the velocity *v(t)* and acceleration *a(t)* of the tip are related to its position z(t) through the following derivatives:

$$v(t) = \frac{dz}{dt} \qquad a(t) = \frac{dv}{dt} = \frac{d^2z}{dt^2}$$

Newton's third law *(F = ma)* relates the forces on the tip to its motion. We already mentioned that the cantilever behaves much like a spring, and will we approximate the restoring force using Hooke's law relating spring constants and restoring forces ($F = -kz$). Combining these two equations gives us the following equation of motion:

$$F = ma = -kz$$
$$m\frac{d^2z}{dt^2} = -kz$$

The tip and cantilever are real materials moving through air, so the motion is also damped by both air friction and by losses in the spring. These losses are both approximately proportional to the velocity and so we modify our equation of motion with a "drag force" or damping term $-bv$:

$$F = ma = -kz - bv$$
$$m\frac{d^2z}{dt^2} = -kz - b\frac{dz}{dt}$$

Rearranging a bit, we can write this as a differential equation describing basic motion of the tip far away from any substrate (and still without any driving force yet either)

$$m\frac{d^2z}{dt^2} + b\frac{dz}{dt} + kz = 0$$
$$\frac{d^2z}{dt^2} + \beta\frac{dz}{dt} + \omega_0^2 z = 0$$

where $\omega_0^2 \equiv k/m$ and $\beta \equiv b/m$. ω_0 is the natural frequency of the cantilever.

Most non-contact/intermittent contact SPM is performed while applying a sinusoidally oscillating drive force on the tip, so we must also add the driving force to our equation of motion:

$$\frac{d^2z}{dt^2} + \beta\frac{dz}{dt} + \omega_0^2 z = D\cos\omega t$$

This equation may look familiar. It is the classic equation for the damped and driven simple harmonic oscillator. The solution to this equation is a steady-state motion of the system should oscillate with the driving force, plus a potential phase shift δ. You can check that the solution has the form:

$$z(t) = A\cos(\omega t - \delta)$$

where:

$$\delta = \tan^{-1}\left(\frac{\omega\beta}{\omega_0^2 - \omega^2}\right)$$

The amplitude, A, of oscillation is:

$$A = \frac{D}{\sqrt{(\omega_0{}^2 - \omega^2)^2 + \omega^2\beta^2}}$$

The "resonance frequency" of the oscillator is defined as the driving frequency at which A is maximized. If the damping is small, the amplitude is at a maximum when the driving frequency equals the natural frequency ω_0. The amount of damping in a simple harmonic oscillator is commonly characterized by the quality factor, Q. Q is defined as the resonance frequency divided by β, and is a measure of the total energy stored in the oscillator divided by the energy lost per period of oscillation. For systems that are only weakly damped (like an AFM tip vibrating in air), a practical method of determining Q is to divide the resonance frequency by the width of the resonance peak (where the width is taken at the points where the amplitude is equal to $1/\sqrt{2} \approx 0.707$ of the maximum).

AC-Mode Imaging

In a common form of topography imaging, called intermittent-contact mode (or a variation called "Tapping Mode™" by some manufacturers), the AFM is driven at a frequency close to the resonant frequency of the tip. When the tip comes close to the surface, it interacts with the surface through short range forces such as van der Waals forces. These additional interactions change the resonance frequency of the tip, thereby changing the amplitude of oscillation and its phase lag. Typically, an image is formed by using a feedback loop to keep the oscillation amplitude constant by varying the tip sample distance with the z-piezo (see figure below). By plotting the z-piezo signal as a function of position it is then possible to generate an image of the height of features on the surface. It is possible to image in both the attractive, and the repulsive regions of the van der Waals potential, and strictly speaking this divides the classification of AC-Mode imaging techniques into "non-contact" and "intermittent contact" AFM respectively). However, intermittent contact AC-mode imaging is more common for routine imaging.

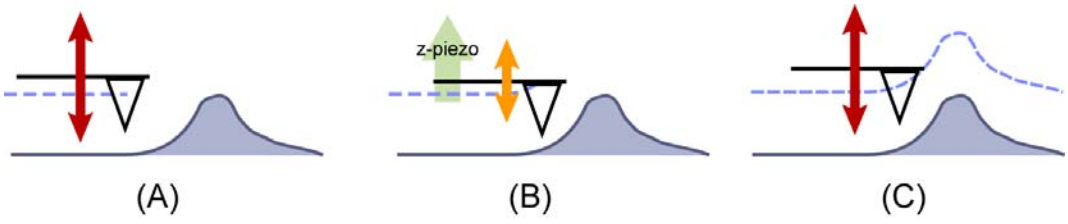

Schematic for intermittent-contact mode AFM. (A) The AFM tip is driven near its natural resonance frequency to obtain a target amplitude of oscillation. (B) As the tip approaches changes in topography, the increasing van der Waals forces shift the resonance frequency, which causes the tip's oscillation amplitude to decrease. In response, the Z-piezo lifts the tip away from the surface so (C) the original oscillation amplitude is reestablished. By tracking the Z-motion of the tip, we obtain the measured topography of the surface (dashed line).

Of course, the material properties of the sample affect tip-surface interactions, so the topography image obtained by AC-mode imaging isn't perfectly free of artifacts (some imaging modes even exploit differences in elastic properties of the surface to differentiate materials). Nevertheless, AC-mode imaging is much gentler and can be used to image a wider variety of soft samples than contact mode imaging.

Electrostatic Force Microscopy

The goal of an EFM experiment is not to image the surface topography, but rather to image the electrical properties of the surface. This is accomplished by vibrating a metal-coated tip some distance away from the surface — beyond the range of short range van der Waals interactions, so that only long-range forces (such as electrostatic forces) remain.

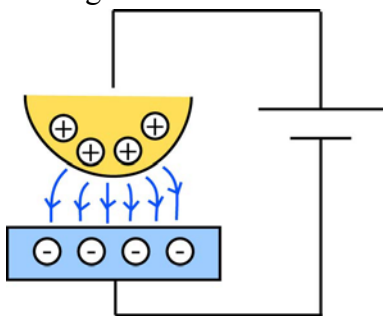

As the tip scans over a surface, its motion is affected by the forces between it and the surface below. To understand EFM, it is useful to think of the tip and sample as forming two plates in a very small capacitor. The potential energy, U, of a capacitor with capacitance C charged to a voltage V is given by:

$$U = \tfrac{1}{2} C V^2$$

The force F, is always given by the first derivative of the potential U, as a function of position z. The force between the tip and the cantilever is then:

$$F = -\frac{dU}{dz} = -\frac{d}{dz}\left(\frac{1}{2} C V^2\right) = -\frac{1}{2}\frac{dC}{dz} V^2$$

This force depends on both the applied voltage (independent of distance) and the capacitance (depends on distance). This is really an electrostatic force (Coulomb's Law) in a different form. The potential difference causes opposite charges to build up on the tip and the substrate (as seen in the cartoon), which pulls the tip towards the substrate.

How does this force affect the tip motion? Well, to first order it doesn't! (You may remember from your physics coursework that the resonant frequency of a spring-mass oscillator doesn't depend on the value of the local gravitational acceleration). It is not the electrostatic force, but rather the *force gradient* that determines the oscillation of the tip. For example, the force gradient using the restoring force from the cantilever (Hooke's Law) is

$$F = -kz$$

$$\frac{dF}{dz} = -k$$

This is the spring constant, which shows up in the natural frequency ω_0 of the oscillator. Any other forces on the cantilever that have a significant force gradient will affect the tip's motion. In this case, we are interested in measuring the electrostatic force by how

it affects our oscillating tip. It is easier to see the effect of this additional force on the tip's motion by writing its contribution to the total force gradient:

$$F = -kz - \frac{1}{2}\frac{dC}{dz}V^2$$

$$\frac{dF}{dz} = -k - \frac{1}{2}\frac{d^2C}{dz^2}V^2$$

Assuming $\frac{d^2C}{dz^2}$ is relatively constant for the range of motion, we can consider this new factor as a change in the spring constant, $k' = k + \Delta k$. **In other words, the electrostatic *force gradient* works like a change in the effective spring constant of the cantilever.** This will change the natural oscillation frequency, now ω_0', and the phase shift δ' between the cantilever and drive signal for some constant driving frequency ω.

$$\omega_0' = \sqrt{\frac{k'}{m}}$$

$$\delta' = \arctan\left(\frac{\omega\beta}{\omega_0'^2 - \omega^2}\right)$$

For small damping factors and a driving frequency at the resonance frequency ($\omega_0 = \omega$), we can approximate the change in phase shift as [3]:

$$\Delta\delta = -\arcsin\left(\frac{Q}{2k}\frac{d^2C}{dz^2}V^2\right)$$

In real experiments, the phase shift versus voltage curve has a non-zero offset, V_0:

$$\Delta\delta = -\arcsin\left(\frac{Q}{2k}\frac{d^2C}{dz^2}(V - V_0)^2\right)$$

This offset is attributed to the difference in work function between the tip and the sample.

Applications

Electrostatic force microscopy and variations of EFM (such as scanning Kelvin probe microscopy (SKPM), measuring differences in surface potential; magnetic force microscopy (MFM), measuring magnetic moments) can be used to characterize many different samples, such as dopant profiles in silicon-based transistors, polarization in piezoelectric materials, and charge distributions in organic semiconductors. In this lab, you apply EFM to characterize metal films as well as semiconducting polymer blends.

References

1. *Scanning Probe Microscopy and Spectroscopy: Techniques, and Applications.* Edited by Dawn Bonnell, Wiley-Interscience Publication, 2nd Ed., New York, 2001.
2. *Classical Dynamics of Particles and Systems*. Jerry B. Marion and Stephen T. Thornton, Harcourt Brace & Company, 4th Edition, 1995.
3. C H Lei, A Das, M Elliot, J E Macdonald, "Quantitative electrostatic force microscopy-phase measurements." *Nanotechnology.* **15** (2004) 627-634.

LAB UNIT 3: Force Spectroscopy Analysis

Specific Assignment: Adhesion forces in humid environment

Objective

This lab unit introduces a scanning force microscopy (SFM) based force displacement (FD) technique, *FD analysis*, to study local adhesion, elastic properties, and force interactions between materials.

Outcome

Learn about the basic principles of force spectroscopy and receive a theoretical introduction to short range non-covalent surface interactions. Conduct SFM force spectroscopy measurements as a function of relative humidity involving hydrophilic surfaces.

Synopsis

The SFM force spectroscopy probes short range interaction forces and contact forces that arise between a SFM tip and a surface. In this lab unit we examine the adhesion forces between hydrophilic surfaces of silicon oxides within a controlled humid atmosphere. While at low humidity Van der Waals forces can be observed, capillary forces dominate the adhesive interaction at higher humidity. We will discuss relevant tip-sample interaction forces, and geometry effects of the tip-sample contact. Furthermore, we will be able to estimate the true tip contact area – something that generally evades the SFM experimentalist.

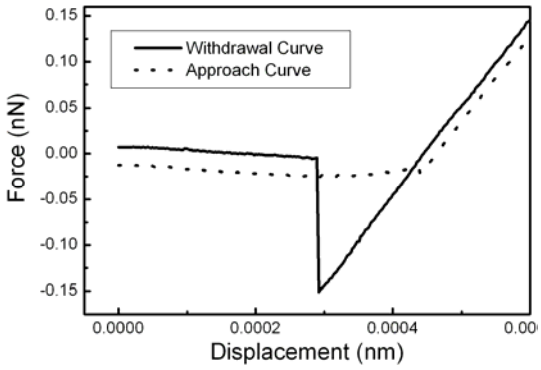

Force Displacement Curve

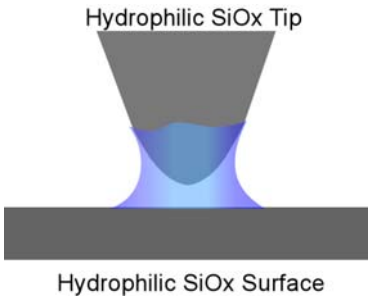

Nanoscale contact of two hydrophilic objects in humid air

Materials

(111) Silicon oxide wafers

Technique

SFM force spectroscopy

Table of Contents

1. Assignment

The assignment is to experimentally determine the effect of humidity on adhesion forces for hydrophilic surfaces and to employ the theories and background information to discuss the experimental results. The steps are outlined here:

1. Familiarize yourself with the background information provided in Section 4.
2. Test your background knowledge with the provided Quiz in Section 2.
3. Conduct the adhesion-humidity experiments in Section 3. Follow the step-by-step experimental procedure.
4. Analyze your data as described in Section 3
5. Finally, provide a report with the following information:
   (i) Results section: In this section you show your data and discuss instrumental details (i.e., limitations) and the quality of your data (error analysis).
   (ii) Discussion section: In this section you discuss and analyze your data in the light of the provided background information.
   It is also appropriate to discuss sections (i) and (ii) together.
   (iii) Summary: Here you summarize your findings and provide comments on how your results would affect any future AFM work you may do.
   The report is evaluated based on the quality of the discussion and the integration of your experimental data and the provided theory. You are encouraged to discuss results that are unexpected. It is important to include discussions on the causes for discrepancies and inconsistencies in the data.

2. Quiz – Preparation for the Experiment

Theoretical Questions

(1) Given the data below, plot the Lennard Jones potential for N_2-N_2 interaction and Ar-Ar interaction for distances between 0.25 and 1.4 nm. (Hint: assume point-point interaction, use Excel and make the calculation increment 0.01 nm for greatest clarity. Also select a y-axis range from -0.05 to 0.05 eV).

Molecule	ε (eV)	σ (nm)
Ar	0.01069	0.342
N_2	0.02818	0.368

(2) Provide a detailed description (with sketch) of an attractive FD curve. Under what condition is the curve attractive (Hint: Draw the curve for cases where the Hammaker constant A>0 and for A<0).

(3) Consider a force-displacement analysis conducted on 1, 10 and 100 nm radii SiO_x silica particles. Calculate the interaction strength assuming ultra-dry conditions at 27°C assuming a SiO_x silicon SFM tip radius of 5 nm and 50 nm. Compare the results to the capillary force strength in contact with R = 50 nm. (Hint: Use the excel spreadsheet provided to calculate the Hamaker constant.)

Additional data:
h = 6.63E-34 Js
ν_e = 3.00E+15 Hz
D_0 = 1.60E-01 nm
K = 1.38E-23 J/K

	Dielectric Constant	Refractive Index
SiOx	3.78	1.45
Si	12	3.45
Air	1	1

(4) In high resolution SFM imaging of soft surfaces such as DNA strands, it is important not to deform the sample with strong adhesion forces.
   (a) Assuming a SiO_x SFM tip and a dielectric constant for DNA of 1.2 and a refractive index of 1.33, suggest appropriate fluids that provide close zero or repulsive adhesion forces. Are these fluids appropriate for organic matter?
   (b) How about a tip that is hydrocarbon coated (either using thiol and silane chemistry)?

Prelab Quiz

(1) (3pt) A typical force displacement curve is shown below. Indicate the segment of the curve that corresponds to the adhesion force.

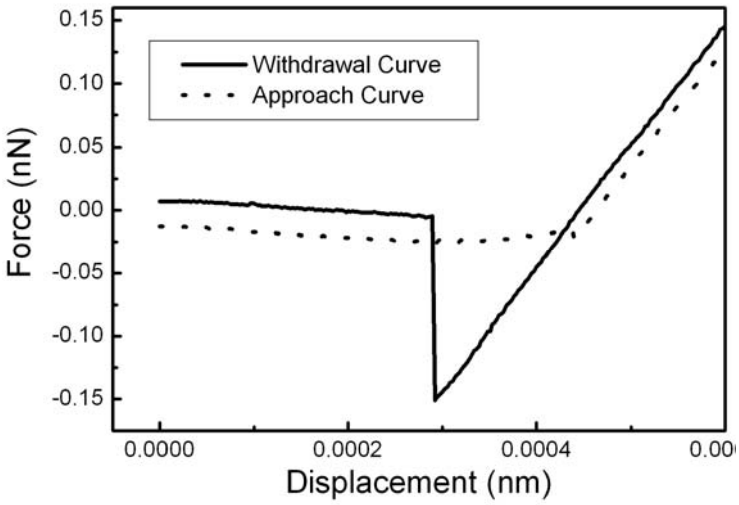

(2) (7pt) The adhesion forces as a function of relative humidity, obtained by He et al. are given below. Follow the analysis procedure described in the experimental section.

a. (4pt) Determine the fit parameters, F_{stv}, $F_{stw} + F_{cap}$, φ_0, and m of the model equation, using the provided excel worksheet.

$$F_{mea} = (F_{stw} + F_{cap}) + \frac{F_{stv} - (F_{stw} + F_{cap})}{1 + \exp[(\varphi_0 - \varphi)/m]}$$

b. (3pt) Determine the tip radius R and the filling angle φ.

Raw data from He et. al.

Relative Humidity (%RH)	Average F_{mea} [nN]
88	25
82	29
76	32
70	33
69	34
62	35
54	33
43	31
40	18
33	12
28	11
23	11
17	11
12	10
9	10
9	10

Additional information

Contact Angle (silicon/water) = 0°

$\gamma_{SiO/air}$ = 100 mJ/m^2

$\gamma_{SiO/waterr}$ = 24.5 mJ/m^2

γ_{water} = 72.8 mJ/m^2

3. Experimental Assignment

Goal

Following the step-by-step instruction below, determine the functional relationship of the adhesion force between two silicon-oxide surfaces with relative humidity from 5-60 %. Analyze and discuss the data with the background information provided in Section 4. Provide a written report of this experiment.

Specifically provide answers to the following questions:

(1) According to the analysis, what was (a) the radius of the SFM tip, (b) the critical relative humidity, and (c) the filling angle?

(2) Compare with the result reported by He et al.[1] how does your result differ/resemble that of He et al? Discuss your findings.

(3) Using the tip radius determined experimentally, determine the interaction strength assuming dry conditions. (Hint: see Background Question (4))

(4) Report values for F_{stv} and F_{stw}. Discuss the difference between values. Do they depend on the Hamaker constant? If so how and why?

(5) Two possible ways to reduce the capillary effects are suggested in background question (4). Discuss the downside of such treatments.

(6) In a previous experimental run the data in the figure below was obtained. Compare these results to your results and suggest reasons for any differences.

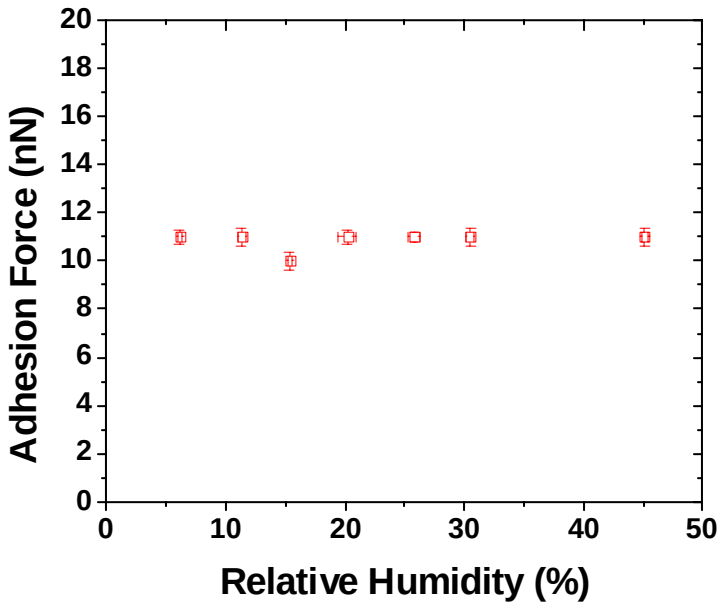

Safety

- Wear safety glasses.
- Refer to the General rules in the AFM lab.
- The gas cylinder valve should be closed when it is not in use.
- Conduct the experiment within the assigned relative humidity range of 5-60% to avoid electric shortages.

Instrumental Setup

- Easy Scan 2 AFM system with contact Mode SFM tip with 0.2 N/m spring constant.
- Environmental enclosure and a hygrometer
- Nitrogen cylinder and valves
- 60 ml beaker within chamber

Materials

- Samples: 2 pieces of ~ 1cm^2 UV treated (111) silicon wafers securely stored in sealed Petri dishes till ready for the experiment.
- N_2 gas
- Ultra pure Milli Q water.

Experimental Procedure

Read the instructions below carefully and follow them closely. They will provide you with information about (i) preparation of the experiment, (ii) the procedure for force spectroscopy measurements, (iii) the procedure for closing out the experiment, and (iv) on how to conduct the data analysis. (v) A silicon pretreatment (removal of organic contaminants) is provided at the end of this section.

(i) Preparation of the experiment

(1) System Set-up: (This part will be performed with a TA) Follow the start up procedure **steps 1 – 8**, in the Easy Scan 2 AFM System SOP (Standard Operational Procedure). NOTE: The software leveling step in the SOP is not necessary—skip this step.
   a. Place a CONTR cantilever with the spring constant of 0.2 N/ m.
   b. Positioning procedure should be done with a dummy sample to avoid contamination.

(2) Place a sample piece at the center of the sample holder. Connect the ground wire from the sample holder to *Scan Head*.

(3) Make sure that the regulator valve and the rotameter are closed. Open the main cylinder valve.

(4) Control the humidity in the glove box. The force-displacement curve will be taken from low humidity (5%) to high (60%).
   a. Control the humidity using the N_2 gas for the relative humidity between 5% - ambient humidity of the day (~ 40%). The flow will be adjusted by

the rotameter. When conducting the experiment it is generally most efficient to let the humidity increase up to the 15% measurement with the AFM containment in place. For subsequent measurements (20% to room humidity) removing the containment and then adding nitrogen is faster.

b. For the relative humidity between the ambient humidity to 60%, the humidity is controlled using heated water and the N_2 gas.
   i. Place 15mL of ultra pure MilliQ water in a 30 mL beaker.
   ii. According to the ambient humidity, heat the water using a hot plate to the temperature found in Figure 1.

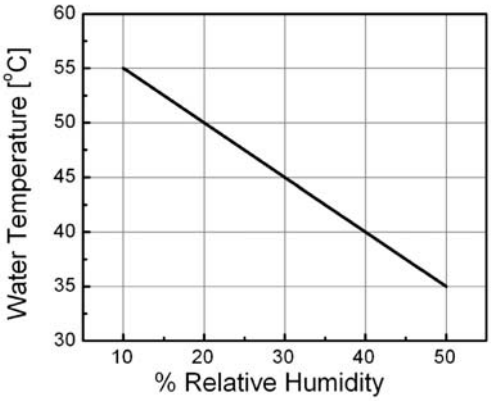

Figure 1: Initial water temperature for specified room humidity.

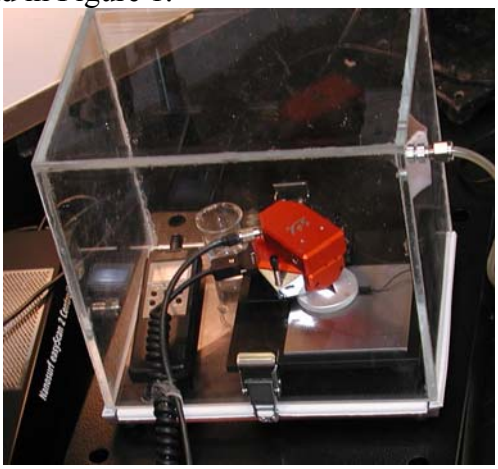

Figure 2: The water beaker is placed in the AFM containment.

   iii. Place the heated beaker in containment with AFM and humidity meter. (Figure 2)
   iv. Place the glove box over the AFM system. Close.
   v. Allow the humidity in the containment to reach the desired humidity. Adjust and keep the humidity by adjusting the N_2 flow through the rotameter.

c. When the humidity is stabilized at desired level, take the AFM measurement.

(ii) Coming to contact

(1) Once the cantilever is approximately 1mm from shadow, automatic approach is used to bring the cantilever into contact.
(2) Open the Z-Controller Panel by clicking the icon in the Navigator bar.
(3) Set the set point to be 5 nN. Use the default values for the P-Gain and I-Gain.
(4) Click the Approach icon in Approach panel on the left side of the Positioning window.
(5) The software lowers the SFM tip till it comes in contact with the sample surface.
(6) Once the approach is complete a message 'Approach done' appears and the imaging panel automatically appears in the active window.

(7) Look at the Probe Status Light on the Controller. If it is NOT green, it is not operating correctly. Immediately come out of contact by clicking Withdraw in the Approach Panel. Consult a lab assistant.

Click off the Auto start imaging

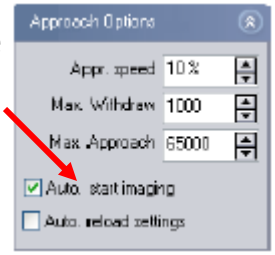

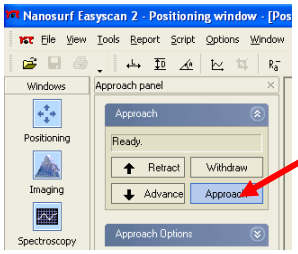

Automatic Approach

(iii) Procedure for force spectroscopy measurement

(1) Follow the procedure described in the Easy Scan 2 force distance measurement SOP.
(2) Initially take multiple data points at low humidity (<~5%). Record these measurements as stipulated in (6) below and continue the measurements until the adhesion force seems to attain a relatively constant value (at least 30 data points). This step is intended to remove tip wear as a variable in the subsequent humidity dependence measurement.
(3) Take data from low humidity to high humidity, with a ~5% increment.
(4) Come out of contact when changing humidity. When removing the containment, the tip should be raised far from the surface to avoid accidentally crashing it into the surface.
(5) For each humidity setting, obtain at least four force-displacement curves at various locations.
(6) Record for each reading,
   a. Adhesion force in unit of nm,
   b. The humidity,
   c. Any other observations that might be relevant in interpreting the result,

(iv) Procedure for closing the experiment

(1) Shut down the AFM system by following the shutdown procedure described in Easy Scan 2 AFM system SOP.
(2) Stop the N_2 gas to the box by closing at the cylinder main valve, the regulator, and the rotameter.
(3) Remove the glove box.
(4) Drain the Milli Q water into sink. Clean the beaker.
(5) Store samples in a Petri dish with a parafilm seal.

(v) Instruction for data analysis

(1) Convert the adhesion force F_{AD} in unit of nm, into in unit of nN by multiplying it with the spring constant of the cantilever C_N used,

$$F_{AD}[nN] = F_{AD}[nm] \cdot C_N[N/m]$$

(2) Calculate the average value and the standard deviation of the adhesion forces for each relative humidity.

(3) Construct the adhesion force verses the relative humidity plot. Include the standard deviation as an error bar.
(4) Using the sigmoidal function model (Eq. (16)), obtain the fitting parameters, F_{stv}, $F_{stw} + F_{cap}$, φ_o, and m. This can be done using the solver function of the provided Excel program (Figure 3).
   a. Input the relative humidity (x-axis) and the average adhesion force (y-axis) into the cells (light green) of the Excel work sheet. The program will generate the plot.
   b. Set the F_{cap}+F_{stw} cell to the maximum observed adhesion force and the F_{stv} to the minimum observed adhesion force as initial guesses. Initial guesses for φ_o, and m should be 100 and 5, respectively.
   c. Open *Tool* on the tool bar and select *Solver*
   d. Set the *Target Cell* by selecting the yellow cell indicated in the work sheet.
   e. Select *Equal to* "Min" (minimize)
   f. Select *By Changing Cells* the parameter cells indicated by purple in the worksheet.
   g. Click on *Solve* to obtain the best values for the fit parameters.
   h. The fit parameters will appear automatically in the purple cells.
   i. If the fit curve does not substantially resemble the data different initial guess values may be required. Consult your teaching assistant.

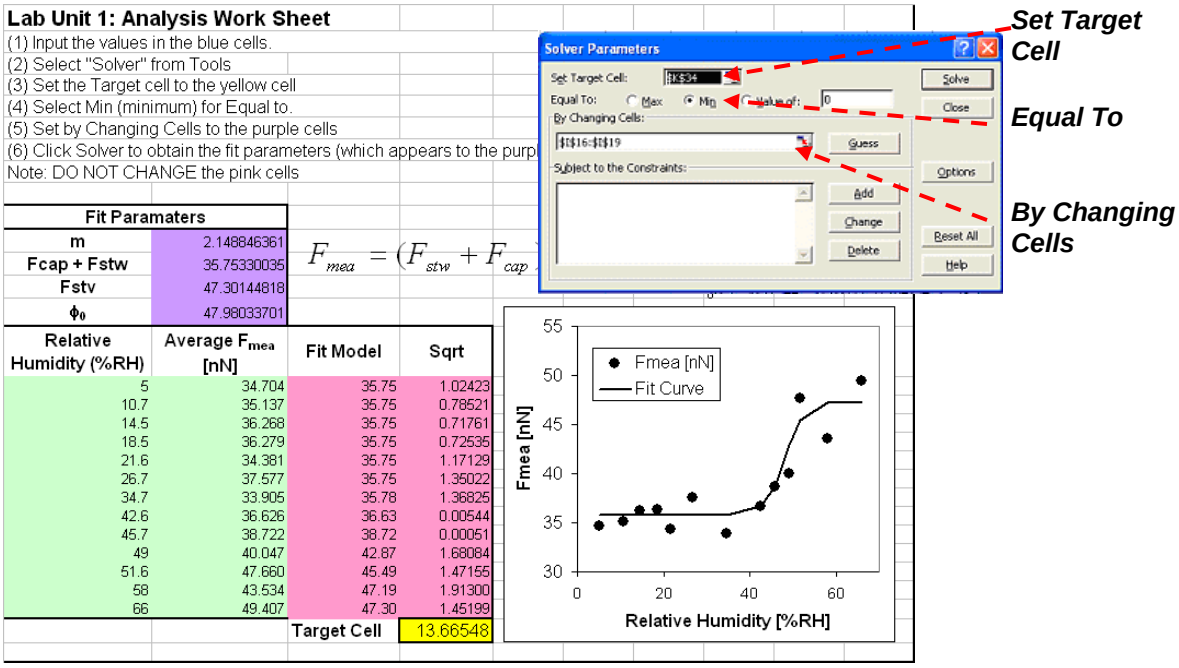

Figure 3: Data analysis within Excel (use of *Solver Function*)

(5) Using the value of F_{stv} obtained experimentally, the tip radius R can be deduced using Eq. (17a). The W_{stv} can be obtained through Eq. (18).
(6) Using the value R, calculate F_{stw} (Eq. (17b)).

(7) F_{cap} is calculated by subtracting F_{stw} from experimentally determined value of (F_{stw} + F_{cap}) (from step (4)).
(8) Using the capillary equation with geometric coefficient K (Eq. (19)), calculate the filling angle ϕ.

Additional information:

Contact Angle (silicon/water) = 0°
$\gamma_{SiO/air}$ = 100 mJ/m^2
$\gamma_{SiO/waterr}$ = 24.5 mJ/m^2
γ_{water} = 72.8 mJ/m^2

(v) Silicon Treatment Prior to Experiment

The pretreatment of silicon addresses organic condamination.

Safety

(1) Follow the general rules for Nanotechnology Wet-Chemistry Lab at your Institution.
(2) The UV/Ozone cleaner should be **OFF** before opening the sample tray.
(3) Always handle silicon wafers with tweezers, not with your fingers. Wafer edges can be very sharp.
(4) All solvent wastes are disposed into designated waste bottles located under the hood.
(5) All silicon waste are disposed into the sharp object waste box.

Depending on the degree of condamination solvent cleaning and UV/Ozone treatment are recommended.

Materials

(1) 4 pieces of Silicon wafers (~1cm^2 size pieces)
(2) Millipore H_2O
(3) Acetone
(4) Methanol
(5) A 150 ml beaker, a caddy and a watch glass for sonication
(6) A waste beaker for organic solvent
(7) A plastic waste beaker.
(8) Fine point tweezers
(9) N_2 gas with 0.2 micron filter.
(10) 3 Petri dishes and para-film for finished samples.
(11) UV/Ozone cleaner.
(12) Sonicator
(13) DI water

Procedure

(1) **Solvent cleaning:** Removes organics off of the silicon surfaces.
   a. Place silicon wafers in the caddy fitted in a 150 ml beaker and pour Acetone to fill upto~ 60 ml.
   b. Fill the sonicator with water. Place the beaker and adjust amount of water so that the water in the sonicator is about at the surface level of Acetone in the beaker.
   c. Cover with the watch glass.
   d. Turn on the sonicator and run for 15 minutes.
   e. Turn off the sonicator and remove the beaker.

f. Lift up the caddy (with silicon wafers) and drain the acetone into a waste beaker. Place the caddy back into the beaker.
g. Pour small amount of methanol for rinsing. Drain the methanol into the waste beaker. Repeat once.
h. Fill the beaker with Methanol upto ~ 60 ml.
i. Place the beaker back in to the sonicator. Cover with the watch glass.
j. Sonicate for 30 minutes. Take the beaker out when done.
k. Lift the caddy and pour out the methanol into the waste beaker. Rinse with Millipore water at least three times. Return the caddy back into the beaker and fill with Millipore water.
l. Pick up a piece of wafers with tweezers and rinse with flowing Millipore water. Blowdry it with N_2 gas.
m. Place the dried silicon wafers in a Petri dish. Cover the Petri dish.
n. Transfer the waste solvent mixture (of acetone, methanol and water) into the designated solvent waste bottle. Rinse the waste beaker with DI water. The spent water is also drained into the waste bottle. Note: Don't use this waste beaker for the HF process.
o. Empty out the sonicator and allow drying.

(2) **UV/Ozone treatment**: Removes any trace of organics off of the surface.

a. Make sure the UV/Ozone cleaner is OFF.
b. Open the sample tray and place two of the silicon wafers. Leave the other two for HF treatment.
c. Close the tray.
d. Turn on the power switch.
e. Set a timer to 30 minutes and start.
f. Turn of the power switch when done. Open the sample tray and take the silicon wafers out and place them into a Petri dish and seal it with parafilm.

4. Background: Non-Covalent Short Range Interactions

Table of Contents:

Motivation

As technology moves more towards miniaturization in novel product developments, it is imperative to integrate interfacial interactions into design strategies. Consequently, interfacial forces have to be explored. Interfacial forces are on the order of 10^{-6} to 10^{-10} N, strong enough, for instance, to freeze gears in micro-electrical mechanical systems (MEMS), to affect the stability of colloidal system, or to wipe out magnetically stored data information in hard drives. There are multiple ways of exploring the strength of interfacial interactions, one of which is by force spectroscopy, also known as force-displacement (FD) analysis. The FD analysis involves a nanometer sharp scanning force microscopy (SFM) tip that is moved relative to the sample surface in nanometer to micrometer per second, as illustrated at end of this document in Figure 10. Before we discuss FD analysis, we first discuss interaction forces, particularly weak interactions between molecules and solids.

Short Range Interactions and Surface Forces

There are three aspects that are of particular importance for any interaction: Its strength, the distance over which it acts, and the environment through which it acts. Short range interactions, as summarized in Table 1, can be of following nature: ionic, covalent, metallic, or dipolar origin. Ionic, covalent, metallic and hydrogen bonds are so-called atomic forces that are important for forming strongly bonded condensed matter. These short range forces arise from the overlap of electron wave functions. Interactions of dipolar nature are classified further into strong hydrogen bonds and weak Van der Waals

(VdW) interactions. They arise from dipole-dipole interactions. Both hydrogen and VdW interactions can be responsible for cooperation and structuring in fluidic systems, but are also strong enough to build up condensed phases. Following is a description of these short range forces:

A. *Ionic Bonds*: These are simple Coulombic forces, which are a result of electron transfer. For example in lithium fluoride, lithium transfers its 2s electron to the fluorine 2p state. Consequently the shells of the atoms are filled up, but the lithium has a net positive charge and the Flourine has a net negative charge. These ions attract each other by Coulombic interaction which stabilizes the ionic crystal in the rock-salt structure.

B. *Covalent Bond*: The standard example for a covalent bond is the hydrogen molecule. When the wave-function overlap is considerable, the electrons of the hydrogen atoms will be indistinguishable. The total energy will be decreased by the "exchange energy", which causes the attractive force. The characteristic property of covalent bonds is a concentration of the electron charge density between two nuclei. The force is strongly directed and falls off within a few Ångstroms.

C. *Metallic Bonds and Interaction*: The strong metallic bonds are only observed when the atoms are condensed in a crystal. They originate from the free valence electron sea which holds together the ionic core. A similar effect is observed when two metallic surfaces approach each other. The electron clouds have the tendency to spread out in order to minimize the surface energy. Thus a strong exponentially decreasing, attractive interaction is observed.

D. *Dipole Interactions*:

D.1. Hydrogen Bond Interaction: Strong type of directional dipole-dipole interaction

D.2. Van der Waals Interaction: The relevance of VdW interactions goes beyond of building up matter (e.g., Van der Waals organic crystals (Naphthalene)). Because of their "medium" range interaction length of a few Ångstroms to hundreds of Ångstroms, VdW forces are significant in fluidic systems (e.g, colloidal fluids), and for adhesion between microscopic bodies. VdW forces can be divided into three groups:

- *Dipole-dipole force*: Molecules having permanent dipoles will interact by dipole-dipole interaction.
- *Dipole-induced dipole forces:* The field of a permanent dipole induces a dipole in a non-polar atom or molecule.
- *Dispersion force:* Due to charge fluctuations of the atoms there is an instantaneous displacement of the center of positive charge against the center of the negative charge. Thus, at a certain moment, a dipole exists and induces a dipole in another atom. Therefore non-polar atoms (e.g. neon) or molecules attract each other.

Table 1: Short Range Interaction Forces

Nature of Bond	Type of Force	Energy (kcal/mol)	Distance
Ionic bond	Coulombic force	180 (NaCl) 240 (LiF)	2.8 Å 2.0 Å
Covalent bond	Electrostatic force (wave function overlap)	170 (Diamond) 283 (SiC)	N/A
Metallic bond	free valency electron sea interaction (sometimes also partially covalent (e.g., Fe and W)	26 (Na) 96 (Fe) 210 (W)	4.3 Å 2.9 Å 3.1 Å
Hydrogen Bond	a strong type of directional dipole-dipole interaction	7 (HF)	
Van der Waals	(i) dipole-dipole force (ii) dipole-induced dipole force (iii) dispersion forces (charge fluctuation)	2.4 (CH_4)	significant in the range of a few Å to hundreds of Å

Van der Waals Interactions for Point Interactions

The attractive VdW pair potential between point particles (i.e., atoms or small nonpolar spherical molecule) is proportional to $1/r^6$, where r is the distance between the point particles. The widely used semi-empirical potential to describe VdW interactions is the Lennard-Jones (LJ) potential, referred to as the 6-12 potential because of its $(1/r)^6$ and $(1/r)^{12}$ distance r dependence of the attractive interaction and repulsive component, respectively. While the 6-potential is derived from point particle dipole-dipole interaction, the 12-potential is based on pure empiricism. The LJ potential is provided in the following two equivalent forms as function of the particle-particle distance r:

$$\phi(r) = -\frac{C_{vdw}}{r^6} + \frac{C_{rep}}{r^{12}} = 4\varepsilon\left[\left(\frac{\sigma}{r}\right)^{12} - \left(\frac{\sigma}{r}\right)^{6}\right] \quad (1a)$$

where

$$\sigma = \left(\frac{C_{rep}}{C_{vdw}}\right)^{\frac{1}{6}}; \quad \varepsilon = \frac{C_{vdw}{}^2}{4C_{rep}} \quad (1b)$$

C_{vdw} and C_{rep} are characteristic constants. $C = C_{vdw}$ is called the VdW interaction parameter. The empirical constant ε represents the characteristic energy of interaction between the molecules (the maximum energy of attraction between a pair of molecules). σ, a characteristic diameter of the molecule (also called the *collision diameter*), is the distance

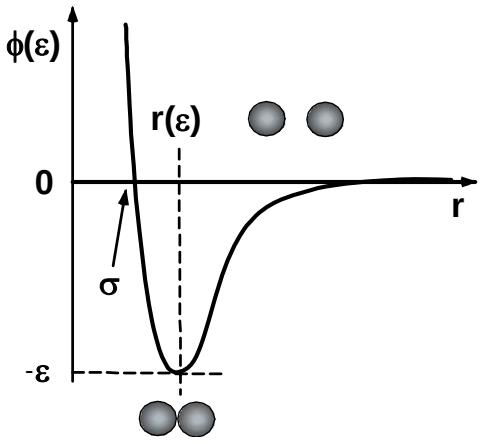

Figure 4: Lennard Jones (6-12) potential (empirical Van der Waals Potential between two atoms or nonpolar molecules).

between two atoms (or molecules) for $\phi(r) = 0$. The LJ potential is depicted in Figure 4..

Surface Forces

The integral form of interaction forces between surfaces of macroscopic bodies through a third medium (e.g., vacuum and vapor) are called *surfaces forces*. To apply the VdW formalism to macroscopic bodies, one has to integrate the point interaction form presented above. Consequently, the dipole-dipole interaction strength C but also the exponent of the distance dependence become geometry dependent. For instance, while for point-point particles the exponent is -6, it is -1 and -3 for macroscopic sphere-sphere and sphere-plane interactions, respectively. Thus, while, VdW point particle interactions are very short ranged ($\sim 1/r^6$), macroscopic VdW interactions are long ranged (e.g., sphere-sphere: $\sim 1/D$, where D represents the shortest distance between the two macroscopic objects). Table 3 provides a list of geometry dependent non-retarded VdW interaction strengths and exponents.

In vacuum, the main contributors to long-range surface interactions are the Van der Waals and electromagnetic interactions. At separation distance < 2 nm one might also have to consider short range retardation due to covalent or metallic bonding forces. Van der Waals and electromagnetic interactions can be both attractive or repulsive. In the case of a vapor environment as the third medium (e.g., atmospheric air containing water and organic molecules), one also has to consider modifications by the vapor due to surface adsorption or interaction shielding. This can lead to force modification or additional forces such as the strong attractive capillary forces.

The SFM tip-sample interaction potential W are typically modeled as a sphere-plane interaction, i.e.,

$$W(D) = \frac{-AR}{6D} \tag{2a}$$

with the force

$$-\frac{\mathrm{d}W}{\mathrm{d}D} = F(D) = \frac{-AR}{6D^2} \tag{2b}$$

where R is the radius of curvature of the tip, and D is the distance between the tip and the plane. The interaction constant A, is called the *Hamaker constant*, defined as $A = \pi^2 C \rho_1 \rho_2$, with the interaction parameter of the point-point interaction C, and the number density of the molecules in both solids ρ_i (i = 1,2). The Hamaker constant is based on the mean-field Lifshitz theory. If known, A provides the means to deduce the material specific (i.e., geometry independent) interaction parameter C. Typical values for A, C and ρ are provided in Table 2. Table 3 summarizes the Van der Waals interaction potential for various geometries.

Table 2: Hamaker constants of Hydrocarbon, CCl_4, and water.

Medium	C (10^{-79} Jm^6)	ρ [10^{28}m^{-3}]	A [10^{-19} J]
Hydrocarbon	50	3.3	0.5
CCl_4	1500	0.6	0.5
Water	140	3.3	1.5

Table 3: Van der Waals interaction Potential

	Geometry of Interaction		Interaction Potential (W)
Point Interaction	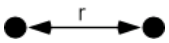	Two Atoms	$\frac{-C}{r^6}$
	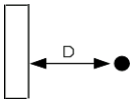	Atom-Surface	$\frac{-\pi C\rho}{6D^3}$
Body Interaction	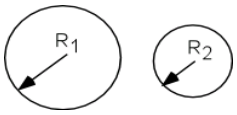	Sphere-Sphere	$\frac{-A}{6D}\frac{R_1R_2}{(R_1+R_2)}$
	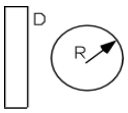	Plane-Sphere	$\frac{-AR}{6D}$
	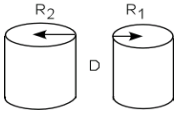	Two Cylinders	$\frac{AL}{12\sqrt{2}D^{3/2}}\left(\frac{R_1R_2}{(R_1+R_2)}\right)^{1/2}$
	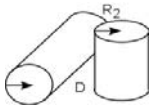	Two Crossed Cylinders	$\frac{-A\sqrt{R_1R_2}}{6D}$
	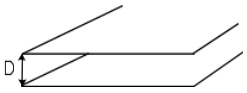	Plane-Plane	$\frac{-A}{12\pi D^2}$
	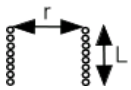	Two Parallel Chain Molecules	$\frac{-3\pi CL}{8\sigma^2 r^5}$

Hamaker Constant

Originally the Hamaker constant was determined based on a purely additive method in which polarization was ignored. The Lifshitz theory has overcome the problem of additivity. It is a continuum theory which neglects the atomic structure. The input parameters are the dielectric constants, ε, and refractive indices, n. The Hamaker constant for two macroscopic phases 1 and 2 interacting across a medium 3 is approximated as:

$$A \approx \frac{3}{4}kT\left(\frac{\varepsilon_1-\varepsilon_3}{\varepsilon_1+\varepsilon_3}\right)\left(\frac{\varepsilon_2-\varepsilon_3}{\varepsilon_2+\varepsilon_3}\right)+\frac{3h\upsilon_e}{8\sqrt{2}}\frac{\left(n_1^{\,2}-n_3^{\,2}\right)\left(n_2^{\,2}-n_3^{\,2}\right)}{\sqrt{\left(n_1^{\,2}+n_3^{\,2}\right)}\sqrt{\left(n_2^{\,2}+n_3^{\,2}\right)}\left\{\sqrt{\left(n_1^{\,2}+n_3^{\,2}\right)}+\sqrt{\left(n_2^{\,2}+n_3^{\,2}\right)}\right\}} \quad (3)$$

where ν_e is the absorption frequency (e.g., for H_2O: $\nu_e = 3 \times 10^{15}$ Hz). Table 4 provides non-retarded Hamaker constants determined with the Lifshitz theory (eq. 3).

In general, there is an attractive VDW interaction for $A > 0$, and the two macroscopic phases are attracted to each other. In cases where it is desired to have repulsive forces, the medium must have dielectric properties which are intermediate to the macroscopic phases.

Table 4: Non-retarded Hamaker constants for two interacting media across a vacuum (air) (Source: intermolecular & Surface Forces, J. Israelachvili, Academic Press) [3]

Medium	Dielectric constant ε	Refractive Index n	Absorption frequency[a] ν ($10^{15}s^{-1}$)	Hamaker Constant $A_{medium/air/medium}$ (10^{-20})
Acetone	21	1.359	2.9	4.1
Benzene	2.28	1.501	2.1	5.0
Calcium Flouride	7.4	1.427	3.8	7.0
Carbon tetrachloride	2.24	1.460	2.7	5.5
Cyclohexane	2.03	1.426	2.9	5.2
Ethanol	26	1.361	3.0	4.2
Fused quartz	3.8	1.448	3.2	6.3
Hydrocarbon (crystal)	2.25	1.50	3.0	7.1
Iron oxide (Fe_3O_4)		1.97	3.0 est	21
Liquid He	1.057	1.028	5.9	0.057
Metals (Au. Ag, Cu)			3-5	25--40
Mica	7.0	1.60	3.0	10
n-Pentane	1.84	1.349	3.0	3.8
n-Octane	1.95	1.387	3.0	4.5
n-Dodecane	2.01	1.411	3.0	5.0
n-Tetradecane	2.03	1.418	2.9	5.0
n-Hexadecane	2.05	1.423	2.9	5.1
Polystyrene	2.55	1.557	2.3	6.5
Polyvinyl chloride	3.2	1.527	2.9	7.5
PTFE	2.1	1.359	2.9	3.8
Water	80	1.333	3.0	3.7

[a]UV absorption frequencies obtained from Cauchy plots mainly from Hough and White (1980) and H. Christenson (1983, thesis).

Van der Waals Retardation Effects

The van der Waals forces are effective from a distance of a few Ångstroms to several hundreds of Ångstroms. When two atoms are a large distance apart, the time for the electric field to return can be critical, i.e., comparable to the fluctuating period of the dipole itself. The dispersion can be considered to be retarded for distances more than 100 Å, i.e., the dispersion energy begins to decay faster than $1/r^6$ ($\sim 1/r^7$). It is important to note that for macroscopic bodies retardation effects are more important than for atom-atom interactions. This is of particular importance for the SFM force displacement method.

Adhesion and Surface Energies

The energy of adhesion (or just *adhesion*), W'', i.e., the energy per unit area necessary to separate two bodies (1 and 2) in contact, defines the interfacial energy γ_{12} as:

$$W'' = 2\gamma_{12}; \quad \gamma_{12} = \gamma_1 + \gamma_2 - 2\sqrt{\gamma_1\gamma_2} \tag{4}$$

where γ_i (i= 1,2) represent the two surface energies. Assuming two planar surfaces in contact, the Van der Waals interaction energy per unit area is

$$W_1(D) = \frac{-A}{12\pi D^2} \text{ (see above)} \tag{5}$$

which was obtained by pairwise summation of energies between all the atoms of medium 1 with medium 2. The summation of atom interactions within the same medium have been neglected, which yields additional energy terms, i.e.,

$$W_2 = -const. + \frac{A}{12\pi D_o^{\,2}} \tag{6}$$

consisting of a bulk cohesive energy term (assumed to be constant), and an energy term related to unsaturated "bonds" at the two surfaces in contact (i.e., $D = D_o$). Notice that contact cannot be defined as $D = 0$ due to molecular repulsive forces. D_o is called the "cutoff distance". Hence the total energy of two planar surfaces at a distance $D \geq D_o$ apart is (neglecting the bulk cohesive energy)

$$W = W_1 + W_2 = -\frac{A}{12\pi}\left(\frac{1}{D_o^{\,2}} - \frac{1}{D^2}\right) = \frac{A}{12\pi D_o^{\,2}}\left(1 - \frac{D_o^{\,2}}{D^2}\right). \tag{7}$$

In contact (i.e., $D=D_o$) $W = 0$. In the case of isolated surfaces, i.e., $D = \infty$,

$$W = \frac{A}{12\pi D_o^{\,2}}. \tag{8}$$

Thus, in order to separate the two surfaces one has to overcome the energy difference

$$\Delta W = W(D_o) - W(D=\infty) = -\frac{A}{12\pi D_o^{\,2}}, \tag{9}$$

which corresponds to the adhesive energy per unit area of $W'' = 2\gamma_{12}$. Hence, the interfacial energy can expressed as function of the Hamaker constant and the cutoff distance:

$$\gamma_{12} = \frac{A}{24\pi D_o^2}, \tag{10}$$

Cutoff Distance for Van der Waals Calculations

The challenge is to determine the repulsive cutoff distance D_o, which unfortunately cannot be set equal to the collision diameter, σ (i.e., the distance between atomic centers). Let us assume a planar solid consisting of atoms that are close-packed. Each surface atom (of diameter σ) will have nine nearest neighbors (instead of 12 as in the bulk). When surface atoms come into contact with a second surface each atom will gain (12-9)w=3w=$3C/\sigma^6$ in binding energy. Thus, the energy per unit area, $S=\sigma^2\sin(60\text{ deg}) = \sigma^2\sqrt{3}/2$, is

$$\gamma_{12} = \frac{1}{2}\left(\frac{3w}{S}\right) = \frac{\sqrt{3}C}{\sigma^8} = \frac{\sqrt{3}C\rho^2}{2\sigma^2}; \quad \rho = \frac{\sqrt{2}}{\sigma^3}, \tag{11}$$

where ρ reflects the bulk atom density for a close packed system. Introducing the definition of the Hamaker constant, it follows

$$\gamma_{12} = \frac{\sqrt{3}C\rho^2}{2\sigma^2} = \frac{\sqrt{3}A}{2\pi^2\sigma^2} \approx \frac{A}{24\pi\left(\frac{\sigma}{2.5}\right)^2}, \tag{12}$$

For σ = 0.4 nm and $\gamma_{12} = A/(24\pi D_o^{\,2})$ it follows that D_o = 0.16 nm. D_o = 0.16 nm is a remarkable "universal constant" yielding values for surface energies γ that are in good agreement with experiments as shown in the Table 5.

Table 5: Surface energies based on Lifshitz theory and experimental values.(Source: intermolecular & Surface Forces, J. Israelachvili, Academic Press) [3]

		Surface Energy, γ (mJ/m^2)	
Material	**A** (10^{-20})	**Lifshiz Theory** $A/24\pi D_o^2$ {D_o=0.165nm}	**Experimental*** (20°C)
Liquid helium	0.057	0.28	0.12 - 0.35(at 4-1.6K)
Water	3.7	18	73
Acetone	4.1	20.0	23.7
Benzene	5.0	24.4	28.8
CCl_4	5.5	26.8	29.7
H_2o_2	5.4	26	76
Formamide	6.1	30	58
Methanol	3.6	18	23
Ethanol	4.2	20.5	22.8
Glycerol	6.7	33	63
Glycol	5.6	28	48
n- Pentane	3.75	18.3	16.1
n -Hexadecane	5.2	25.3	27.5
n -Octane	4.5	21.9	21.6
n -Dodecane	5.0	24.4	25.4
Cyclohexane	5.2	25.3	25.5
PTFE	3.8	18.5	18.3
Polystyrene	6.6	32.1	33
Polyvinyl chloride	7.8	38.0	39

Capillary Forces due to Vapor Condensation

In the discussion above we have considered a continuous medium in-between the two surfaces to deduce the surface forces. Thereby, we have assumed that this third medium fills up the vacuum space entirely, i.e., does not introduce interfaces. We have to drop this assumption, however, should the third medium form a finite condensed phase within the interaction zone of the two bodies. Any condensed phase within the interaction zone will exhibit interfaces towards the vapor, and thus, if deformed (e.g., stretched) contribute to the acting forces. These new forces, called *capillary forces*, are on the order of 10^{-7} N for single asperity contacts with radii of curvatures below 100 nm.

Capillary forces are meniscus forces due to condensation. It is well known that micro-contacts act as nuclei of condensation. In air, water vapor plays the dominant role. If the radius of curvature of the micro-contact is below a certain critical radius, a meniscus will be formed. This critical radius is defined approximately by the size of the Kelvin radius $r_K = l/(l/r_1 + 1/r_2)$ where r_1 and r_2 are the radii of curvature of the meniscus. The Kelvin radius is connected with the partial pressure p_s (saturation vapor pressure) by

$$r_K = \frac{\gamma_L V}{RT\, log\left(\frac{p}{p_s}\right)}, \tag{13}$$

where γ_L is the surface tension, R the gas constant, T the temperature, V the mol volume and p/p_s the relative vapor pressure (relative humidity for water). The surface tension γ_L of water is 0.074N/m (T=20°C) leading to a critical Van der Waals distance of water of $\gamma_L V/RT$ = 5.4 Å. Consequentially, we obtain for $p/p_s=0.9$ a Kelvin radius of 100 Å. At small vapor pressures, the Kelvin radius gets comparable to the dimensions of the molecules, and thus, the Kelvin equation breaks down.

The meniscus forces between two objects of spherical and planar geometry can be approximated, for D « R, as:

$$F^{R>>D} = \frac{4\pi R\gamma_L \cos\Theta}{(1 + D/d)}, \tag{14}$$

where R is the radius of the sphere, d the length of $\overline{PQ}$, see Figure 5, D the distance between the sphere and the plate, and θ the meniscus contact angle.

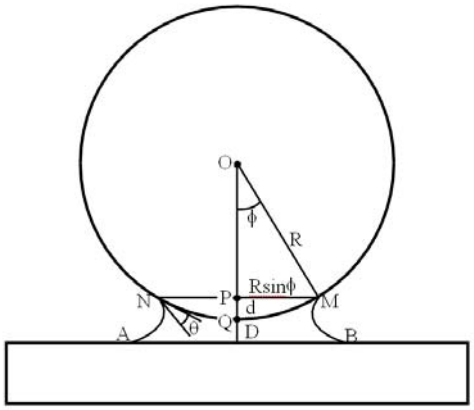

Figure 5: Capillary meniscus between two objects of spherical and planar geometry

The maximum force, found at at D = 0 (contact), is $F_{max}^{R>>d} = 4\pi R\gamma \cos\theta$. While this expression estimates the capillary forces of relatively large spheres fairly accurately, the capillary forces of highly wetted nanoscale spheres requires a geometrical factor K.

$$K = \frac{(1+\cos\phi)^2}{4\cdot\cos\phi} \tag{15}$$

where ϕ is the filling angle.

Critical Humidity for Capillary Neck Formation

SFM force displacement analysis studies involving hydrophilic counter-surfaces and water vapor have identified three humidity regimes with significantly different involvement of the third medium, as shown in Figure 6. At very low humidity (regime I), below a critical relative humidity (RH) of ~40 %, no capillary neck is developed, and the forces measured truly reflects VdW interactions. A capillary neck is formed at about 40 % RH, which leads to a force discontinuity observed between regimes I and II. We can understand this transition-like behavior of the pull-off force by considering the

minimum thickness requirement of a liquid precursor film for spreading. The height of the precursor film can not drop below a certain minimum, *e*, which is

$$e = a_0\left(\frac{\gamma}{S}\right)^{1/2} \;;\; a_0 = \left(\frac{A}{6\pi\gamma}\right)^{1/2} \;;\; S = \gamma_{SO} - \gamma_{SL} - \gamma\,, \tag{15}$$

where a_o is a molecular length, S the spreading coefficient, A the Hamaker constant, γ_{SO} the solid-vacuum interfacial energy, and γ_{SL} the solid-liquid interfacial energy. As the water vapor film thickness depends on the RH (i.e., p/p_s), a relative humidity smaller than 40 % does not provide a minimum thickness for the formation of a capillary neck. Once a capillary neck forms between the SFM tip and the substrate surfaces, the pull-off force increases suddenly, and provides over regime II a pull-off force that contains both, VdW and capillary forces. VdW forces from SFM FD analysis as determined, for instance, from regime I, see Figure 6(b), are on the order of 1-10 nN. The capillary force, on the other hand, is on the order of up to 100 nN, and thus, dominates VdW interactions in regime II.

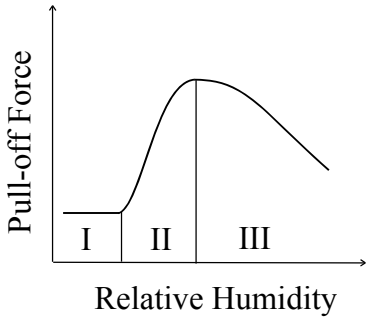

Figure 6(a): Generic sketch of the functional relationship between the pull-off force and the relative humidity (RH). Regimes I, II and III represent the van der Waals regime, mixed van der Waals – capillary regime, and capillary regime decreased by repulsive forces, respectively.

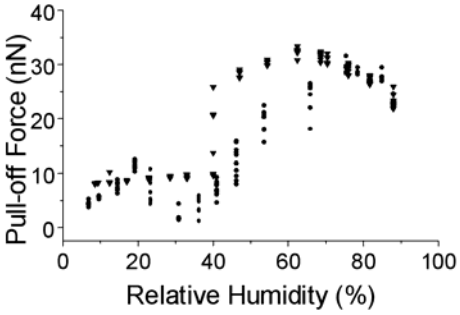

Figure 6(b): Pull-off force vs. RH measured between a hydrophilic silicon oxide SFM tip and a ultra-smooth silicon oxide wafer. λ measured for increasing RH, τ measured for decreasing RH. .[1]

In the high RH regime (III) the pull-off force decreases with increasing RH for hydrophilic counter-surfaces. At such high humidity, the water vapor film thickness dimensions exceeds the contact size (→ asperity flooding), and the effect of the capillary interface decreases.

Estimation of the Tip Radius Utilizing the Capillary Effects

The capillary effect, commonly not desired, can be useful in estimating the SFM tip radius. Assuming the absence of the flooding effect and the ionic salvation effect within regime III, as discussed in the previous section, the humidity dependent adhesion forces can be described as a mathematical model of sigmoidal form[4],

$$F_{mea} = (F_{stw} + F_{cap}) + \frac{F_{stv} - (F_{stw} + F_{cap})}{1 + \exp[(\varphi_0 - \varphi)/m]} \tag{16}$$

where F_{mea} is the experimentally determined pull-off forces,
F_{stv} is the van der Waals interaction force between the sample and the tip in water vapor,
F_{stw} is the van der Waals interaction force between the sample and the tip in liquid water,
F_{cap} is the capillary force, ϕ is the relative humidity (in fraction),
φ_0 is the mid-point of the transition regime, and
m is the transition width.

As shown in Figure 7, the forces, F_{stv}, F_{stw}, and F_{cap}, *are* components of the measured pull-off force F_{mea}. When the relative humidity is below the transition regime, i.e., $\varphi < \varphi_0$, the F_{mea} consists F_{stv} only, represents the lower limit of the sigmoidal fit. Above the transition regime, F_{mea} is the sum of F_{stw} and F_{cap}, represents the upper limit of the sigmoidal fit.

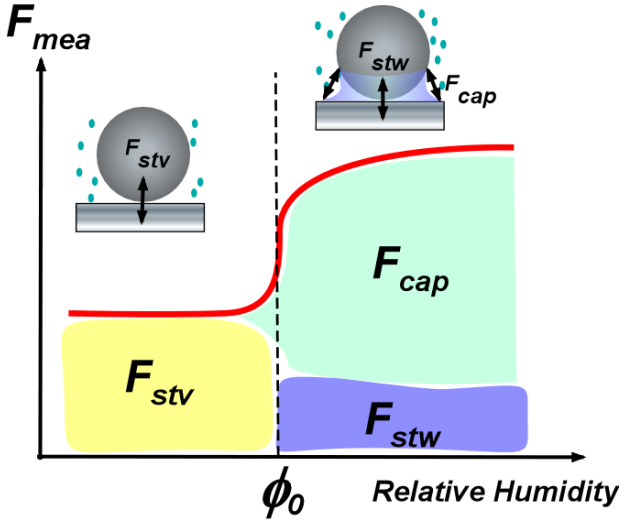

Figure 7: The components of full-off forces in humid environment.

The F_{stw} and F_{stv} can be expressed by assuming that the contact is between an incompressible sphere and a hard flat surface, i.e. Bradley's model (see page 24),

$$F_{stv} = 2\pi \cdot R \cdot W_{stv} \text{ or } F_{stw} = 2\pi \cdot R \cdot W_{stw} \qquad \text{(17a or 17b)}$$

where R is the sphere radius (i.e. SFM tip radius), W is the work of adhesion which is expressed as,

$$W_{ijm} = \gamma_{im} + \gamma_{jm} + \gamma_{ij} \qquad (18)$$

where γ is the interfacial energies of the two materials, and i, j, m represents solid i, solid j, and the medium m in which the contact take place, respectively. If the contact is between two solids with the same material, i.e., $i = j$, Eq. (18) reduces to $W_{ijm} = 2\gamma_{im}$.

In order to determine the tip radius R, Eq. (17a) is solved for R using experimentally determined F_{stv}. The R value is then used to determine F_{stw} through Eq. (17b), and F_{cap} is deduced. Employing the geometric coefficient K for the capillary force equation,

$$F_{cap} = 4\pi \cdot R \cdot \gamma_{water} \cos\theta \cdot \frac{(1+\cos\phi)^2}{4 \cdot \cos\phi} \qquad (19)$$

the filling angle ϕ can be deduced. For example, the result obtained by He et. al.[1] on the silicon wafer surface, was analyzed using this model. Using the value of $\gamma_{SiO/air}$ 100 mJ/m^{25}, $\gamma_{SiO/water}$ 24.5 mJ/m^{25}, γ_{water} 72.8 mJ/m^2, and the contact angle Θ of 0 °, the tip radius R and the filling angle ϕ was determined to be 8.7 nm and 85.6 ° respectively.

Modification of Hydrophobicity (Wettability)

Capillary effect is absent when the surface is hydrophobic, i.e., non-wetting, and hydrophobic silicon surfaces can be created with appropriate treatment. In general, the degree of hydrophobicity (wettability) depends on the surface chemistry and micro roughness. One most common technique to measure hydrophobicity is the contact angle measurement. As shown in Figure 8, a droplet of water is placed on a surface of interest and the angle Θ which the water forms with the surface is evaluated. When the angle is smaller than 90 °, the surface is said to be more hydrophilic or wetting. When the angle is larger than 90 °, the surface is rather hydrophobic (non-wetting). The contact angle results from the energy balance between the solid surface, vapor, and the liquid, hence the contact angle, although it is not straightforward, can be used to deduce the surface energy γ. It should be noted that the surface energy (interchangeably called interfacial energy, surface tension), is an important parameter in evaluating the surface forces, as it can be seen in multiple equations presented in previous sections.

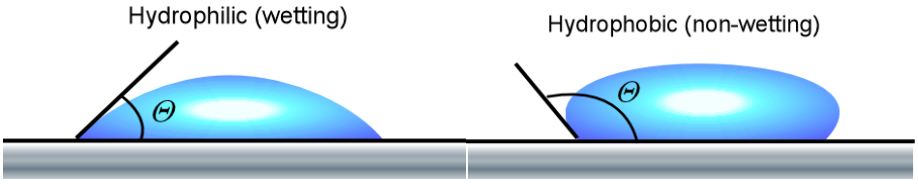

Figure 8: The contact angle measurement. The contact angle Θ is the measure of hydrophobicity (wettability). Left: hydrophilic surface. Right: hydrophobic surface.

The hydrophobicity is a major concern in semiconductor industries, such as IC (integrated circuit) board manufactures and microelectronic technology. Because such devices are used in ambient environment, i.e. humid air, the surfaces are prepared carefully to have both the desired functionalities and the surface characteristics. A silicon wafer is made out of pure silicon, Si**,** but the surface without any special treatment, is in an oxidized form silicon, SiO_x, a hydrophilic surface. This oxide layer can be etched out by HF (hydrofluoric acid), leaving the surface with hydrogen-terminated silicon, more hydrophobic. Figure 9 is actual photographs of the contact angle measurement on a series of silicon surfaces. Figure 9(b) is as-is silicon surface which is cleaned with organic solvent. This surface is SiO_x covered with residual organic impurities, generating partially wetting (hydrophilic) surface. When the solvent cleaned surface was further treated with UV/Ozone cleaner, which removes the residual organics on the surface, the surface showed complete wetting with the contact angle of 0 °, Figure 9(a). On the other hand, if the surface was treated with HF, the contact angle is rather large ~ 72 °, thus it is rather hydrophobic surface, Figure 9(c). Although this HF treated surface posses desirable hydrophobicity, the surface is not stable due to its high surface energy. Studies found that the hydrogen-terminated surface in ambient air is oxidized within several hours, resulting in creating naturally grown SiO_x layer on the surface.

(a) **(b)** **(c)**

Figure 9: The contact angle measurement of silicon surfaces (a) clean SiOx surface, (b) SiOx covered with organic impurities, (c) HF treated Si surface.

Force Displacement Curves

In SFM force displacement (FD) analysis, the normal forces acting on the cantilever are measured as a function of the tip-sample displacement. In other words, the tip-sample distance could not be precisely controlled due to the flexibility of the cantilever. As a result, the FD curve jumps the path of the force curve as illustrated in Figure 10. Figure 10(a) shows the cantilever approach from point D_0. When the distance reaches point A_0 an instability occurs resulting in a jump into contact to point B_0. On the retraction out of contact an instability occurs at point C_0 causing the cantilever tip to snap out of contact back to point D_0. As a result the typical force distance curve is shown in Figure 10(b). Each segment of the curve is described as follows.

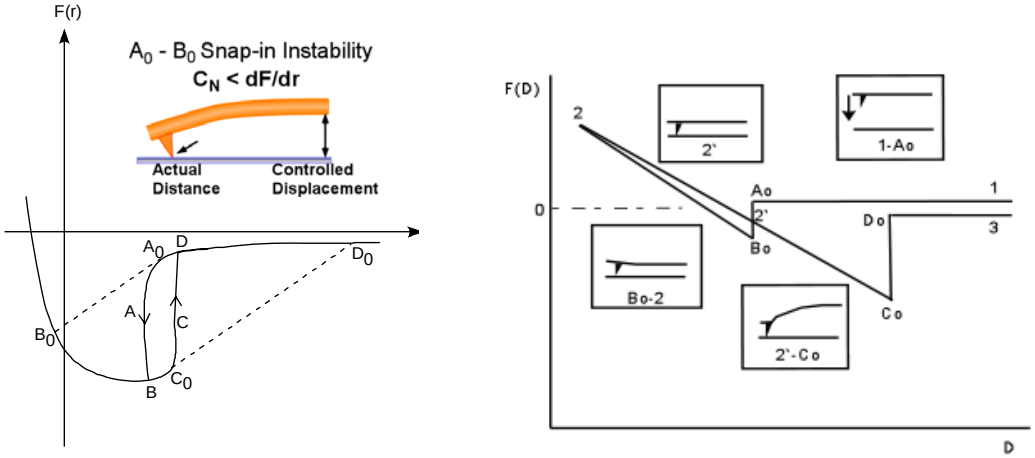

(a) **(b)**

Figure 10: (a) The actual path taken by a SFM cantilever. The inset illustrates the snap-in instability at A_0 where the second derivative of the interaction potential exceeds the spring constant of the cantilever. **(b)** Typical force distance curve. D = displacement, $F(D)$ = force.

1. *Line 1-A_0:* The probe and sample are not in contact but the tip is moving toward the sample.
2. *Line A_0-B_0:* Jump into contact caused by the attractive van der Waals forces outweighing the force of the cantilever spring between the tip and the sample causing the cantilever to bend.
3. *Line B_0-2:* Shows upward deflection of the cantilever in response to the sample motion after they are in contact. The shape of the segment indicates whether the sample is deforming in response to the force from the cantilever. (may not always be straight) If the sample is assumed to be a hard surface, the slope of this line is the sensitivity (springiness) of the cantilever.

4. *Line 2-C_0:* As the tip moves away, the slope follows the slope of line B_0-2 closely. If line *2-C_0* is parallel to line B_0-2, no additional information can be determined. However, if there is a difference in the in and out-going curves (hysteresis) gives information on the plastic deformation of the sample. Once it passes point 2', the cantilever begins to deflect downward due to adhesive forces..
5. Line C_0-D_0: A jump out of contact occurs when the cantilever force exceeds the adhesive forces.

The jump out of contact distance will always be greater than the jump into contact distance because of few possible causes are:

a. During contact, some adhesive bonds are created.
b. During contact, the sample buckles and "wraps" around the tip, increasing the contact area.
c. Hysteresis contributions
d. Capillary forces exerted by contaminants such as water.

FD analysis is widely used for adhesion and force interaction studies. Recently biological materials have been studied by force spectroscopy, such as adsorption strength of proteins on a substrate and folding/unfolding energy of DNAs.

References

1 M. He, A. Blum, D. E. Aston, C. Buenviaje, and R. M. Overney, Journal of chemical physics **114** (3), 1355 (2001).
2 H. Hertz, J. Reine und Angewandte Mathematik **92**, 156 (1882).
3 J. N. Israelachvili, *Intermolecular and surface forces*. (Academic Press, London, 1992).
4 D. L. Sedin and K. L. Rowlen, Analytical Chemistry **72**, 2183 (2000).
5 C. Ziebert and K. H. Zum Gahr, Tribology Letters **17** (4), 901 (2004).
6 J. A. Greenwood, Proc. R. Soc. Lond. A **453**, 1277 (1997).

Recommended Reading

Contact Mechanics by K. L. Johnson, Cambridge University Press, Cambridge, 1985.
Gases, liquids and solids and other states of matter by D. Tabor, Cambridge Univ. Press, Cambridge, 3rd ed. 2000.
Intermolecular and surface forces by J. N. Israelachvili, Academic Press, London, 1992.
Nanoscience: Friction and Rheology on the Nanometer Scale by E. Meyer, R. M. Overney, K. Dransfeld, and T. Gyalog, World Scientific Publ., Singapore, 1998.

5. Appendix

The following MS-Excel based tools are provided. See Excel Toolbox.

Tool for Sigmoidal Data Fit

Lab Unit 1: Analysis Work Sheet

(1) Input the values in the blue cells.
(2) Select "Solver" from Tools
(3) Set the Target cell to the yellow cell
(4) Select Min (minimum) for Equal to.
(5) Set by Changing Cells to the purple cells
(6) Click Solver to obtain the fit parameters (which appears to the purple cells)
Note: DO NOT CHANGE the pink cells

Fit Paramaters	
m	0.80950955
$F_{cap} + F_{stw}$	32.86757066
F_{stv}	10.58973278
φ_0	40.39442756

$$F_{mea} = (F_{stw} + F_{cap}) + \frac{F_{stv} - (F_{stw} + F_{cap})}{1 + \exp[(\varphi - \varphi_0)/m]}$$

Relative Humidity (%RH)	Average F_{mea} [nN]	Fit Model	Sqrt
88.00	25.05	32.87	7.81293
81.70	29.40	32.87	3.46988
76.00	31.63	32.87	1.23269
70.40	33.33	32.87	0.46706
68.60	34.15	32.87	1.28173
62.39	35.05	32.87	2.18528
53.94	32.87	32.87	0.00002
42.51	31.34	31.34	0.00001
39.84	18.04	18.04	0.00001
33.00	11.57	10.59	0.97950
28.50	11.37	10.59	0.77533
22.90	11.04	10.59	0.45478
17.00	10.59	10.59	0.00000
12.40	10.43	10.59	0.16249
9.30	10.21	10.59	0.38416
8.50	10.01	10.59	0.57933
		Target Cell	19.78519

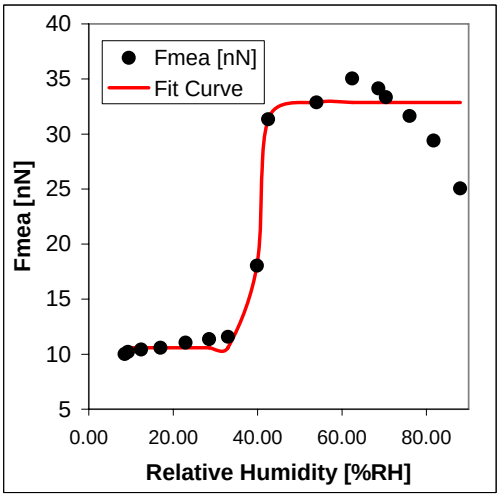

Tool for Hamaker Constant Calculation (provided in Excel Toolbox)

Lab Unit 1: Hamaker Constant Calculation
(1) Enter the given input parameters in the yellow boxes
(2) Enter the given dielectric constants and refractive indices in the orange and green boxes respectively
(3) The Hamaker constant and the interaction strength are given in the highlighted cells

Parameters	
T (K)	300
k (J/K)	1.38E-23
h (Js)	6.63E-34
υ_e (Hz)	3.00E+15
R (nm)	50
D_0 (nm)	0.16

$$A \approx \frac{3}{4} kT \left(\frac{\varepsilon_1 - \varepsilon_3}{\varepsilon_1 + \varepsilon_3} \right) \left(\frac{\varepsilon_2 - \varepsilon_3}{\varepsilon_2 + \varepsilon_3} \right) + \frac{3h\upsilon_e}{8\sqrt{2}} \frac{\left(n_1^2 - n_3^2 \right) \left(n_2^2 - n_3^2 \right)}{\sqrt{\left(n_1^2 + n_3^2 \right)} \sqrt{\left(n_2^2 + n_3^2 \right)} \left\{ \sqrt{\left(n_1^2 + n_3^2 \right)} + \sqrt{\left(n_2^2 + n_3^2 \right)} \right\}}$$

$$W(D) = \frac{-AR}{6D}$$

Material Properites				
	Dielectric Constants		Refractive Indices	
Phase 1	ε_1	3.78	n_1	1.45
Phase 2	ε_2	3.78	n_2	1.45
Medium	ε_3	1	n_3	1

A[J]	W[J]
5.97E-20	-3.11E-18

LAB UNIT 4: Force Modulation Microscopy

Specific Assignment: Thermomechanical Viscoelastic Response Study

Objective

This lab unit introduces a scanning force microscopy (SFM) based mechanical (sinusoidal) perturbation method referred to as force modulation microscopy, to explore thermomechanical properties in polymers around the glass transition.

Outcome

Learn about the basic principles of contact mechanics and polymer viscoelasticity, and conduct force modulation studies as a function of temperature below and above the polymer glass transition.

Synopsis

Force modulation microscopy provides surface sensitive local information about nano-mechanical properties, such as material stiffness (moduli), hardness, elastic-plastic yield points, and viscosity. As SFM based methods operate with nanoscale probing areas, perturbation-induced material activation into metastable configurations can be to a great part avoided, which makes force modulation microscopy very sensitive to “true” (equilibrated) material properties. This is illustrated with this project utilizing with small amplitude normal modulations at a variety of temperatures around the glass transition of poly-t-butylacrylate and polystyrene thin films.

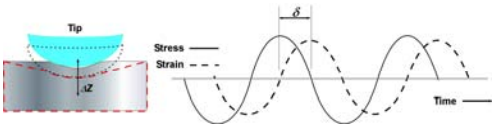

Force Modulation Spectroscopy applied to Local Glass Transition at Polymer Surface

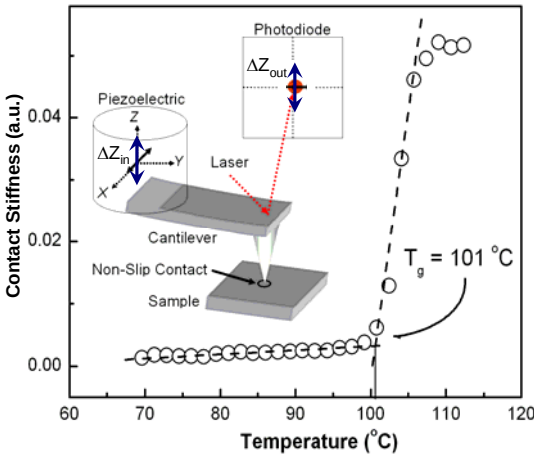

Materials

Poly-t-butylacrylate spin-coated film (> 100 nm) on silicon substrates.

Technique

SFM force modulation microscopy

Table of Contents

1. Assignment

The assignment is to locally investigate the nano-thermomechanical properties of thin film polymers utilizing normal force modulation microscopy, and to employ the theories and background information to discuss the experimental results. The steps are outlined here:

1. Familiarize yourself with the background information provided in Section 4.
2. Test your background knowledge with the provided Quiz in Section 2.
3. Conduct the force modulation experiments in Section 3. Follow the experimental step-by-step procedure.
4. Analyze your data as described in Section 3
5. Finally, provide a report with the following information:
   (i) Result section: In this section you show your data and discuss instrumental details (i.e., limitations) and the quality of your data (error analysis).
   (ii) Discussion section: In this section you discuss and analyze your data in the light of the provided background information.
   It is also appropriate to discuss section (i) and (ii) together.
   (iii) Summery and outlook: Here you summarize your findings and provide an outlook on how one could proceed.
   The report is evaluated based on the quality of the discussion and the integration of your experimental data and the provided theory. You are encouraged to discuss results that are unexpected. It is important to include discussions on the causes for discrepancies and inconsistencies in the data.

2. Quiz – Preparation for the Experiment

Theoretical Questions

(1) (*3pts*) Determine the contact area for a JKR contact at which the contact becomes unstable.

(2) (*3pts*) Describe the two terms *solid-like* and *liquid-like* using the two simple models of Hooke's law of elasticity and Newton's law of viscosity.

(3) (*3pts*) List methods that are use to determine the glass transition temperature. What property are they actually sensitive to?

(4) (*3pts*) At the glass transition temperature, the response signal of SM-FM that is proportional to the contact stiffness is increasing noticeably. Considering that the modulus for many polymers decreases by orders of magnitude from the glassy state to the rubbery state (e.g., in the case of polystyrene PS by about 4 orders of magnitude from 10^9 N/m^2 to 10^5 N/m^2), the probing contact area of SM-FM has to increase substantially to compensate for the reduction in the material stiffness. This is based on the Herzian relationship between the contact stiffness and the modulus, i.e, $k_c = 2aE$ (for normal distortion), or $k_c=8aG$ (for lateral distortion).
Evaluate with the Hertzian model, the relative degree of contact area increase for polystyrene.

(5) (*3pts*) Glass transition and Gibbs free energy.
(a) Show in a V(T) diagram the distinct difference between melt/freezing transition and a glass transition
(b) How are changes related to the specific heat and volume obtained from Gibbs free energy.

Prelab Quiz

(1) (*10 pts*) For a sinusoidal FM microscopy experiments, the input modulation amplitude A_{in} and the output signal amplitude A_{out} shall be known in volts that are applied to the piezo (PZ) and received from the photo diode (PD), respectively. The conversion sensitivity factors S_{PZ} and S_{PD} are used to convert the two signals into nanometer.
(a) Determine formally the root mean square (RMS) amplitudes in nanometer.
(b) With the appropriate RMS amplitudes determine the force that is acting on a cantilever with spring constant k_L.
(c) Assuming an ideal spring model as depicted in Figure 3, what is the force acting on the sample?
(d) Provide an expression for the sample deformation δ as function of A_{in} and A_{out}.
(e) Express the the contact stiffness as function of δ, A_{in}, A_{out}.*and* k_L.

(2) (*10 pts*) FM microscopy utilized a function generator with a sinusoidal input modulation to the piezo. The cantilever response modulation signal $A_{out}\sin(\omega t+\phi_{out})$ is detected with a laser detection scheme by the photodiode. Because the signals are very small, i.e., within the noise level of the signal, a lock-in technique is used. The lock-in amplifier, a phase sensitive detector (PSD), compares the photodiode signal with the input signal to the piezo, $A_{in}\sin(\omega t+\phi_{in})$, as a reference signal. Note that both signals are not only defined by their amplitude and frequency but also by their phase ϕ. The output signal of the lock-in amplifier V_{psd} is the product of two sine waves, i.e.,

$$V_{PSD} = A_{in}A_{out}\sin(\omega t+\phi_{in})\sin(\omega t+\phi_{out})$$

This signal is composed of two AC signals, one with frequency $\omega_{in}+\omega_{out}$ and $\omega_{in}-\omega_{out}$ and is heavily low pass filtered. Consequently, as in our case, only a non-zero DC signal comes through for $\omega_{in} = \omega_{out} = \omega$. In other words the lock-in technique is frequency discriminating the signal it receives based on the reference signal. The quantities that matter are the amplitudes, and the phase shift $\phi = \phi_{in} - \phi_{in}$. As the phase of the phase signal of the input signal to the piezo is arbitrary, we will define it generally as zero, i.e., $\phi_{in} = 0$. The situation described here, is illustrated in the figure below, expressing the frequency discriminated signal V_{PSD} in complex form, i.e.,

$$V_{PSD}^{*} = Re^{(\omega t+\phi)}$$

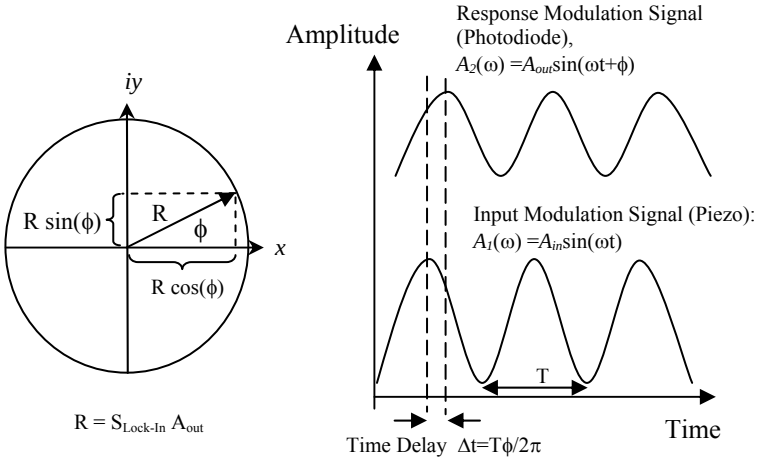

Describe the operation of the function generator. How would you expect the phase angle to differ between solid-like and liquid-like materials?

3. Experimental Assignment

Goal

Following the step-by-step instruction below, determine the glass transition temperature of the polystyrene film. Analyze and discuss the data with the background information provided in Section 4. Provide a written report of this experiment.

Specifically provide answers to the following questions:

(1) What is the observed glass transition temperature for poly (t-butyl acrylate)? Does this value correlate with the literature value? What factors would cause the observed *Tg* value to be different from the literature?
(2) Why is Modulated Force Microscopy effective at determining the glass transition temperature?
(3) What is the magnitude of the cantilever modulation?
(4) What is the relationship between contact stiffness and normal load? Does this relationship depend on temperature?
(5) What is the relationship between contact stiffness and adhesion force?

Safety

- Wear safety glasses.
- Refer to the General rules in the AFM lab.
- The heating module should be off when it is not in use.

Instrumental Setup

- Easy Scan 2 AFM system with long contact Mode SFM tip with 0.2 N/m spring constant with NO Aluminum coating.
- Heating stage with controller.
- Lock-in amplifier with two long BNC cables

Materials

- Samples: 2 pieces of $\sim 1 cm^2$ Spin-coated PtBA film on silicon substrate, stored in sealed Petri dishes until ready for the experiment. The sample PtBA (M_w = 137.3k) is spin cast onto an organic contaminant-cleaned (possibly also oxide treated) silicon wafer and annealed above its glass transition temperature in a vacuum oven. Preferred film thicknesses are between 100 to 500 nm. Recommended pretreatments of the silicon substrate: (i) sonication, (ii) UV/ozone cleaning, and (iii) hydrofluoric acid treatment. More information is provided at the end of the experimental procedure.

Experimental Procedure

Read carefully the instructions below and follow them closely. They will provide you with information about (i) preparation of the experiment, (ii)) the procedure for force modulation microscopy and temperature control, (iii) the procedure for closing the experiment, and (iv) on how to conduct the data analysis.

(i) Preparation of the experiment

(1) System Set-up: (This part will be performed with a TA) Place BT00250 silicon sample grid on heater stage

(2) Follow the start up procedure **step 1 – 8**, in Easy Scan 2 AFM System SOP (Standard Operational Procedure).
   a. Place a CONTR cantilever with the spring constant of 0.2 N/ m.

(3) Connect BNC cables:
   a. from Function Generator *Function* output to *Excitation* Input on Nanosurf Break Out Box
   b. from Function Generator Function output to Lock-In *REF IN* signal (reference)
   c. from *Current or Deflection* Output on Nanosurf Break Out Box to Oscillscope Signal *1*
   d. From Oscilloscope Signal *1* to Lock-In Signal *A*

(ii) Determining Probe/Photodiode Sensitivities

(1) Under **Positioning Window:Approach Options** uncheck **Auto. Start imaging**

(2) Under **Positioning Window:Video Options** set **Illumination, Brightness** and **Contrast** to 0, 0 and 0 respectively

(3) Come in to contact with the sample and scan enough lines to clearly see grid pattern

(4) Under **Z-Controller:Z-Controller Mode** set **Z-Feedback algorithm** to **Standard PID**

(5) Under **Z-Controller** set **Set point** to 100nN

(6) Under **Z-Controller** set **P-Gain**, **I-Gain** and **D-Gain** (**PID)** to 0,0 and 0 respectively

(7) On the oscilloscope, determine in mV the height of the grid step (corresponds to 100nm actual height)

(8) Stop the scan

(9) Turn on the function generator
   a. Set frequency: Push **FREQ – 50 – Hz/V_{pp}**
   b. Set Amplitude: Push **AMPL – 5 – Hz/V_{pp}**

(10) On the oscilloscope measure the peak to peak height of the probe oscillation (in mV)

(11) Repeat for multiple frequencies, filling out the following table (use result from **ii-6** to determine displacement)

Frequency (Hz)	Amplitude (mV)	Sensitivity(nm/mV)	Displacement (nm)
50			
100			
150			
200			
300			
500			
750			
1000			

(12) Withdraw probe and set function generator amplitude to 0
(13) Set **Illumination, Brightness** and **Contrast** to 50, 50 and 50 respectively

(iii) Determining PtBA Glass Transition

(1) Replace Si grid with PtBA sample
(2) Reset **PID** gains to 10,000 , 1000 and 0 respectively
(3) Under **Approach Options** set **Tip-Position** to 4μm advanced
(4) Set **Illumination, Brightness** and **Contrast** to 0, 0 and 0 respectively
(5) Approach sample and come into contact
(6) Scan sample surface and identify a clean, smooth area between 1μm and 5 μm in size
(7) **Zoom** in on smooth area
(8) After ~5 scan lines, stop scan and set **PID** gains to 0, 5 and 0 respectively
(9) Set function generator amplitude to 5V and frequency to 200 Hz
(10) Open heater software at **Desktop:contactlab:HEATER-CONTROL: TC-36-25RS232rev.A.exe**
(11) Initialize Heater in Heater program
   a. Set **FIXED SET TEMP** to 25.00
   b. Set **SELECT COMM PORT** to COM2
   c. Click **CommCheck** (if system ready, proceed. Otherwise seek TA)
   d. Click **INITIALIZE**
      Verify that **OUTPUT ON/OFF** is now **ON**
(12) Wait 4-5 minutes for equilibrium
(13) By hand, record for ~30 seconds the **R** value from the lock-in
(14) For the first (25°C) and last (45°C) temperatures record **R** as a function of load (**Set point**) (make sure to use 100nN for all other temperatures)

Load (nN)	$R_{25°C}$ (mV)	$R_{45°C}$ (mV)
20		
40		
60		
80		
100		

(15) By changing **FIXED SET TEMP** in the heater program, repeat steps 11-15 for temperatures from 27 to 45°C in increments of 2°C
(16) Cool system back to 25°C
(17) Obtain a force-distance curve for each temperature:
   a. Set modulation amplitude to 0
   b. Set **PID** gains to 10000, 1000 and 0 respectively
   c. Scan image for at least 15 lines
   d. Follow Easyscan2 AFM F-D SOP to determine F_{ADH}
   e. If F_{ADH} exceeds the range of the z-piezo, a value can be extrapolated
(18) Fill in all data in the table below

Temperature (°C)	R (mV)	F_{ADH} (nm)
25		
27		
29		
31		
33		
35		
37		
39		
41		
43		
45		

(19) Withdraw tip, set heater temperature to 25°C, set function generator amplitude to 0

(20) Shut down the AFM system by following the shutdown procedure described in Easy Scan 2 AFM system SOP

(iv) Instructions for Data Analysis

(1) T_g analysis

a. Plot R vs temperature and the identify transition onset.

b. How large is the change in R as the sample goes through its transition?

c. What other parameters could be investigated to maximize T_g sensitivity?

(2) Contact mechanics analysis

From the back ground:

$$\frac{k_c(\omega)}{k_c(\omega)\big|_{L=0}} = \left[\frac{1+\sqrt{1-L/F_{adh}}}{2}\right]^{2/3}$$

a. Using the load dependence data above and below T_g, determine the limiting value of R as load goes to 0 (i.e. plot R vs Load and determine R intercept). Do you observe a difference in load dependence below and above T_g? Why might the behavior differ above and below T_g? Is your data consistent with this rationale?

b. Given that R is proportional to contact stiffness, plot R vs

$$\left[\frac{1+\sqrt{1-L/F_{adh}}}{2}\right]^{2/3}.$$

What is the nature of the observed trend? If the above equation were perfectly obeyed, how should the plot appear? Sketch this expectation on your same plot. Do you think the equation is valid for describing you system below T_g? Above T_g?

c. Plot R vs F_{adh} and describe the observed trend.

(v) Silicon Pretreatment Prior to Spin Coating

The pretreatment of silicon addresses (A) organic condamination and (B) and control of the oxide surface via HF treatment. Best treatment is achieved with (A) and (B). As HF surface treatment has to follow very strict safety requirements, it might be better that the proecude is conducted by a well trained TA instead of undergraduate students.

Safety

(1) Follow the general rules for Nanotechnology Wet-Chemistry Lab at your Institution.
(2) This lab uses **Hydrofluoric Acid (HF)**. Exposure to HF is extremely dangerous. Prior to the use of HF, read the **emergency procedures for HF exposure in the appendix and consult the safety regulations in your institution**, and receive a **formal HF handling training** prior to working with HF.
(3) The UV/Ozone cleaner should be **OFF** before opening the sample tray.
(4) Always handle silicon wafers with tweezers, not with your fingers. Wafer edges can be very sharp.
(5) All solvent wastes are disposed into designated waste bottles located under the hood.
(6) All silicon waste are disposed into the sharp object waste box.

(A) Removal of Organic Condaminants

Depending on the degree of condamination solvent cleaning and UV/Ozone treatment are recommended.

Materials

(1) 4 pieces of Silicon wafers (~1cm^2 size pieces)
(2) Millipore H_2O
(3) Acetone
(4) Methanol
(5) A 150 ml beaker, a caddy and a watch glass for sonication
(6) A waste beaker for organic solvent
(7) A plastic waste beaker.
(8) Fine point tweezers
(9) N_2 gas with 0.2 micron filter.
(10) 3 Petri dishes and para-film for finished samples.
(11) UV/Ozone cleaner.
(12) Sonicator
(13) DI water

Procedure

(1) **Solvent cleaning:** Removes organics off of the silicon surfaces.
   a. Place silicon wafers in the caddy fitted in a 150 ml beaker and pour Acetone to fill upto~ 60 ml.
   b. Fill the sonicator with water. Place the beaker and adjust amount of water so that the water in the sonicator is about at the surface level of Acetone in the beaker.
   c. Cover with the watch glass.
   d. Turn on the sonicator and run for 15 minutes.
   e. Turn off the sonicator and remove the beaker.
   f. Lift up the caddy (with silicon wafers) and drain the acetone into a waste beaker. Place the caddy back into the beaker.
   g. Pour small amount of methanol for rinsing. Drain the methanol into the waste beaker. Repeat once.
   h. Fill the beaker with Methanol upto ~ 60 ml.
   i. Place the beaker back in to the sonicator. Cover with the watch glass.
   j. Sonicate for 30 minutes. Take the beaker out when done.

k. Lift the caddy and pour out the methanol into the waste beaker. Rinse with Millipore water at least three times. Return the caddy back into the beaker and fill with Millipore water.
l. Pick up a piece of wafers with tweezers and rinse with flowing Millipore water. Blowdry it with N_2 gas.
m. Place the dried silicon wafers in a Petri dish. Cover the Petri dish.
n. Transfer the waste solvent mixture (of acetone, methanol and water) into the designated solvent waste bottle. Rinse the waste beaker with DI water. The spent water is also drained into the waste bottle. Note: Don't use this waste beaker for the HF process.
o. Empty out the sonicator and allow drying.

(2) **UV/Ozone treatment**: Removes any trace of organics off of the surface.

a. Make sure the UV/Ozone cleaner is OFF.
b. Open the sample tray and place two of the silicon wafers. Leave the other two for HF treatment.
c. Close the tray.
d. Turn on the power switch.
e. Set a timer to 30 minutes and start.
f. Turn of the power switch when done. Open the sample tray and take the silicon wafers out and place them into a Petri dish and seal it with parafilm.

(B) HF Treatment

Hydrofluoric acid (HF) is used to remove the oxide layer and hydrogen passivate the surface, i.e., generates a hydrophobic surface. This surface is known to still grow an oxide layer (~ 2 nm think over ½ hour).

Additional Materials for HF treatment
(14) HF and HF handling tool kit (vials, vial stand, teflon coated tweezers)
(15) An extra large (~1000ml) waste beaker for HF

Procedure

- Be well prepared for the HF procedure. Wear TWO LAYERS of NITRILE gloves, a lab coat and a goggle. Make sure to be covered as much as possible. If you have long hair, tie it back. If you have facial hair, you might want to wear a mask.
- Decide who is operating the main HF procedure (Leader) and who is operating the sub-tasks around the main HF procedure (Assistant).
- Alert others that you are about to work with HF.
- Have the third person ready for any assistance. This person can remind you and your partner the steps in the procedure, interact with others in the lab, open and close the N_2 gas tank, etc.

g. Clear the working surface in the hood.
h. Fill an extra large waste beaker with water filled 70%. Place it under the hood.
i. Place a plastic waste beaker under the hood.
j. Have Millipore water and DI water filled in squeeze bottles. Place them under hood.
k. From this point on, separate tasks as directed.
l. **Leader** Place the HF tool kit basket under the hood. Places the vials in the vial stand in front of the basket.
m. **Leader** pours the Millipore water into the 4 HF vials up to the 15 ml mark.
n. **Leader** places the Teflon coated tweezers into the #4 vial. Note that the Teflon coated tweezers will be placed in the #4 vial whenever it is not used.
o. **Leader** opens the HF bottle. The mouth should be facing the back of the hood, not you. Add 5-6 drops of HF in the vial #1.

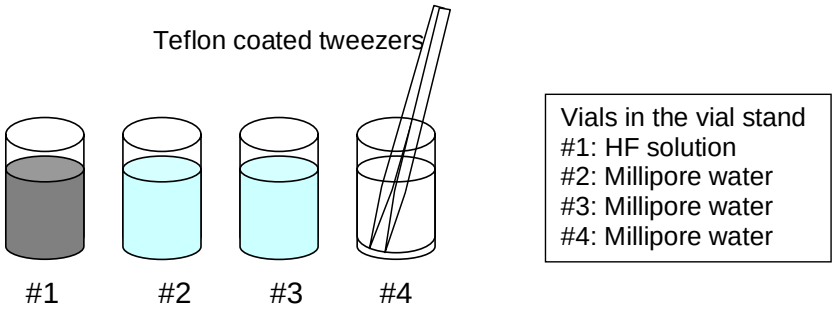

p. **Assistant** places a silicon wafer in HF vial #1 using a tweezers. Don't submerge the tweezers in the HF solution. Wait for 5 minutes or more.
q. **Leader** takes the silicon wafer out using the Teflon coated tweezers and place it in the vial #2, and transfer it into the vial #3.
r. **Leader** takes the silicon wafer in the vial #3 out. Hold it over the plastic waste beaker for rinsing with copious amount of flowing Millipore water.
s. **Assistant** takes over the silicon piece with a tweezers. Blow Dry it with N_2 gas. Make sure it is completely dry. Place it in a Petri dish.
t. Repeat for the second silicon piece.
u. HF treatment is done. Follow the **cleaning procedure**.
v. **Leader** pours the HF solution out of the vial #1 into the extra large waste beaker. Rinse it with copious amount of flowing DI water.
w. **Leader** places the clean vial back to the vial stand.
x. Repeat for the vial #2, #3, and #4. Rinse the Teflon coated tweezers likewise. Lay on the vial stand.
y. **Leader** places the vial stand into the HF tool kit basket. Place the basket into a designated storage location. Ask the third person for opening drawers/doors.
z. **Assistant** Transfer the extra large waste beaker and the plastic waste beaker into a sink with flowing water. Let it rinse it for 5 minutes.
aa. **Leader and Assistant** take the top layer of the gloves off. Through them out INSIDE OUT in a regular trash can.
bb. While **Leader** wipes the working surfaces with wet/dry paper towels, **Assistant** finish washing the waste beakers.
cc. Make sure to clean everywhere Leader and Assistant touched: the N2 gas nozzle tube, water squeeze bottles, the water faucet.
dd. When done, take the second layer of gloves off INSIDE OUT. Through it in a regular trash can.

4. Background: Contact Mechanics and Viscoelastic Phenomena of Polymers

Table of Contents:

Contact Mechanics – Fully Elastic Models

Hertz analyzed the stresses at the contact of two elastic solids, and thereby assumed small strains within the elastic limit. The contact radius *a* is considered significantly smaller than the radius of curvature *R,* and the two contacting surfaces, as depicted in Figure 1, assumed to be non-conformal. Furthermore, creep at the interface is neglected; i.e., a frictionless contact assumed.

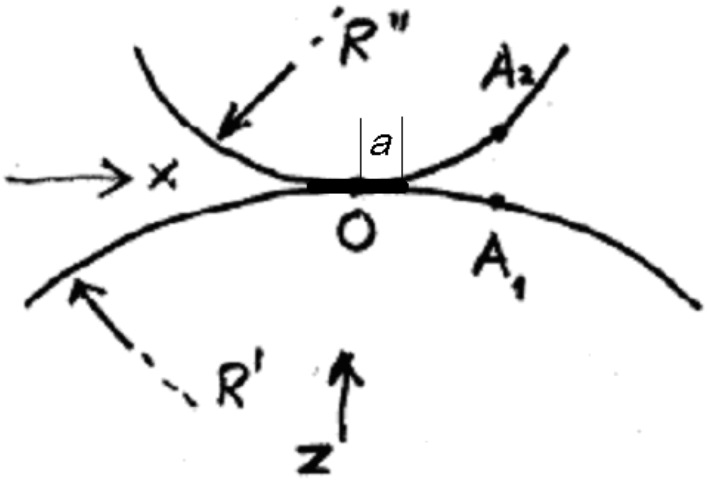

Figure 1: Contact of two elastic spheres.

Based on this assumption, the contact radius *a*, the contact area *A*, and both the maximum pressure p_{max} and the mean pressure p_m can be determined with an elastic infinite half-space analysis as:

Hertz contact radius: $a = \left[\frac{3LR}{4E^*}\right]^{1/3}$

Hertz area of contact: $A = \pi a^2 = \pi\left[\frac{3LR}{4E^*}\right]^{2/3}$

Mutual approach: $\delta = \frac{a^2}{R}\left[1 - \frac{2}{3}\left(\frac{a_o}{a}\right)^{3/2}\right]$ with $a_o = a\big|_{L=0}$

Hertz pressure: $p_{max} = \frac{3L}{2\pi a^2} = \frac{3}{2}p_m\left[\frac{6L\left(E^*\right)^2}{\pi^3 R^2}\right]^{1/3}$

with the applied normal force (load) L, and the combined Young's modulus and radius of curvature of the two materials (1 and 2), i.e.,

$$E^* = \left(\frac{1-\nu_1^2}{E_1} + \frac{1-\nu_2^2}{E_2}\right)^{-1} \text{ and } R = \left(\frac{1}{R_1} + \frac{1}{R_2}\right)^{-1}$$

where ν is the Poisson ratio ($\nu \approx 0.5$ for polymers). Neglected in the Hertz model are adhesive interactions, as seen at zero loads where the contact area vanishes.

The adhesion force between two rigid spheres can be expressed as

$$F_{adh} = -2\pi R^* \Delta\gamma\,; \quad \Delta\gamma = \gamma_1 + \gamma_2 - \gamma_{12}$$

where $\Delta\gamma$ is called the "work of adhesion" per unit area. This force-adhesion relationship is named after *Bradley*. Neither elastic nor plastic deformations are considered in Bradley's model. Johnson, Kendal and Roberts introduced a very successful elastic model - named JKR model. Based on this model, the area of contact $A = \pi a^2$ can be easily deduced from the JKR contact radius, i.e.,

$$a = \left[\frac{3R}{4E^*}\left(L + 3\pi R\Delta\gamma + \sqrt{6\pi R\Delta\gamma L + \left(3\pi R\Delta\gamma\right)^2}\right)\right]^{1/3}.$$

Note, for vanishing work of adhesion, the JKR expression for a corresponds to the Hertzian contact radius. For non-zero adhesion forces, the significant difference of the two models is illustrated in Figure 2. With the JKR model, a negative loading regime between L = 0 and the instability load, i.e., the adhesion force

$$L = F_{adh}{}^{JKR} = -\frac{3}{2}\pi R^* \Delta\gamma \text{ , is possible.}$$

Considering that the JKR adhesion force equation is seemingly independent of any elastic modulus, there seems to be an inconsistency, if compared to the Bradley model above. The apparent discrepancy was resolved by David Tabor (1977) who introduced the following parameter:

$$\mu = \frac{\left(R^*\right)^{1/3}\left(\Delta\gamma\right)^{2/3}}{\sigma\left(E^*\right)^{2/3}}, \qquad \textit{"Tabor Coefficient"}$$

where E^* and R^* are the combined curvature and modulus, respectively, and σ the characteristic atom-atom distance. The Tabor coefficient μ expresses the relative

importance of the adhesive interaction versus the elastic deformation. For $\mu > 5$, which is typical for soft organic materials, the JKR model is appropriate.

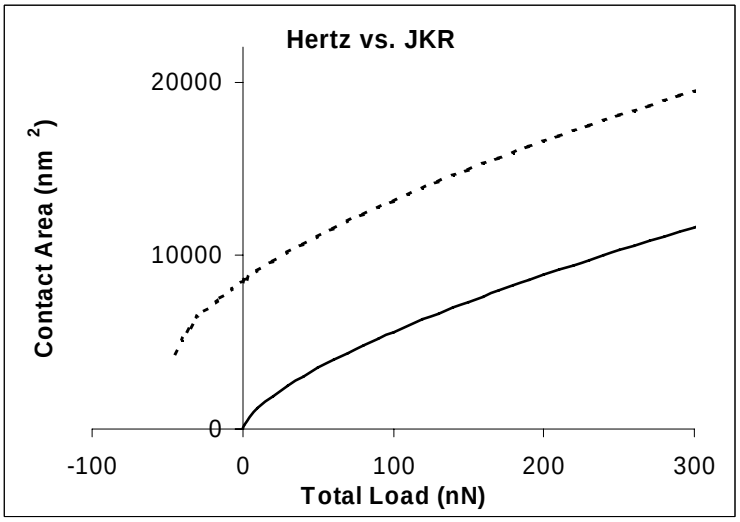

Figure 2: Hertzian elastic contact and JKR adhesive-elastic contact as function of load.

Force Modulation SFM and Hertzian Theory

The Hertzian theory of elastic circular point contact for a planar surface and an assumed spherically caped tip, Fig. 3, describes the contact radius as

$$a = \left[\frac{3LR}{4E}\right]^{1/3},$$

where R is the radius of curvature of the probing SFM tip, and E is the modulus of the sample only, if the sample material stiffness is much smaller than the modulus of the cantilever material. The mutual relative approach of distant points δ between the sample and probing tip, i.e., the sample indentation for an incompliant tip material, is given by the Hertzian theory as

$$\delta = \left[\frac{9L^2}{16RE}\right]^{1/3}$$

For a fully elastic sample and a incompliantly stiff probing SFM tip, δ reflects the elastic strain deformation (indentation) of the sample material. For a force modulated relative approach, the load varies around the equilibrium load L_o as

$$L = L_o + \frac{\partial L}{\partial \delta}\delta$$

As we consider only the sample being deformed, a one-dimensional sample stiffness (generally referred to as contact stiffness) can be introduced as the derivative of the load, i.e.,

$$k_c \equiv \frac{\partial L}{\partial \delta} = \left(6E^2 L_o R\right)^{1/3}.$$

The equation above is synonymous with the non-adhesive Hertzian expression

$$k_c = 2aE \,.$$

Higher order derivatives provide anharmonic distortions (dissipation) that can be neglected. The equilibrium load can be expressed by the normal spring constant of the cantilever k_L and the equilibrium deflection z_o as $L_o = k_L z_o$.

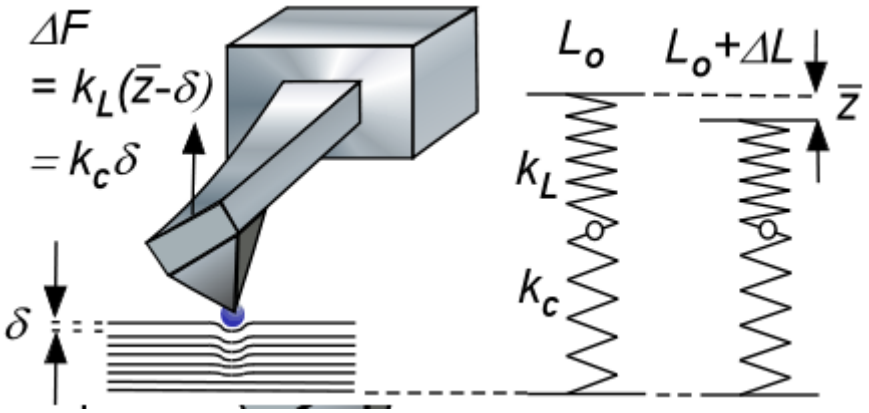

Figure 3: Elastic sample deformation involving rigid SFM tip.

Thus, for a sinusoidal normal stress disturbance, $z = A \sin(\omega t)$, with a root mean square amplitude

$$\bar{z} = \frac{1}{\sqrt{2}} A$$

the dynamic force acting on the cantilever is proportional to the net displacement (input modulation minus sample deformation), i.e.,

$$\Delta F = k_L \left(\bar{z} - \delta \right).$$

Analogous, the force modulation can also be described from the sample perspective as

$$\Delta F = k_c \delta \,.$$

The "normal force", ΔF, acting on the SFM lever in the process of an indentation can be expressed in Hooke's limit as

$$\Delta F = k_{sys} \bar{z} = k_c \delta = k_L \Delta z_L \quad \text{with} \quad \Delta z_L = \bar{z} - \delta \,,$$

as illustrated in Figure 3. The system combined spring constant, k_{sys}, is then given as

$$k_{sys} = \left(\frac{1}{k_c} + \frac{1}{k_L} \right)^{-1} .$$

Analogous relationships exist also for elastic shear modulation.

Contact Stiffness

In the previous paragraph, we have assumed that only the sample is deformed and the material response is rate independent. If both bodies are compliant, the non-adhesive Hertzian contact stiffness is given as

$$k_c = 2aE^* \text{ with } E^* = \left(\frac{1-\nu_1^2}{E_1} + \frac{1-\nu_2^2}{E_2} \right)^{-1}$$

where E_i and ν_i (I = 1,2) are the reduced material Young's moduli and Poisson ratios, respectively. This equation has also been found to be applicable for viscoelastic materials, i.e.,[1]

$$k_c(\omega) = 2aE^*(\omega).$$

where $k_c(\omega)$ and $E(\omega)$ reflect effective stiffnesses.

If we consider now also adhesion to take place in the contact area the Hertzian theory would have to be replaced by the JKR theory, which leads to the following expression for a normalized contact stiffness to zero load:[1]

$$\frac{k_c(\omega)}{k_c(\omega)\big|_{L=0}} = \left[\frac{1+\sqrt{1-L/F_{adh}}}{2} \right]^{2/3}, \text{ with}$$

$$k_c(\omega)\big|_{L=0} = 2a_o E^*(\omega) = 2E^*(\omega) \left[\frac{9\pi R^2 \Delta\gamma}{2E^*\big|_{\omega\to 0}} \right]^{1/3}$$

FM and Polymer Relaxation Properties

Controlled temperature experiments involving force modulation microscopy, provides the opportunity to investigate relaxation properties of polymeric and organic materials. Thereby, the contact stiffness is monitored as a function the temperature, as illustrated below with shear modulation force microscopy (SM-FM) employed to thin polystyrene films. Due to the small probing area even the smallest changes in the polymer internal pressure, modulus and surface energies can be detected. SM-FM is allows for accurate determination of transition properties, such as the glass transition temperature,* T_g, of nanoconstrained systems, such as ultrathin polymer films with a thickness below ~100 nm, Fig. 4(a).

The SM-FM method is briefly described as follows: A nanometer sharp SFM cantilever tip is brought into contact with the sample surface, Figure 4(b). While a constant load is applied, the probing tip is laterally modulated with a "no-slip" nanometer amplitude, ΔX_{IN}. The modulation response, ΔX_{OUT}, is analyzed using a two-channel lock-in amplifier, comparing the response signal to the input signal. The modulation response, i.e., the effective stiffness, is a measure of the contact stiffness. Thermally activated transitions in the material, such as the glass transition, T_g, are determined from the "kink" in the response curve, as shown in Figure 4(b).

Conceptually, the force modulation FM approach is a nanoscopic analogue to dynamic mechanical analysis (DMA). In essence, mechanical responses to external shear forces with varying temperature entail a material's viscoelastic properties, such as the modulus.

* Background information regarding the glass transition of viscoelastic material is provided below.

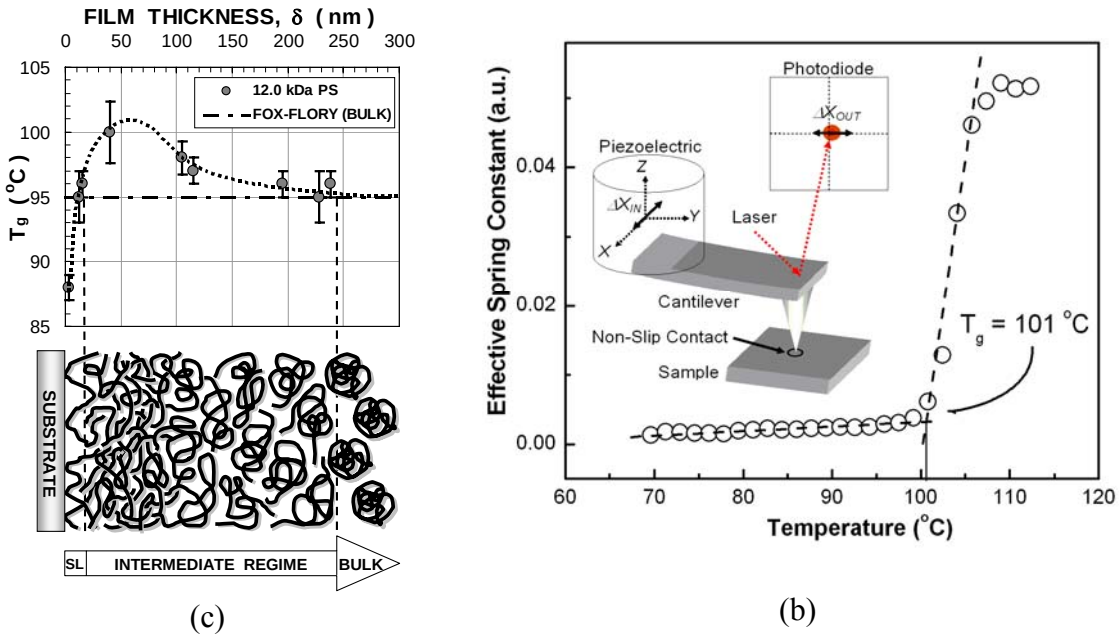

Figure 4. (a) Nanoscale constrained glass transition profile below 100 nm thick polymer films. (b)Working principle of Shear Modulation Force Microscopy (SM-FM)

Transition and Viscoelasticity

It is hard to imagine life without plastics, looking at water bottles, car bumpers, backpacks, computer casings, and many more products that involve synthesized organic materials – called polymers. There are numerous reasons to list why the last one hundred years can be called the *Plastic Age.* Polymers are light weight, formed in any shapes and colors, and can be produced with a simple scheme at low cost. One major advantage of polymers over traditional materials such as metals is their versatility in their mechanical property. Polymers can be soft and flexible like rubber bands and chewing gums, but also stiff and tough like the aircraft body of the new Boeing 787.

One critical parameter in designing polymeric product is the glass transition temperature T_g. The glass transition can be pictured, although with some caution, as a structural order-disorder transition that is observed in non-structured (amorphous) solids. One of the main features of the glass transition is the change in the mechanical and diffusive properties of the material below and above T_g. For instance, below T_g the material starts to act stiff and is brittle (i.e., glass like), and above T_g, still in the solid (condensed) phase, it exhibits high mechanical flexibility due to the existence of molecular chain mobility. Despite the importance of the glass transition of polymeric materials, the glass transition phenomena and its underlying viscoelastic behavior are not completely understood. These shortcomings have however not stopped mankind from designing continuously new polymer based products on a macroscopic level. However, the ambiguity in our current fundamental understanding of the glass forming process in polymers is being challenged by the recent nanotechnology spurt. As the dimension of solid systems approach the nanoscale, a dimension that is comparable to the size of polymer chains, it matters from an effective design perspective to grasp the exact relaxation mechanism behind the glass transition process.

One of today's most common ways to determine the glass transition temperature is the measurement of the change in the specific heat capacity $C_p(T)$ as a function of temperature by differential scanning calorimetry (DSC). Although widely used because of its convenience, DSC is also known for its inaccurately. One of the main reasons is that the glass transition process takes place not only at a specific temperature, like a typical first order phase transition, but over a range of temperatures[2]. Thus, T_g as determined by DSC has to be assigned, to some degree arbitrarily within a critical temperature range, as illustrated in Figure 5. Another reason for the difficulties in determine T_g originates from the viscoelastic nature of polymers, which makes the material temperature rate dependent with a high possibility of aging during the characterization process. DSC information is usually obtained from the polymer in powder form, to reduce effects based on thermal history and process engineered properties.[3] In other words for T_g determination, DSC is restricted to the characterization of bulk materials, like other widely used techniques, as the dynamic mechanical analysis (DMA), Fig. 5. DMA is sensitive to changes in the in-phase G' and out-of-phase modulus response G". The ratio of these two moduli components, define the loss modulus (also referred to as loss tangent tanδ), with which T_g can be identified. Due to imposed macroscopic mechanical constraints this value is often different from the DSC calorimetric glass transition.

There is currently not only a need for new techniques to provide a more fundamental understanding of the glass transition process, but also for methods that are applicable to small scale systems; e.g., thin films, and polymeric heterosystems (e.g., polymers blends and polymer nanocomposites). A technique that has been found to address the experimental shortcomings of DSC and DMA is shear modulation force microscopy (SM-FM), as introduced above.

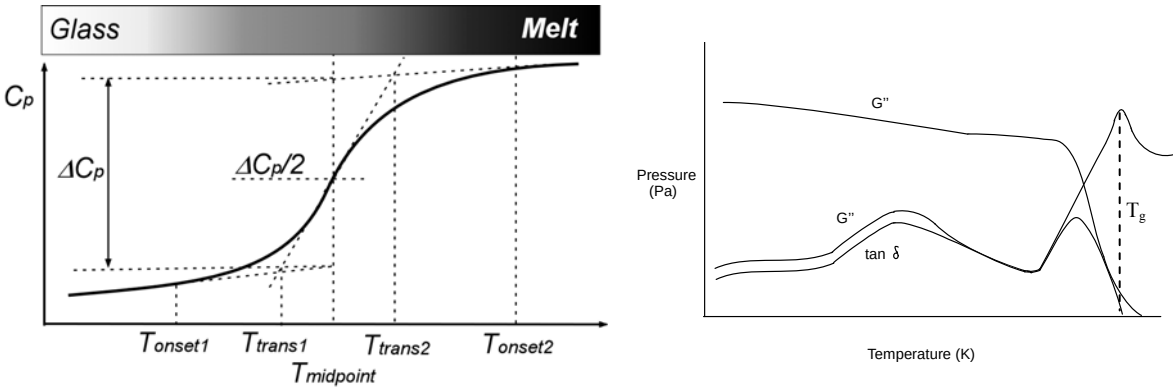

Figure 5 : (left) Schematic thermogram of $C_p(T)$. Shows the various distinct temperatures used to define the midpoint temperature T_g. (right) Schematic thermomechanical results, as obtainable by DMA.

Introduction to Linear Viscoelasticity

The science that deals with the mechanical properties of condensed phases under external stresses is called Rheology. We will limit our discussion to a subdiscipline of rheology, i.e., linear viscoelasticity, with which we conceptually separate the *liquid-like* (viscous) behavior from the *solid-like* (elastic) behavior. Thereby, a material that exhibits

ideal solid-like behavior under stress can be described with a simple stress-strain relationship, and a material with *ideal liquid-like* behavior shows a simple stress-strain-rate dependence. With *stress* we define the external force per unit area that is imposed on the condensed phase. The resulting deformation (e.g., length or angular deformation (ΔL or γ) for a uniaxial length extension, or simple shear, respectively) defines a strain ratio (e.g., $(L_o+\Delta L)/L_o$ or $\tan\gamma$). It is convention to use for uniaxial stress and strain the Greek symbols σ and ε and for the shear stress and strain τ and γ. Strain rates reflect the time derivative of the strain.

Ideal solid-like and ideal liquid-like

Ideal solid-like materials deform and relax instantaneously with changes in the applied external stresses. *Hooke's Law* is a manifestation of a solid-like behavior. Thus, an ideal solid-like behavior is synonymous with *ideal elastic*. Mechanical energy is stored in an ideal elastic material without exhibiting any form of energy dissipation. The energy is instantaneously regained with the discharge of the external stresses. Note, with this definition of a material behaving ideal solid-like, no structural arrangements, such as for instance *"crystallinity*", were imposed. In ideal elastic materials the stress is linearly related to the strain and the proportionality factor is called a *stiffness modulus*. In the case of a uniaxial elongation/compression in x-direction or simple shear in y-direction of an isotropic material, Hooke's law has the following simple form:

$$\sigma_{xx} = E\varepsilon_{xx} \quad \text{(unaxial deformation)}$$
$$\tau_{xy} = G\gamma_{xy} \quad \text{(simple shear deformation)}$$

with the modulus of elasticity (Young's modulus) E and the shear modulus G. The forces per unit area, i.e., $F_x/A = \sigma_{xx}$ and $F_y/A = \tau_{xy}$ are the normal and lateral stresses, respectively, which are imposed on the elastic solid. ε and γ are the corresponding strains; i.e., normalized dimensionless displacements.

The conceptual counter behavior to ideal solid-like is ideal liquid-like as found in a *Newtonian liquid*. The basic equation of simple flow is described one-dimensionally by *Newton's law of viscosity*,

$$\tau_{yx} = -\eta\frac{dv_x}{dy},$$

which relates proportionally the shear force per unit area, $F_x/A = \tau_{xy}$, to the negative of the local velocity gradient (time derivative of the deformation) with a constant viscosity value, η. The velocity gradient represents a strain rate. If a stress is applied to a Newtonian liquid no strain is built up. The material is incapable of mechanical energy storage. Once the stress is removed the material does not relax. The material resistance to shear manifests itself in the rate with which the stress is imposed. In a perfect liquid we find a linear relationship between the stress and the strain rate. The proportionality factor is called *viscosity*.

In general, any realistic liquid and solid matter will behave in a mixed manner, solid-like and liquid-like, depending on the degree and time scale over which external stresses are acting.

Linear Viscoelasticity

Mixed liquid-like and solid-like characteristics of viscoelastic materials suggest that the external forces applied are partially stored and partially dissipated. This is nicely described by a simple constitutive equation based on a periodic deformation process. If the viscoelastic behavior is in a linear region, a shear sinusoidal stress that is applied to a viscoelastic body exhibits a sinusoidal strain with a phase lag that is expressed as follows:

$$\gamma = \gamma_0 \sin(\omega \cdot t),$$

$$\sigma = \sigma_0 \sin(\omega \cdot t + \delta),$$

ω is the angular frequency, and δ is the phase lag, and γ_0 and σ_0 are the maximum magnitudes of the strain and the stress. The expression of the sinusoidal stress can be expanded to elucidate the two components, i.e., in phase component and out of phase component,

$$\sigma = \sigma_0 \sin(\omega \cdot t)\cos(\delta) + \sigma_0 \cos(\omega \cdot t)\sin(\delta).$$

The in phase component,t $\sigma_0 \cos(\delta)$ is referred to as the storage modulus *G'*, and the out of phase component, $\sigma_0 \sin(\delta)$ is called the loss modulus *G"*. The stress relationship then writes as

$$\sigma = \gamma_0 \cdot G' \cdot \sin(\omega \cdot t) + \gamma_0 \cdot G'' \cdot \cos(\omega \cdot t),$$

Expressed in complex notation the strain and stress are:

$$\gamma = \gamma_0 \exp(i \cdot \omega \cdot t),$$

$$\sigma = \sigma_0 \exp\left(i \cdot (\omega \cdot t + \delta)\right),$$

and thus, we can introduce a complex modulus *G** as,

$$\frac{\sigma}{\gamma} = G^* = \frac{\sigma_0}{\gamma_0}(\cos\delta + i \cdot \sin\delta) = G' + i \cdot G'',$$

The *storage modulus G'* represents the storage capability of the systems and the *loss modulus G"* describes the dissipation character of the system in form of plastic deformation or flow. The ratio of the loss and the storage component is referred to as the loss tangent,

$$\tan\delta = \frac{G''}{G'},$$

and reflects the relative viscous and elastic properties. The smaller the loss tangent is the more elastic is the material. tanδ is often the most sensitive indicator of various molecular motions within the material. Figure 6 provides a response visualization of a simple shear phenomenon.

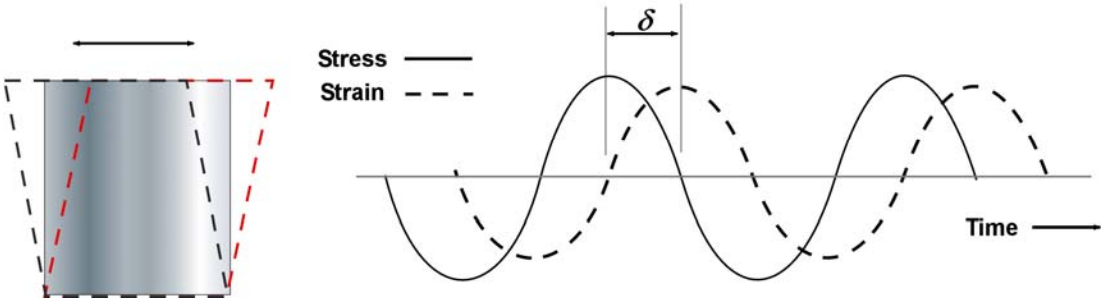

Figure 6: Dynamic shear stress-strain visualization.

The response of a viscoelastic material can be described by a simple combination of dashpots (dissipative) and springs (elastic). The simplest model of a spring and a dashpot in series is the Maxwell's model (Figure 7(a) with

$$\frac{d\gamma}{dt} = \frac{1}{G}\frac{d\sigma}{dt} + \frac{1}{\eta}\sigma$$

where η is the viscosity, we have introduced above. The solution to this differential equation is,

$$\sigma(t) = \gamma_0 \cdot G \cdot exp\left(-\frac{t}{\eta/G^*}\right)$$

with $G^* = \sigma/\gamma$. This model predicts a time sensitive modulus, i.e.,

$$G(t) = G \cdot exp\left(-\frac{t}{\tau_\gamma}\right),$$

where τ_γ is the characteristic relaxation time, and t is the observation time. Thus, if the deformation process is very fast compared to the material relaxation time, i.e., $t \gg \tau_\gamma$ the elastic behavior will dominate. For very slow deformation ($t \ll \tau_\gamma$), the system's viscous behavior dominates. Another basic viscoelastic setup is obtained by operating a spring in parallel with a viscous dashpot. (Kelvin-Voigt Model,Fig. 2(b))The Kelvin-Voigt model provides the following relationships:

$$\sigma = G \cdot \gamma + \frac{\eta \cdot d\gamma}{dt}$$

and the solution with a constant stress σ_0 is,

$$\gamma(t) = \frac{\sigma_0}{G}\left[1 - exp\left(-\frac{t}{\tau_\sigma}\right)\right]$$

where τ_σ is the retardation time of the strain.

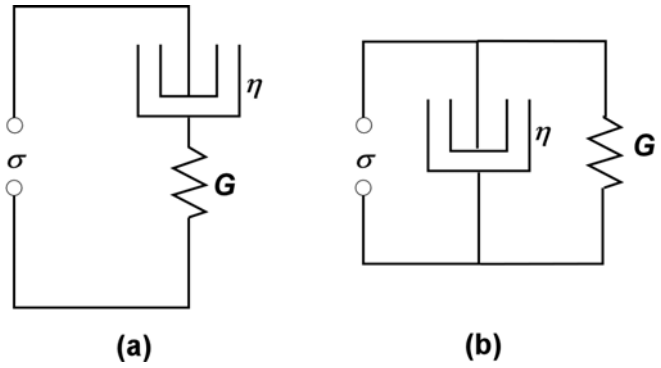

Figure 7: Dashpot spring model of (a) Maxwell Model (b) Kelvin-Voigt Model.

While the Maxwell model describes the stress relaxation but not creep, the Kelvin-Voigt model describes creep but not stress relaxation. For viscoelastic material, the simplest model would be the combination of the two, [4]

$$\sigma + \left(\frac{\eta_1 + \eta_2}{G_1} + \frac{\eta_2}{G_2}\right)\frac{d\sigma}{dt} + \frac{\eta_1\eta_2}{G_1G_2}\frac{d^2\sigma}{dt^2} = \eta_2\frac{d\gamma}{dt} + \frac{\eta_1\eta_2}{G_1}\frac{d^2\gamma}{dt^2}$$

as G_1, G_2, η_1 and η_2 are corresponding to two springs and two dashpots, Fig. 8. If this is solved with the sinusoidal stress,

$$\frac{G'-G_0}{G_\infty - G_0} = \frac{\omega^2 \cdot \tau_\gamma^2}{1+\omega^2 \cdot \tau_\gamma^2}$$

$$\frac{G''}{G_\infty - G_0} = \frac{\omega \cdot \tau_\gamma}{1+\omega^2 \cdot \tau_\gamma^2}$$

$$\tan\delta_m = \frac{G_\infty - G_0}{G_0 + G_\infty \omega^2 \cdot \tau_m^2}$$

where G_0 and G_∞ are *relaxed* and *unrelaxed* moduli, respectively, and τ_m is derived as:

$$\tau_m = (\tau_\sigma \tau_\gamma)^{1/2} = \left(\frac{\eta_1}{G_1}\frac{\eta_1}{G_1+G_2}\right)^{1/2}$$

The maximum of the loss curve then corresponds to $\tau_m\omega_0 = 1$. The product $\tau_m\omega_0$is referred to in the literature as the Deborah number, and reflects the ratio of the externally imposed time disturbance and the intrinsic relaxation time[4]

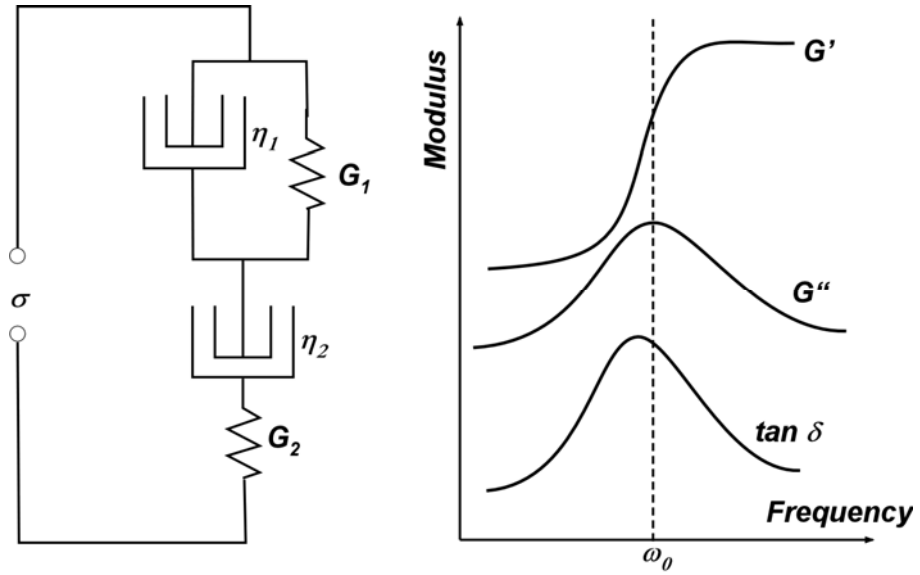

Figure 8: A combination of the Maxwell and Kelvin-Voigt Model.

Many more combinations of springs and dashpots are possible and in detail described in the literature.[3]

Time-Temperature Equivalence of Viscoelastic Behaviors

We showed in the previous section that the viscoelastic behavior is strongly affected by the temperature and the observation time (frequency). Here the concept of time-temperature equivalence is introduced. Consider a glass window. Glass windows are made with an amorphous inorganic (silica mixture) material that appears in daily life to be "solid-like. However, it is more appropriate to consider glass to be in a highly viscous condensed phase that appears to be at equilibrium in a solid-like state during the

time of observation. By controlling the temperature without imposing any transitions we can accelerate or slow down the flow process In that sense, the viscoelastic behavior of the material is affected similarly by either changes in the temperature and or time. This is called a time-temperature equivalence and is illustrated in Figure 9. Figure 9(a) and 9(b) reflect the modulus in a time (i.e., frequency) domain, and in a temperature domain, respectively. Valuable information about the viscoelastic behavior of materials can be deduced from such measurements and will be discussed in the following sections.

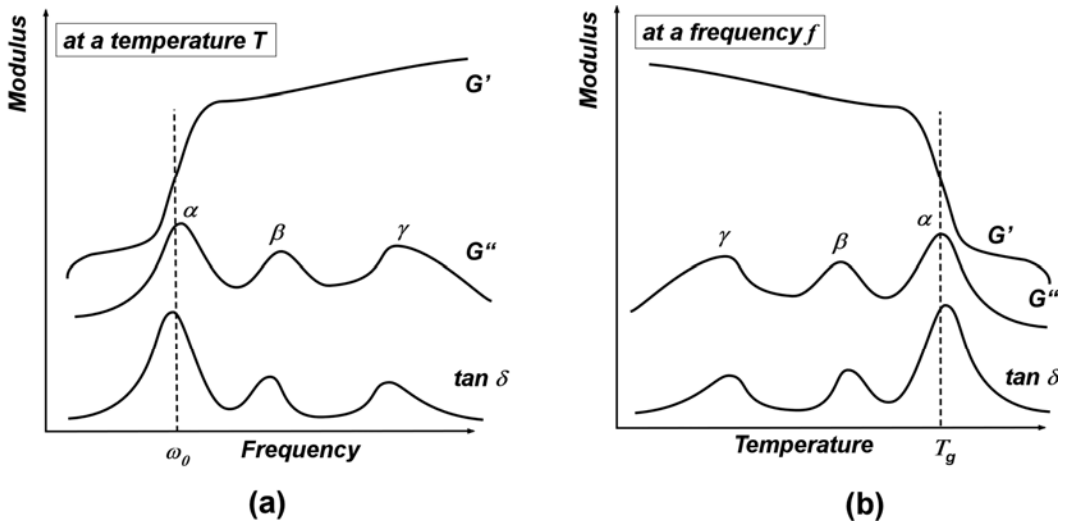

Figure 9: Modulus spectrums in (a) time domain, and in (b) temperature domain.

Glass Transition

The *glass transition* T_g is defined as the reversible change in an amorphous material (e.g., polystyrene) or in amorphous regions of a partially crystalline material (e.g., polyethylene), from (or to) a viscous or rubbery condition to (or from) a hard and relatively brittle one.[5] As shown in the previous section, Fig. 9(b), this transition corresponds to a temperature at which the modulus drastically changes. Above the glass transition temperature the material, still a solid, reveals a strongly rubbery behavior that is to part liquid-like. Below the transition temperature the material behaves like a brittle solid-like material. The glass transition itself, as illustrated in Figure 10, exhibits a strong cooling rate dependence and is in appearance significantly different from melting (first order phase) transition. Also the frequency of the applied macroscopic stresses is affecting the temperature of the transition.

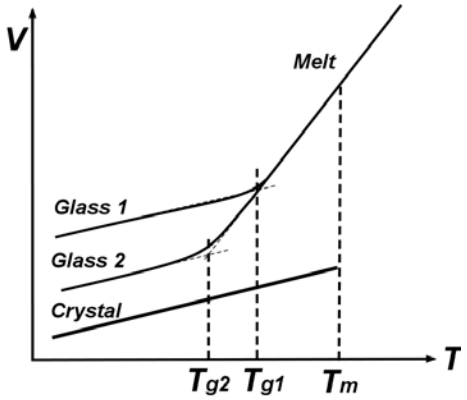

Figure 10: Specific volume change as function of temperature. Depending on the cooling rate any liquid can freeze into a glass phase (fast quenching; e.g. of metallic glasses). Depending on the cooling rate, T_g can significantly shift as indicated with Glass 1 and Glass 2. In polymers, the transition from a melt to a glass is not discontinuous as the first order phase transition (indicated with melting temperature T_m). Hence the assignment of a single transition value for T_g seems to be ambiguous on first sight.

Thermodynamically, the free energy changes between equilibrium states are usually identified by a discontinuity in the first partial derivatives of the Gibbs free energy G = H -TS, with respect to the relevant state variable (pressure P and temperature T), as illustrated Figure 11. Discontinuities, as expressed in the first partial derivatives of the Gibbs free energy

$$\left(\frac{\partial G}{\partial P}\right)_T = V ,$$

$$\left(\frac{\partial G}{\partial T}\right)_P = -S ,$$

$$\left(\frac{\partial (G/T)}{\partial (1/T)}\right)_P = H ,$$

are found in the property-temperature relationships, i.e., the volume V, the entropy S and enthalpy H.

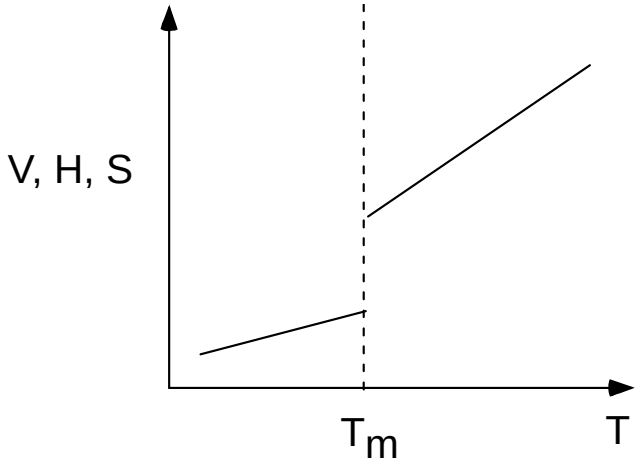

Figure 11: Volume discontinuity. First-order transition between liquid and solid. (T_m melting temperature).

The second derivatives of the Gibbs free energy introduces the heat capacity C_p, compressibility κ and thermal expansion coefficient α.

Heat Capacity, C_p : $$-\left(\frac{\partial^2 G}{\partial T^2}\right)_P = \left(\frac{\partial S}{\partial T}\right) = \frac{C_p}{T}$$

$$\frac{\partial}{\partial T}\left[\left(\frac{\partial (G/T)}{\partial (1/T)}\right)_P\right]_P = \left(\frac{\partial H}{\partial T}\right)_P = C_P$$

Compressibility, κ: $$\left(\frac{\partial^2 G}{\partial P^2}\right)_T = \left(\frac{\partial V}{\partial P}\right)_T = -\kappa V$$

Therm. Expansion Coeff., α: $$\left[\frac{\partial}{\partial T}\left(\frac{\partial G}{\partial P}\right)_T\right]_P = \left(\frac{\partial V}{\partial T}\right)_P = \alpha V$$

Figure 12 provides a rough classification based on the changes of the free energy and derivatives with temperature. While, column (i) illustrates the qualitative behavior of a first-order phase transition (i.e., a melting/freezing transition), column (ii) and (iii) are found for second order and glass transitions, respectively. A second order phase transition (e.g., an order-disorder transition) exhibits no discontinuity in *V* and *H*, and *S*. But there are discontinuities in C_p, κ and α.

First and second order transitions are illustrated in Figure 12. If compared to property changes in glasses around the glass transition temperature, one finds some similarity between the glass transition and the second order transition. There are however significant differences. C_p, κ and α values are always smaller and closely constant below the glass transition temperature, T_g, if compared to the values above T_g. This is in contrast to the second-order transition.

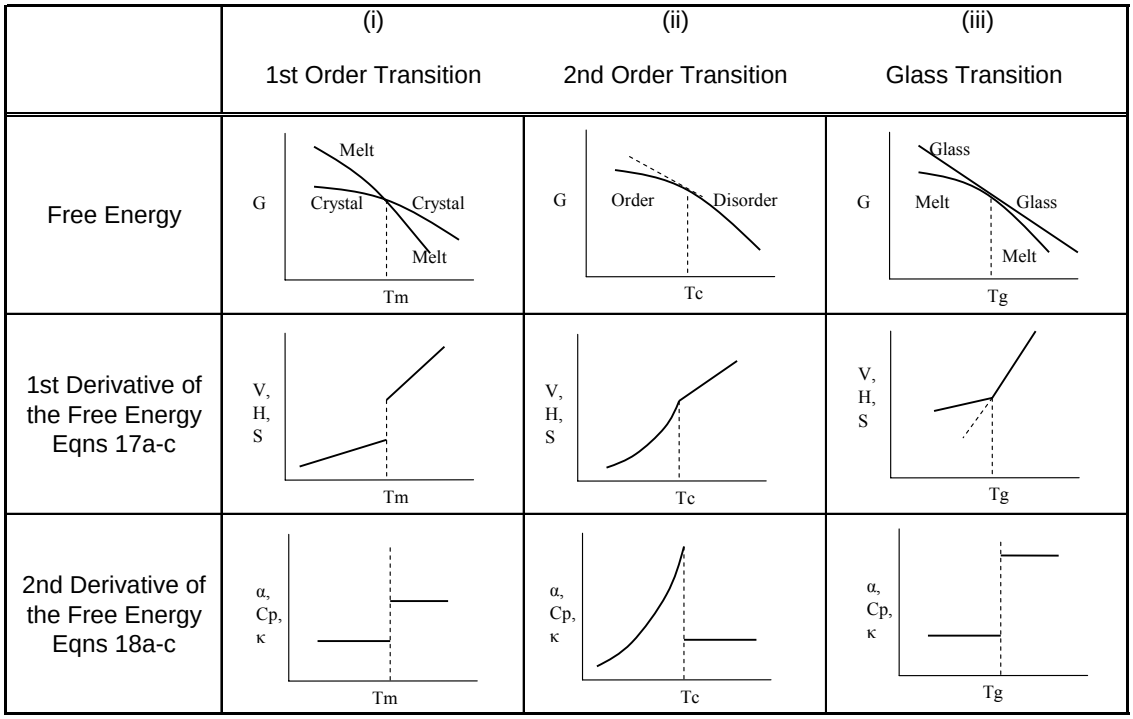

Figure 12: Schematic representation of the changes with temperature of the free energy and its first and second derivatives for (i) first order, (ii) second order and (iii) glass transition.

References

1. D.M. Ebenstein and K. J. Wahl, Coll. Interf. Sci. **298**, 652 (2006).
2. J. J. Aklonis and W. J. MacKnight, *Introducrtion to polymer viscoelasticity*, 2nd ed. (Wiley-Interscience Publication, New York, 1983).
3. D. W. Van Krevelen, *Properties of polymers*. (Elsevier Scienfitic Publishing Company, Amsterdam, 1976).
4. P. Hedvig, *Dielectric spectroscopy of polymers*. (John Wiley & Sons, New York, 1977).
5. A. S. f. T. M. A. E1142.
6. T. G. Fox and P. J. Flory, J. Appl. Phys. **21**, 581 (1950).
7. C. Buenviaje, F. Dinelli, and R. M. Overney, in *American Chemical Society Symposium Series*, edited by J. Frommer and R. M. Overney (University Press, 2000).

Recommended Reading

Introduction to Polymer Viscoelasticity by John J. Alkonis and William J. MacKnight, Wiley-Interscience Publication, 2nd Ed., New York, 1983.

Mechanical Properties of Solid Polymers by I. M. Ward, Wiley-Interscience Publication, London, 1971.

Nanoscience: Friction and Rheology on the Nanometer Scale by E. Meyer, R. M. Overney, K. Dransfeld, and T. Gyalog, World Scientific Publ., Singapore, 1998.

Appendix: EMERGENCY PROCEDURES FOR HYDROLFUORIC ACID (HF) EXPOSURE

SEEK IMMEDIATE MEDICAL ATTENTION
CALL 911

SERIOUS TISSUE DAMAGE WITH DELAYED ONSET
BEGIN FIRST AID IMMEDIATELY

FIRST AID FOR SKIN CONTACT

1. IMMEDIATELY (within seconds) proceed to the NEAREST SAFETY SHOWER. While showering REMOVE ALL CONTAMINATED CLOTHING and WASH THE AFFECTED AREA FOR 5 MINUTES.
2. USING NITRILE 22 MIL (MFG> RECOMMENDED) GLOVES MASSAGE CALCIUM GLUCONATE GEL into the affected area. If calcium gluconate gel is not available, wash area for at least 15 minutes or until emergency medical assistance arrives.
3. RE-APPLY CALCUIM GLUCONATE GEL and massage it into affected area EVERY 15 MINUTES until medical assistance arrives or pain disappears.

FIRST AID FOR EYE CONTACT

1. IMMEDIATELY (within seconds) proceed To THE NEAREST EYEWASH STATION.
2. Thoroughly WASH EYES WITH WATER FOR AT LEAST 15 MINUTES while holding eyelids open.
3. DO NOT APPLY CALCIUM GLUCONATE GEL TO EYES.

FIRSTS AID FOR INHALATION

GET MEDICALASSISTANCE by calling 9-911.

ASK THE MEDICAL ASSISTANCE TO TAKE YOU TO A **MEDICAL BURN CENTER FOR TREATMENT, NOT ANYWHERE ELSE.**

LAB UNIT 5: Scanning Tunneling Microscopy

Specific Assignment: STM study of HOPG and Gold films

Objective

This lab unit introduces scanning tunneling microscopy (STM) technique, used to obtain real space atomic resolution images of conductive surfaces. The tunneling spectroscopy mode of STM is employed to examine local density of state (LDOS) of the surface.

Outcome

Learn about the basic principles of scanning tunneling microscopy, including a short introduction of the tunneling phenomena, and learn how the STM images can be correctly interpreted. Attain STM images and the local density of state of a HOPG (highly ordered pyrolytic graphite) and gold (Au) sample in ambient atmosphere.

Synopsis

The STM provides real space atomic resolution images through tunneling current between a conductive tip and a conductive/semiconductive surface. In this lab unit, we employ two STM modes, i.e., constant current imaging mode and tunneling spectroscopy mode, to study HOPG (graphite) and gold (Au). HOPG is one of well studied materials and serves as a standard for STM technique, and the interpretation of the STM images as well as the spectroscopic analysis are debated actively in literatures. Here, taking into consideration of artifacts such as thermal drift, students will determine the lattice constant and the atom-to-atom distances of HOPG. The contrasting spectroscopic data of the HOPG and Au will illustrate the difference in electronic structure between semi-metals and metallic systems.

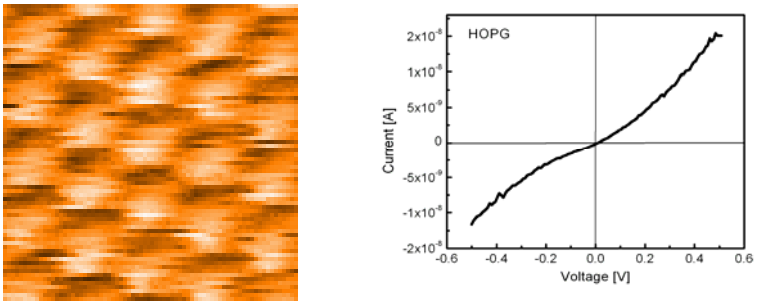

A STM image (Left, 9 Å x 9 Å) and a voltage dependent tunneling spectroscopy curve (Right) of HOPG

Materials

Highly Ordered Pyrolytic Graphite (HOPG) and Gold (Au) film

Technique

STM in imaging mode and tunneling spectroscopy mode

Table of Contents

1. Assignment

The assignment is to study the layered structure of HOPG and Au films. Specifically, the lattice constant and the atom-to-atom distances of HOPG will be determined from the STM images. Conductivity, i.e., band structure, of HOPG and Au are also discussed by analyzing the tunneling spectroscopy data. The steps are outlined here:

1. Familiarize yourself with the background information provided in Section 4.
2. Test your background knowledge with the provided Quiz in Section 2.
3. Conduct the STM experiments in Section 3. Follow the experimental step-by-step procedure.
4. Process images and analyze the spectroscopy data as described in Section 3
5. Finally, provide a report with the following information:
   (i) Result section: In this section you show your data and discuss instrumental details (i.e., limitations) and the quality of your data (error analysis).
   (ii) Discussion section: In this section you discuss and analyze your data in the light of the provided background information.
   It is also appropriate to discuss section (i) and (ii) together.
   (iii) Summery and outlook: Here you summarize your findings and provide an outlook on how one could proceed.

   The report is evaluated based on the quality of the discussion and the integration of your experimental data and the provided theory. You are encouraged to discuss results that are unexpected. It is important to include discussions on the causes for discrepancies and inconsistencies in the data.

2. Quiz – Preparation for the Experiment

Theoretical Questions

(1) Sketch the tunneling phenomena between a metallic STM tip and a metallic sample surface at (a) no bias voltage, (b) positive voltage, and (c) negative voltage.
(2) How does a contamination of a STM tip, with organic molecules for example, influence the tunneling current, i.e., the tunneling barrier? Discuss.
(3) Sketch the electronic structures and I-V curves of tunneling spectroscopy of the four systems; metallic, semi-metallic, semiconductive, and non-conductive.
(4) What is "three-fold-hexagon" of HOPG? Explain.

Prelab Quiz

(1) (6pt) The STM image (below) of a HOPG shows honeycomb structure, known as "three-fold-hexagon" pattern. Determine the lattice constant and the atom-to-atom distance of HOPG of the STM image below.

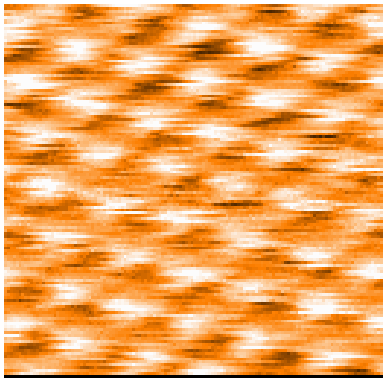
(1.4 nm x 1.4 nm)

(2) (2pt) An actual I-V curve of a HOPG sample is shown below. Sketch the differential conductance (dI/dV)/(I/V) of this I-V curve in the given space.

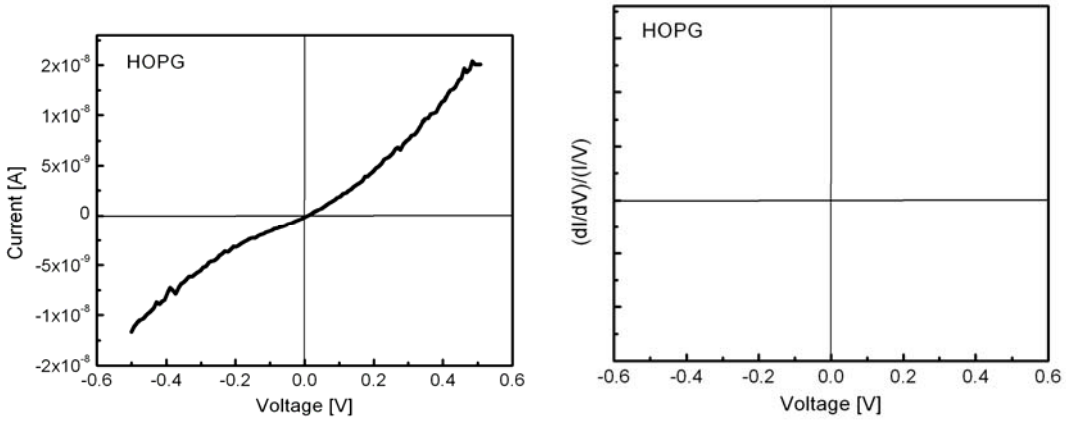

(3) (2pt) List the reasons why the atomic structure of gold sample is difficult (or impossible for our lab) to obtain?

3. Experimental Assignment

Goal

Following the step-by-step instruction below, obtain the STM images and determine the characteristic lattice constant of HOPG. Analyze the tunneling spectroscopy data to determine the conductivity of the systems. Analyze and discuss the data with the background information provided in Section 4. Provide a written report of this experiment.

Specifically provide answers to the following questions:

(1) According to the analysis, what were the lattice constant and the atom-to-atom distance of the HOPG?

(2) Compare the values obtained in (1) with the literature values. How closely does your result agree/disagree that of the literature values? Discuss your findings.

(3) Show the STM images that were obtained at different bias voltage. Discuss how and why they are different/ indistinguishable.

(4) According to the spectroscopic analysis, what type of system is HOPG? How about Au? Explain your conclusion.

(5) STM has been applied to image DNA and other biological macromolecules, which are in general not conductive. How would you image a single biological molecule place on gold substrate?

Safety

- Wear safety glasses.
- Refer to the General rules in the AFM lab.
- Wear gloves when handling ethanol.

Instrumental Setup

- Easy Scan 2 STM system with 0.25nm (diameter) Pt/Ir wire (STM tip)
- STM granite vibration isolation platform

Materials

- Samples: Highly Ordered Pyrolytic Graphite (HOPG) and a gold film. Samples are kept in designated containers when they are not used to avoid contamination.
- Ethanol in squeeze bottle and cotton swabs for cleaning.
- Scotch tape for cleaving the HOPG layers.

Experimental Procedure

Read carefully the instructions below and follow them closely. They will provide you with information about (i) preparation of the experiment, (ii) the procedure for attaining the STM images, (iii) attaining the tunneling spectroscopy data, (iv) the procedure for closing the experiment, and (v) on how to process/analyze the STM images and to process spectroscopy data.

(i) Preparation of the experiment

(1) Wear gloves whenever handing any part of the STM system. Also never talk/breath to any part of the STM systems. Your breath contains billions of organic substances.

(2) Make the STM tip: (This part will be performed with a TA)

a. Make sure everybody is wearing gloves, again.
b. Clean the wire cutter, the flat nose pliers, pointed tweezers, and rounded tweezers with ethanol. Place them on a Kimwipe. Make sure they are dry. These are the only tools that can come in contact with Pr/Ir wire.
c. Cut out 1 ~ 2 cm of the Pt/Ir wire with the wire cutter.
d. Hold the end of the wire firmly with the pliers. (Figure 3.1) Try not to bend (forming a kink) the wire.
e. Place the wire cutter as obliquely as possible (Figure 3.1). Close the cutters until you can feel the wire, but do not cut the wire.
f. Pull the cutters in the direction shown in the figure. The tip is torn off, rather than cut through, to create a sharp tip.
g. *Do not touch the newly created tip with anything, including the cleaned tools and Kimwipe.*
h. Hold the tip wire at just behind the tip using the pointed tweezers. Release the flat nose pliers.
i. Cut the wire so that the total length of the tip wire is ~ 4mm.

(3) Install the tip into the STM head.

a. Put the tip wire on the tip holder parallel to the groove in the tip holder so that it crosses below the tip clamp. (Figure 3.2(a))
b. Move the tip wire sideways until it is in the groove in the tip holder. (Figure 3.2(b))

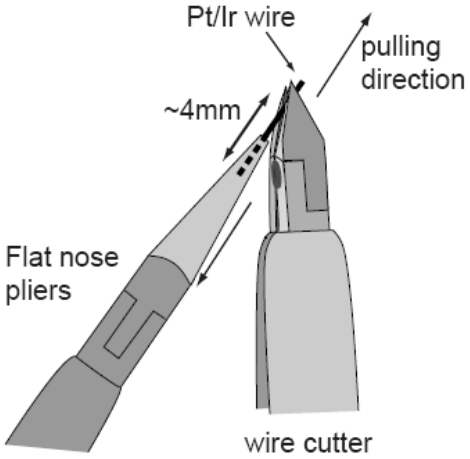

Figure 3.1: Creating a sharp STM tip.

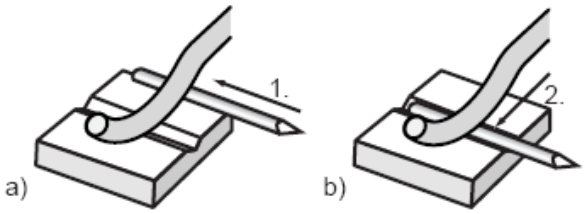

Figure 3.2: Installing the tip into the STM head.

(4) Install the sample.

a. Remove the sample holder from the storage container by holding the black plastic part. DO NOT TOUCH the metal part.
b. Check for any contamination (dust, fingerprint) on the metal part. If cleaning is necessary, follow the cleaning procedure.
    i. Moisten a cotton swab with ethanol and gently clean the surface.
    ii. Allow the alcohol to completely dry.
c. Place it on the sample holder guide bar of the STM head. Make sure it does not touch the tip.
d. Cleave the HOPG (graphite) sample. (Figure 3.3)
    i. Stick a piece of scotch tape gently to the graphite and then gently press with the back, flat part of the tweezers.
    ii. Pull the tape off. The topmost layer of the sample should stick to the tape, leaving a freshly exposed graphite surface.
    iii. Remove any loose flakes with the part of tweezers.

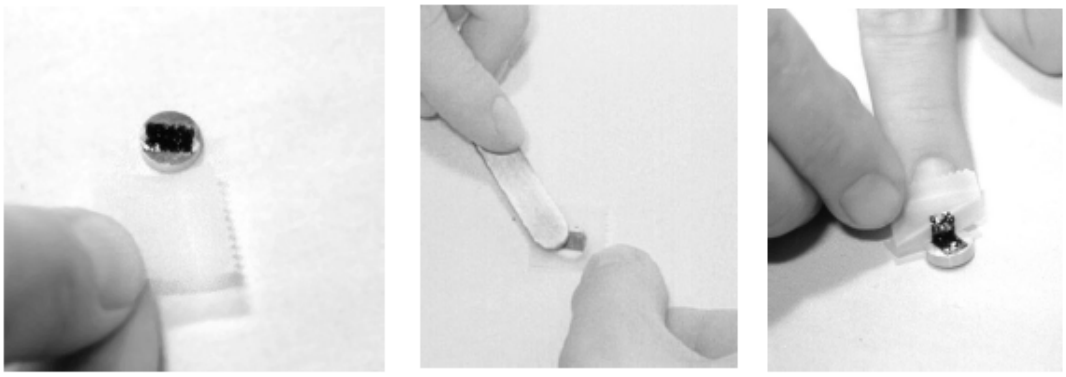

Figure 3.3: Cleaving the graphite sample.

e. Using a tweezers, hold the graphite sample at the magnetic pak.
f. Take the sample holder (handle at the black plastic part), and place the graphite sample on the magnet.
g. Place the sample holder back on the STM head. Make sure it does not touch the tip.

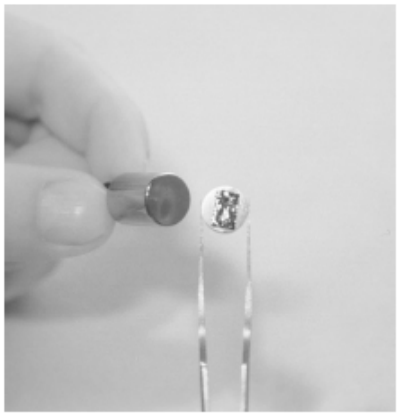

Figure 3.4: Placing the sample on the sample holder.

(5) Turn on the Controller main power switch.
(6) Open the Easy Scan 2 control software.
(7) In the operation mode panel, select STM.

(ii) Procedure for attaining the STM images

(1) Coming in contact.

a. Push the sample holder carefully to within 1mm of the tip. The tip should not touch the sample.
b. Look into the graphite surface. There should be a small gap between the very end of the tip and the reflection of the end of the tip.

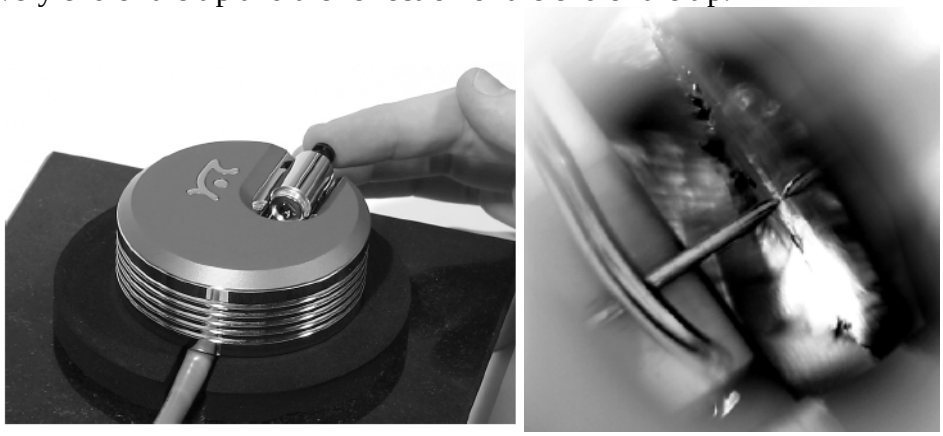

Figure 3.5: Coarse approach.

c. Open the Positioning window.
d. Through the magnifier, watch the distance between the tip and sample as click Advance in the approach panel. The tip should be within a fraction of a millimeter to the surface (i.e., the reflection of the tip).
e. Set control parameters in Z-control panel: Set point 1nA, P-gain 10000, I-gain 1000, Tip voltage 50 mV.
f. Click Approach.

g. If the approach was finished successfully, the probe status light changes from blinking to green and automatically start to scan. If not, retract and try again.

(2) Adjust imaging parameters (scan speed, scan direction, tilt, P-gain and I-gain) as the same manner as for AFM imaging. Set the resolution to 256. For attaining atomic resolution,
   a. For STM, faster scan speed is better for reducing the thermal drift.
   b. Image ~ 500 nm area to find a flat location. Zoom into the flat area.
   c. The atomic resolution images will be ~ 4nm scan size.
   d. If the image does not show atomic features, try different scan direction, reduce the gains.
   e. If none of above work, come out of contact, re-approach. Consult your teaching assistants for further suggestions.

(3) For storing images click Photo in the imaging window. Name files accordingly.

(4) Take images at the bias voltage (tip voltage) of 50mV, 250 mV, -50 mV, and -250 mV. Take at least two STM images for each bias voltage.

(iii) Attain the tunneling spectroscopy data

(1) Stop scanning.

(2) Open the spectroscopy window.

(3) Set parameters: Modulated output is tip voltage, start value -0.5V, end value 0.5 V, modulation time 1s, data point 128, and average 1.

(4) Reset the Z-control parameters in z-control window: set-point 1nA and voltage 50mV.

(5) Click *+Point*, and select a location in the image. Click *Start*.

(6) The obtained I-V curve will appear as a dual line graph.

(7) Save the curve.
   a. Click the I-V curve.
   b. Click Photo from the imaging window tool bar. The STM image and I-V curve appears as a separate window.
   c. From File, select Export, current chart as…, (X, Y, Z)-Points (*csv). Name accordingly.

(8) Take 3 I-V curves at different locations.

(9) Change the modulated output to Z-axis, start value 1nm, and end value 36 fm.

(10) Select a point and start. Save the data. Attain three I-z curves.

Do the same for GOLD film.
   a. Au film can't be cleaned, so handle with extra care not to contaminate.
   b. Atomic resolution of Au is very hard to attain. For this lab, it is sufficient to image the surface of Au and I-V curves.

(iv) Procedure for the closing experiment

(1) Wear gloves.

(2) Retract the STM tip as far as possible by auto-positioning.

(3) Close the Easy Scan 2 software window.

(4) Leave the STM tip on the head.

(5) Take the sample off of the sample holder. Place the sample in its case.
(6) Clean the sample holder with ethanol and a cotton swab. Let it dry.
(7) Place the sample holder in the case. Close the cap tightly.
(8) Place the STM cover over the STM head.
(9) Turn off the controller power switch.

(v) Instruction for data analysis

(1) Open the Easy Scan 2 program to process images. Save the images with scale bar.
(2) The Report program is also used to measure the lattice distance and the atom-to-atom distance of HOPG sample. It will be helpful to also to show the images with the measuring lines, etc. in your final report. So save images as you take measurements (to be imported to your report).
(3) Open the spectroscopy files with Excel.
(4) Generate columns: ln(I), ln(V), and d(ln(I))/d(ln(V)). Calculate ln |I| and ln |V|.
(5) Create two plots of ln(I) vs ln(V), one for $V_{bias} < 0V$ and one for $V_{bias} > 0V$.
(6) Using *Add trendline* function, obtain the fit curves for the ln(I) vs ln(V) curves separately for $V_{bias} < 0V$ and one for $V_{bias} > 0V$. Use either 2nd order or 3rd order polynomial, whichever gives a better fit.
(7) Differentiate the fit curve that is equal to d(ln(I))/d(ln(V)). Type the derivative equation in the cells of the d(ln(I))/d(ln(V)) column.
(8) Create a plot of I vs V (current as a function of voltage, raw data), and differential conductance ((dI/dV)/(I/V) = d(ln(I))/d(ln(V)) as a function of voltage.
(9) Also Plot I-z curve, i.e. current as a function of the z distance in semi-log scale.
(10) According to Equation 2,

$$\log(I) = -A\sqrt{\phi} \cdot z + C$$

determine the barrier height ϕ.

4. Background: Scanning Tunneling Microscopy and Spectroscopy

Table of Contents

Motivation

With the development of quantum mechanics in the early 20th century, mankind's perception of nature was stretched to a great degree leading to new axioms, and the recognition of the particle-wave dualism. It was found that particles with small masses such electrons could interchangeably be described as waves or as corpuscular objects. With the wave character of matter, particles exhibit a probability of existence at places, where they can classically not exist. One of these phenomena is the tunnel effect, which describes the ability of an electron to tunnel through a vacuum barrier from one electrode to the other. Since 1960 tunneling has been extensively studied experimentally. This led in 1981 to the first microscopic tool with which atoms could be observed in real space – the scanning tunneling microscopy. In addition to the atomic resolution imaging capability of STM, tunnel currents could be studied with this tool in a spectroscopy manner providing insight into the local density of state (LDOS) of material surfaces.

Scanning Tunneling Microscopy

While vacuum tunneling was theoretically predicted by Folwer and Nordheim 1928,[1], it was not until 1981 with G Binnig and H. Rohrer's introduction of the scanning tunneling microscope (STM) that provided the first observation of vacuum tunneling between a sharp tip and a platinum surface.

Wavefunction Overlap, Electron Probability

STM is based on a quantum mechanical phenomenon, called tunneling. In quantum mechanics, small particles like electrons exhibit *wave-like* properties, allowing them to "penetrate" potential barriers, a quantum mechanical probability process that is based on classical Newtonian mechanics impossible.[*] In general, STM involves a very sharp conductive tip that is brought within tunneling distance (sub-nanometer) of a conductive sample surface, thereby creating a metal-insulator-metal (MIM) configuration. In the representation of one-dimensional tunneling (Figure 4.1), the tunneling wave of the sample electrons, $\psi_{s,}$ and the wave of a STM tip electrons, $\psi_{t,}$ overlap in the insulating gap, allowing a current to flow.

[*] A more detailed discussion on barrier tunneling is provided in a later section of this text.

To achieve some understanding of the physical meaning of the wave function ψ, we consider the square magnitude of it, which represents the probability of finding an electron at a given location. Generally, this is visualized with electron clouds for atoms or molecules, or for condensed phases with energy levels, as illustrated with the gray shaded areas in Figure 4.2. In metals, electrons fill the continuous energy levels up to the Fermi level, E_F, which defines an upper boundary, similar to the sea level. Above E_F we find electrons that are activated (e.g., thermally). We can raise the Fermi level (e.g., of the sample) in regards to a second material (e.g., tip) by applying a voltage.

Thus, to observe the tunneling current I of electrons through the vacuum gap between the sample and the tip, a bias voltage, $V_{bias,}$ is applied, as shown in Figure 4.2. At $V_{bias} = 0$, the electrons cannot flow in either direction since the Fermi level, $E_{f,}$ of both the tip and the sample is equal, i.e., the gradient is zero. When $V_{bias} > 0$ (positive bias), the Fermi level of the sample is raised by V_{bias}, and the electrons in the occupied state (filled with electrons) of the sample can tunnel into the unoccupied state of the tip. Similarly, when $V_{bias} < 0$ (negative bias), the electrons in the occupied state of the tip tunnel into the unoccupied state of the sample.

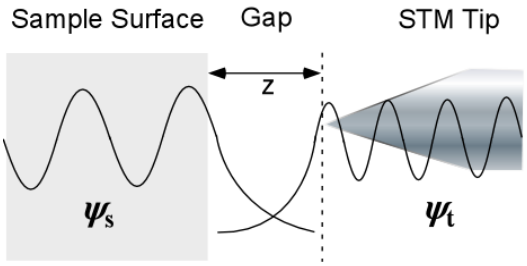

Figure 4.1: Schematic of STM one-dimensional tunneling configuration.

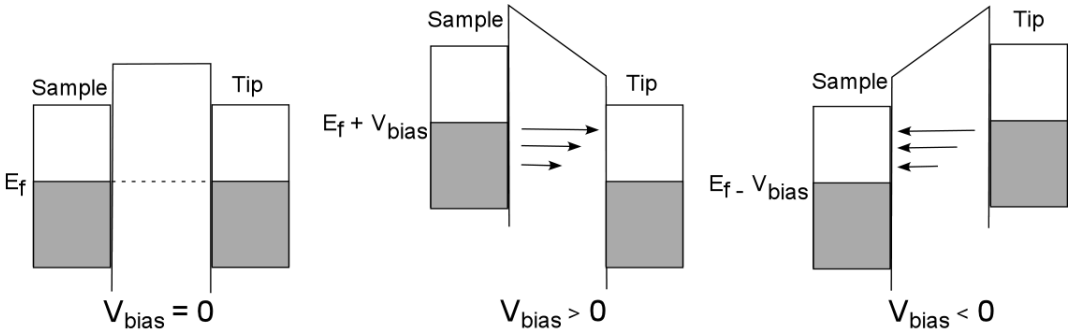

Figure 4.2: Schematic of a metal-insulator-metal tunneling junction. The grey area represents electron filled states (occupied level) and the white area is empty states, ready to accept electrons (unoccupied level).

STM images represent the local magnitude of the tunneling current in the x-y plane. As the tunneling current strongly depends on the tip-sample distance (i.e., the width of the vacuum gap or insulator air gap) the convoluted information it provides are composed of (a) topographical changes and (b) surface electronic anisotropy.

Tunnel Current, Vacuum Gap Size and Density of States

The tunneling current decays exponentially with the distance gap distance z, and is strongly affected by the density of states (DOS) of the sample at the Fermi level, $\rho_s(E_f)^2$; i.e.,

$$I \propto V_{bias}\rho_s(E_F)\exp\left[-2\frac{\sqrt{2m(\phi-E)}z}{\hbar}\right] \propto V_{bias}\rho_s(E_F)\exp(-1.025\sqrt{\phi}\cdot z), \quad (1)$$

where m is the mass of electron and $\hbar$ is the Planck's constant.

An electronic state describes a specific configuration, an electron can possess. For instance, it can have either a spin up or spin down, or a particular magnetic momentum etc. A state is described by a set of quantum mechanical numbers. Each state can only be filled by one electron. Consider a classroom of X chairs with Y < X students. The chairs represent the states and the students the electrons. Let us assume, it is hard to read the board, and the students are all very interested in the subject. Consequently the chairs will be filled up towards the front with some empty seats in the back. This situation is illustrated in Figure 4.3. The chairs in each row are represented by circles. Filled circles represent student occupied chairs. The distance from the board is indicated with x. The number of chairs per row represents the density of states (DOS) for a particular classroom. Two distinctly different classrooms are shown in Figure 4.3. In the second classroom N is a function of the x. The last row that is filled is identified by x_F. Returning to electrons in metals; x_F corresponds to the Fermi energy E_f, N to ρ_s and N(x_F) to $\rho_s(E_f)$. In the case of the free electron model for s-/p-metals at zero Kelvin, $\rho_s(E)$ is proportional to the square root of the energy.

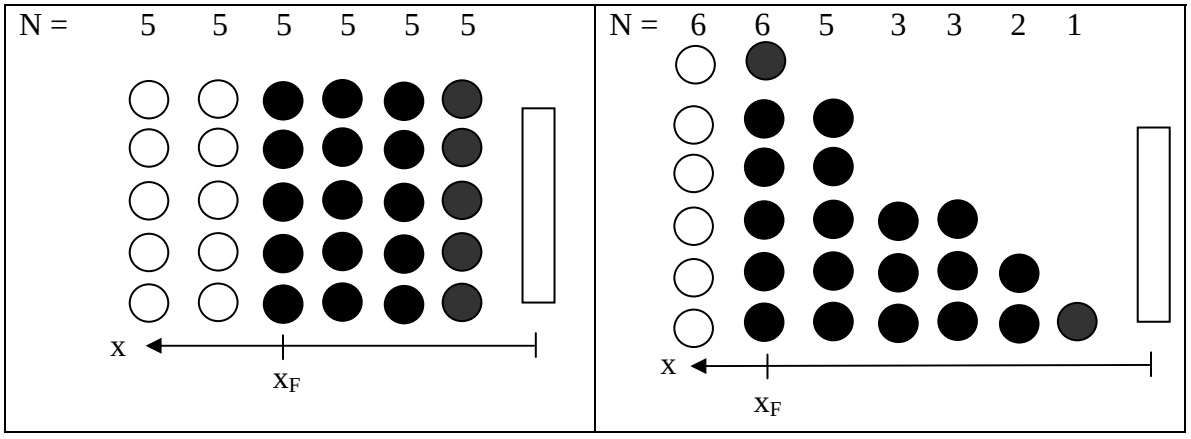

Figure 4.3: Density of state (DOS), N, and Fermi energy x_F in two classroom settings. (left) N is constant. (right) N(x).

Many physical properties are affected or depend on the number of states within an energy range (i.e., the energy density of states). While in metals and semi-metals, there is relatively small variation in the density of states due to the large electron delocalization, the density of energy levels in semiconductors varies noticeably. Thus, knowledge about DOS is of immense importance for electronic applications involving semiconducting materials, where the availability of empty valence and conduction states (states below and above the Fermi level) is crucial for the transition rates. In comparison to Figure 2 that visualizes tunneling between metals, Figure 4.4 illustrates the tunneling mechanism

involving a semiconductor. The filled area (grey) is not uniform, representing the variation in electron density, and the lines in the unoccupied levels represent the variation in density of the energy levels that the tunneling electrons can occupy.

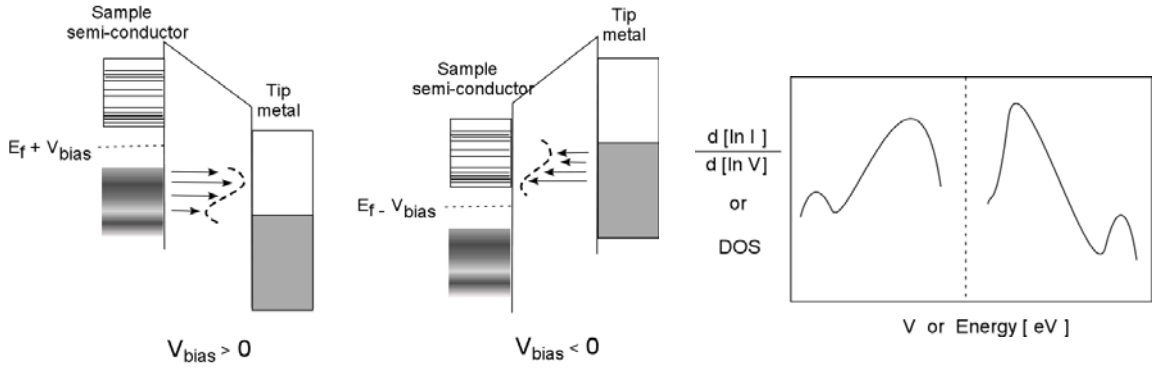

Figure 4.4: (a) Schematic of a metal-insulator-semiconductor tunneling junction and **(b)** corresponding normalized differential tunneling conductance.

STM and Local Density of States

STM constant current maps provide information about the variations in the electron density, and do not necessarily correspond to the location of atoms (nuclei). Figure 4.5 illustrates that a location of high tunneling current in a STM image can be either a compounded affected of two atoms, leading to a current maximum in between the atoms, or be identical with the location of an atom. This is for instance found for the silicon (001) 2x1 surface.[3] A π molecular orbital of the silicon-silicon dimers (Si=Si) creates the highest electron density (probability) at the center of the dimers, while an anti-bonding π^* molecular orbital has a node (a location where the probability is zero) at the center of the dimers. Thus, when a negative bias is applied, the electrons in the π-molecular orbital (occupied state) tunnel and the resulting image, similar to the case shown in Figure 4.5(a), will be obtained. When a positive bias is applied, the electrons of the tip tunnel into the anti-bonding π^* molecular orbital (unoccupied state), revealing a gap between the dimers, as in Figure 4.5(b). When the variation in the local DOS (LDOS) of metals is small, the contour of STM images often can be safely interpreted as the topography of the atomic lattice.[†]

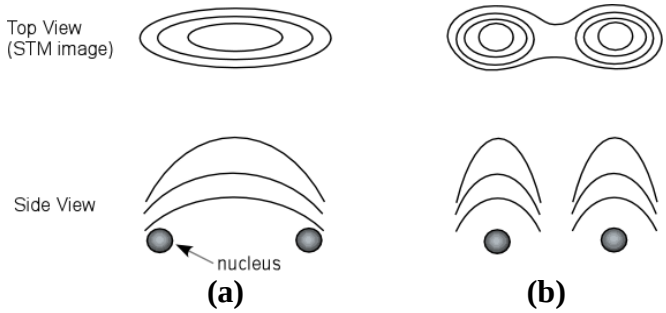

Figure 4.5: Sketch of possible STM images relative to the nucleus locations. Top view is the contouring lines of STM images and the corresponding side view on the bottom. STM image shows high tunneling location **(a)** at center of two nuclei and **(b)** at the top of each nucleus.

[†] See next section on LDOS on variety of systems.

STM Measuring Modes

STM can be operated in three major operation modes: (1) imaging mode, (2) spectroscopy mode, and (3) manipulation mode. There are two imaging modes: Constant current imaging and constant height imaging. In constant current imaging, the vacuum or air insulating gap, *z*, between the tip and the sample is controlled by a current feedback control system. Scanning results in a constant current map of the surface. In contrast, the feedback is turned off, and the tip is scanned at a sample topography independent constant height, which results in a locally changing tunneling current map.

The spectroscopy STM mode, involves either a bias voltage V_{bias} sweep, or distance *z* ramping. The resulting current *I* is monitored as a function of the changing parameters. According to Equation (1), the tunneling current exhibits a log-linear gap distance z relationship. A simplified form of Equation (1) can be used to estimate the barrier height, ϕ, of the tunneling current, i.e.,

$$Log(I) = -A\sqrt{\phi} \cdot z + C \qquad (2)$$

where A is $1.025\sqrt{eV}$ /Å, and C is a constant. I-z spectroscopy is useful for the characterization of the quality of the STM tip, its sharpness and cleanliness. In the groundbreaking article of Binnig and Rohrer, the sensitivity of a STM tip was attained by the I-z curves and was observed to increase with successive cleaning procedures.

Tunneling spectroscopy as a function of the bias voltage, i.e., I-V curves, provides very important information about the surface electronic structure, such as the barrier heights and LDOS of the sample. While the experimental procedures is very similar for large variety of sample systems, i.e., the current is measured as a function of V_{bias}, the data analysis varies from system to system and is in more detail discussed below. As summarized in Figure 4.6, I-V spectroscopy offers with a first order analysis information about the electronics structure, and a second order analysis information vibrational mobilities.

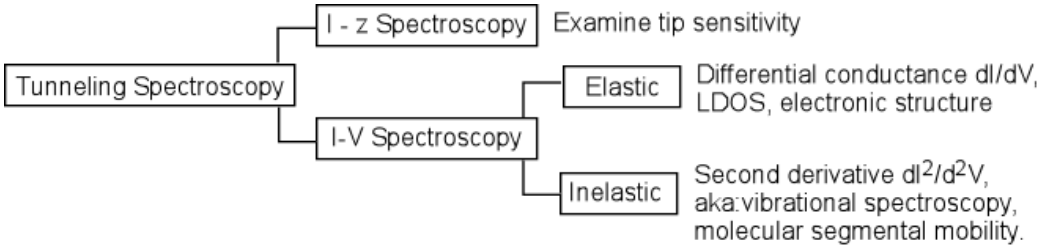

Figure 4.6: Modes of tunneling spectroscopy.

Tunneling Spectroscopy

In the STM imaging mode, the tunneling current *I* is continuously recorded at each location (*x*,*y*) at a constant bias voltage V_{bias}, generating a two-dimensional map of tunneling conductance I/V_{bias}. In contrast, tunneling spectroscopy (I-V curve) focuses on the tunneling conductance, or commonly, a normalized differential tunneling conductance $(dI/dV)/(I/V) = d[\ln(I)] / d[\ln(V)]$. Tunneling spectroscopy studies are usually performed without scanning at a particularly chosen location, based on an initial STM current or height map. However, it is also possible to scan while the bias is ramped (scanning tunneling spectroscopy (STS). Consider the aforementioned example, silicon 001 (2x1), it is evident that the spectroscopy at a location right above a nucleus would exhibit a I-V curve that is different from that of a center of two nuclei. In fact I-V

spectroscopy on silicon 111 (7x7) surface is location specific.[4] Interestingly the average I-V curves at various locations closely resembles to data obtained by ultraviolet photoelectron spectroscopy (UPS) and inverse photoemission spectroscopy (IPS). It suggests that UPS and IPS are the area average of the differential conductance, while STM tunneling spectroscopy is capable of resolving local information, e.g. local DOS rather than average DOS.

The general profile of the density of state around the Fermi level, i.e., $(\mathrm{d}I/\mathrm{d}V)/(I/V)$, can be used to classify the material based on its conductivity, as illustrated in Figure 4.7. As shown, metals do not possess a gap between the occupied states (valence band) and the unoccupied states (conduction band) and the variation in DOS is relatively small. Thus, the I-V curves are linear for the most part, resulting in a very small dI/dV gradient. Semi-metals also do not have a gap between the occupied and unoccupied states. There is, however, a gap in the momentum space (the waves are out of phase) that depresses the conductance around the Fermi level, and consequently bends the density of states at low voltages. For semiconductors and insulators, the conductance around the Fermi level is zero. The threshold voltage, i.e., band gap, $E_g = |V_{+bias}| + |V_{-bias}|$, is relatively small for semiconductor (< 3eV, used as definition for semiconductors). As shown in Figure 4.7, semiconductors show a highly bend DOS, which is flat as for insulators at low voltages, where the energy gap E_g cannot be bridged. It is well known that doping semiconductors with impurities or defect sites affect reduce E_g , and thus, can modify the density of states at the Fermi level to such a degree that it resembles nearly a semi-metal.

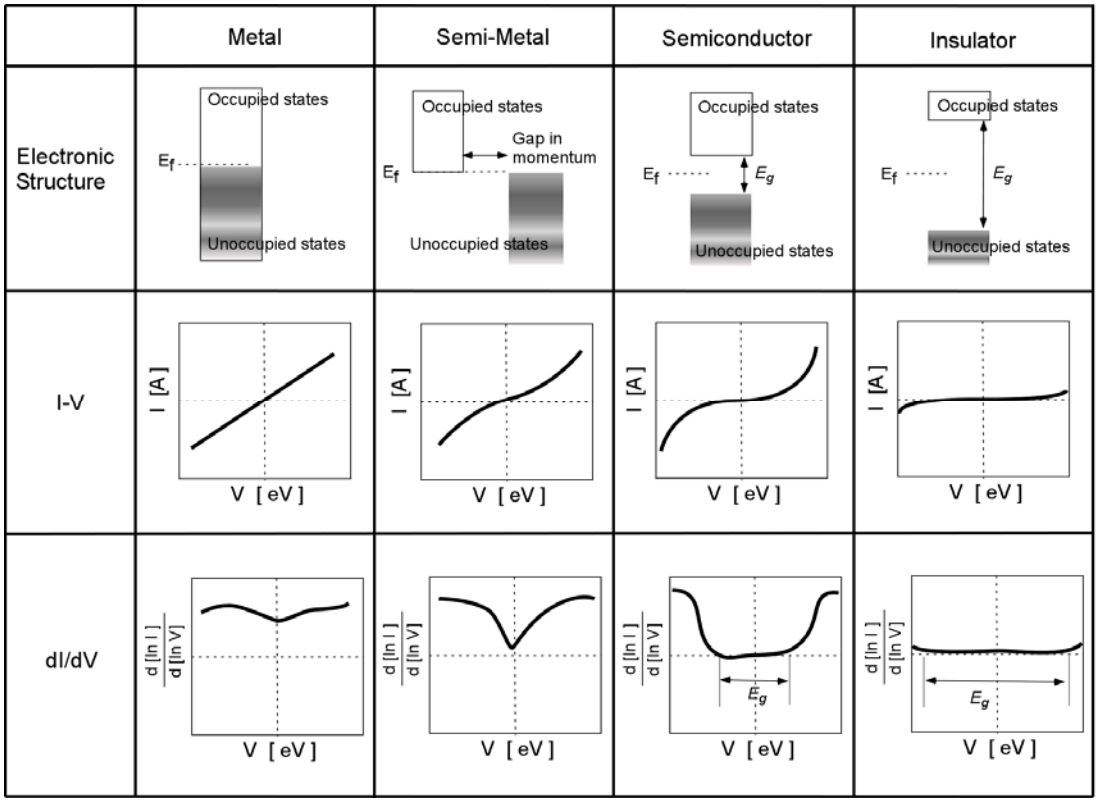

Figure 4.7: The electronic structures and corresponding IV curves and dI/dV curves of tunneling spectroscopy.

So far, we have discussed elastic tunneling spectroscopy, in which the energy of the tunneling electrons is conserved. In inelastic tunneling spectroscopy, the counter electrode is not the material under investigation; rather it is the gap that is examined. In general, the material of interest is placed on top of the counter electrode or fills the insulating gap completely as a thin film. When the tunneling current travels through the material, a part of tunneling electron energy is dissipated by activating various modes of the molecular motion, e.g. C-H stretching of hydrocarbon chains. Thus the modes of the molecular motion can be deduced based on the extensive data base of infrared spectroscopy (IR). Experimentally, the I-V curve is obtained in the same manner as the elastic tunneling spectroscopy. To identify the modes of the molecular motion, the second derivative, dI^2/d^2V, is calculated, which contain multiple number of sharp peaks. The modes of molecular motion are then identified by the locations of the peak V_{peak}.

Layered Structure of HOPG

Highly ordered pyrolytic graphite (HOPG) consists of layers of carbon sheets, forming a semi-metallic system. While the carbons within a sheet are covalently bonded to form a hexagonal lattice structure, the layers are held together by Van der Walls forces. The in-plane lattice constant (repeating unit length) and the z-axis lattice constant are 2.46Å and 6.7 Å respectively and the in-plane atom-to-atom distance is 1.42 Å. The sheets are arranged such that the every other carbon on a layer has a carbon in the neighboring sheets, Figure 4.8. The carbons in the first layer that have a carbon in the second layer right below are called an A-site carbons, and the carbons without a carbon directly below are called B-site carbons.

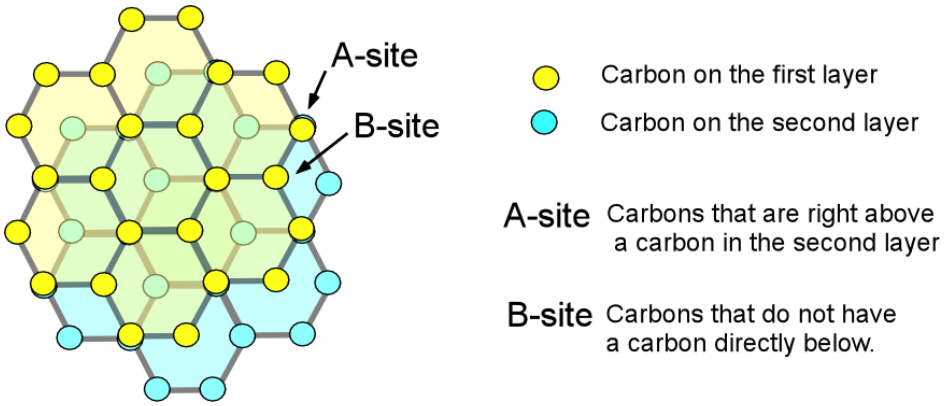

Figure 4.8: Layered structure of HOPG.

In STM images, the two types of carbons (A-site and B-site) appear differently. As shown in Figure 4.9, the B-site carbons exhibit a higher LDOS (i.e., topography) than the carbons at the A-site, exhibiting the *three-fold-hexagon* pattern.

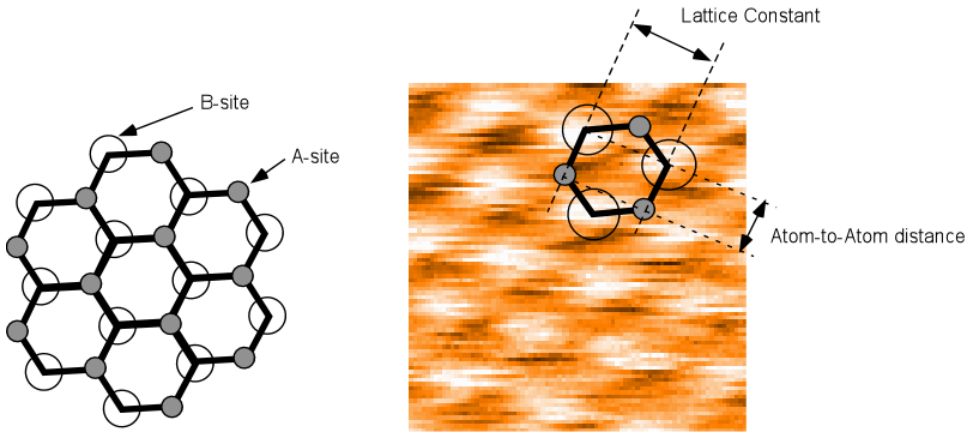

Figure 4.9: Interpretation of HOPG's *three-fold-hexagon* pattern of STM images

While most of STM study of HOPG shows this *three-fold-hexagon* pattern, there are reports on various other patterns of HOPG, such as true hexagon and linear row structure. A possible explanation is given by multiple tip artifacts. Simulations of multiple tip contacts showed superimposed signal collection.

References

1 G. Binnig, H. Rohrer, C. Berber, and E. Weibel, Appl. Phys. Lett. **40** (2), 178 (1981).
2 E. Meyer, H. J. Hug, and R. Bennewitz, *Scanning Probe Microscopy*. (Springer, Berlin, 2004).
3 R. J. Hamers and Y. J. Wang, Chemical Reviews **96** (4), 1261 (1996).
4 R. J. Hamers, R. M. Tromp, and J. E. Demuth, Phys. Rev. Let. 56 (18), 1972 (1986).

Recommended Reading

Quantum Chemistry and Spectroscopy by Thomas Engel and Philip Reid, Pearson/Benjamin Cummings, San Francisco, 2006.

Scanning Probe Microscopy and Spectroscopy, Methods and Applications, by Roland Wiesendanger, Cambridge University Press, Cambridge, 2rd ed. 1994.

Scanning Probe Microscopy-The lab on a Tip, by Ernst Meyer, Hans Josef Hug, Roland Bennewitz, Springer, Berlin, 2004.